AD-A072 867 TEXAS UNIV AT AUSTIN APPLIED RESEARCH LABS F/G 20/1
SHEAR WAVE PROPAGATION IN UNCONSOLIDATED FLUID SATURATED POROUS--ETC(U)
MAY 79 D W BELL N00014-76-C-0117
UNCLASSIFIED ARL-TR-79-31 NL

1 OF 2
ADA
072867

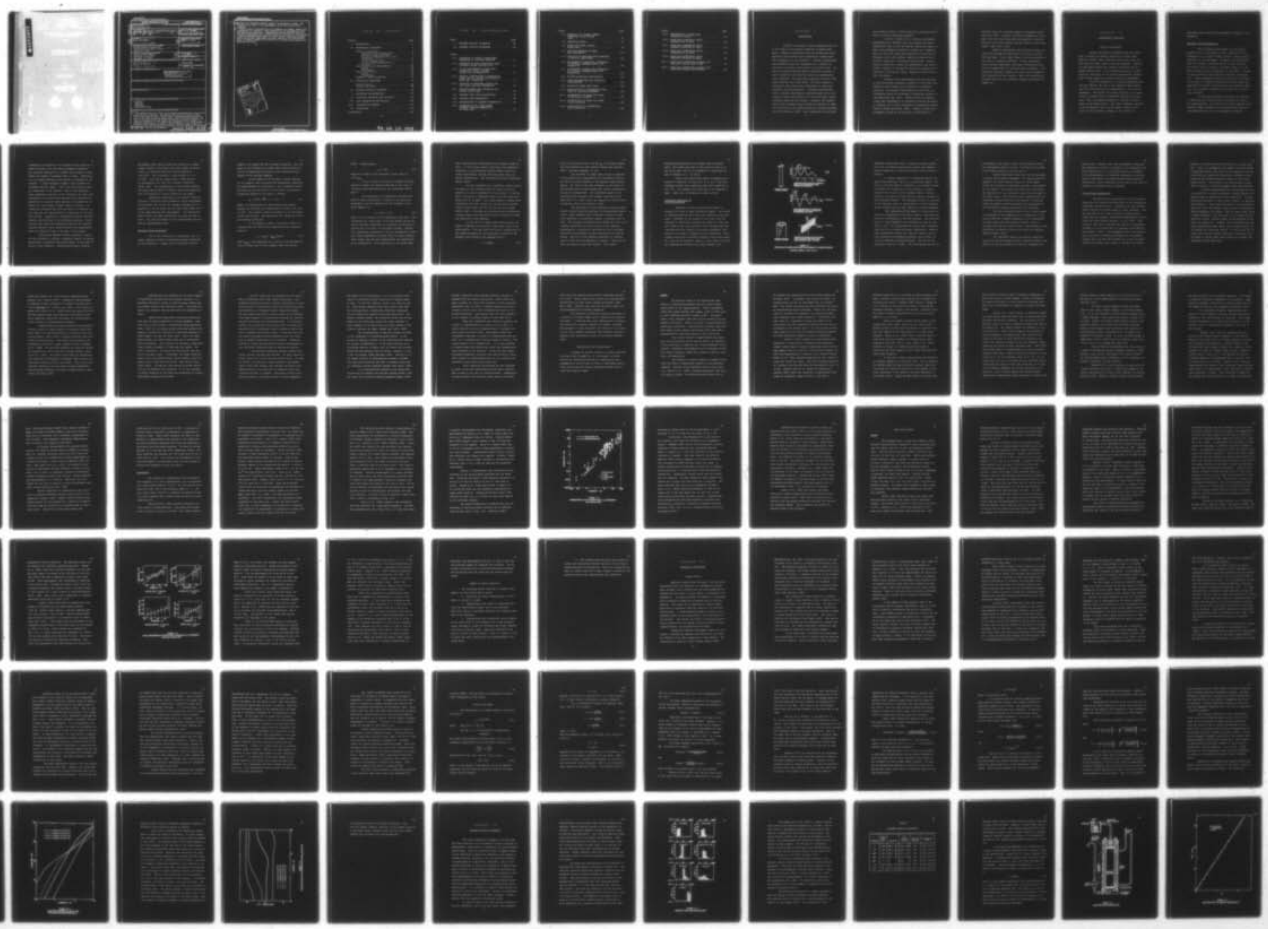

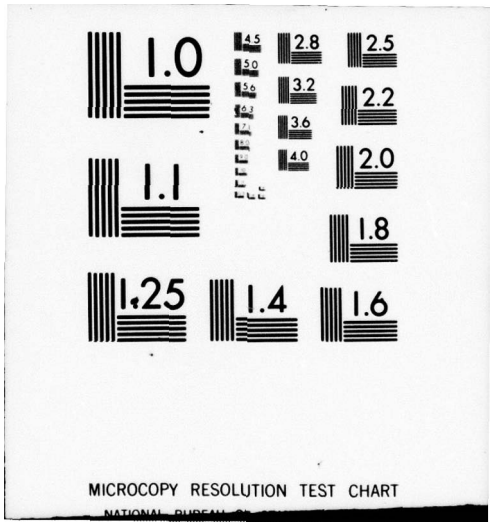
1.0
1.1
1.25
1.4
1.6
1.8
2.0
2.2
2.5
2.8
3.2
3.6
4.0
4.5
5.0
5.6
6.3
7.1
8.0
9.0
MICROCOPY RESOLUTION TEST CHART

UNCLASSIFIED

SECURITY CLASSIFICATION OF THIS PAGE *(When Data Entered)*

REPORT DOCUMENTATION PAGE

READ INSTRUCTIONS BEFORE COMPLETING FORM

1. REPORT NUMBER: ARL-TR-79-31	2. GOVT ACCESSION NO.
3. RECIPIENT'S CATALOG NUMBER	
4. TITLE *(and Subtitle)*: SHEAR WAVE PROPAGATION IN UNCONSOLIDATED FLUID SATURATED POROUS MEDIA	5. TYPE OF REPORT & PERIOD COVERED: Technical Report
	6. PERFORMING ORG. REPORT NUMBER
7. AUTHOR(s): David Warren Bell	8. CONTRACT OR GRANT NUMBER(s): N00014-76-C-0117
9. PERFORMING ORGANIZATION NAME AND ADDRESS: Applied Research Laboratories, The University of Texas at Austin, Austin, TX 78712	10. PROGRAM ELEMENT, PROJECT, TASK AREA & WORK UNIT NUMBERS
11. CONTROLLING OFFICE NAME AND ADDRESS: Office of Naval Research, Department of the Navy, Arlington, VA 22217	12. REPORT DATE: 15 May 1979
	13. NUMBER OF PAGES: 173
14. MONITORING AGENCY NAME & ADDRESS *(if different from Controlling Office)*	15. SECURITY CLASS. *(of this report)*: UNCLASSIFIED
	15a. DECLASSIFICATION DOWNGRADING SCHEDULE: N/A

16. DISTRIBUTION STATEMENT *(of this Report)*

This document has been approved for public release and sale; its distribution is unlimited.

17. DISTRIBUTION STATEMENT *(of the abstract entered in Block 20, if different from Report)*

18. SUPPLEMENTARY NOTES

19. KEY WORDS *(Continue on reverse side if necessary and identify by block number)*

acoustics
sediments
shear wave
compressional wave

20. ABSTRACT *(Continue on reverse side if necessary and identify by block number)*

(U) Experimental shear wave speed and attenuation measurements are reported for seven laboratory sediments. The samples consisted of four sizes of well sorted glass beads and three natural sands. Measurements were obtained for both air and water saturation without application of external pressure. The speed and attenuation for each sample was determined from the change with transducer separation of the transit time and amplitude of an acoustic pulse. Broadband bender elements provided an overall frequency range of 600 Hz to

CONT'D

DD FORM 1 JAN 73 1473 EDITION OF 1 NOV 65 IS OBSOLETE

UNCLASSIFIED 404 434

SECURITY CLASSIFICATION OF THIS PAGE *(When Data Entered)*

CONT

(U) 200 kHz, with individual sediment ranges of approximately a decade. The attenuation was found to vary approximately as the first power of the frequency.

(U) Various physical characteristics of the samples, for example, density and permeability, are reported to allow comparison of the experimental results with theoretical predictions. Supplementary compressional wave speed and attenuation measurements at the single frequency of 120 kHz are also provided. A simple viscoelastic model based on perfect coupling between the sediment grains and the pore fluid predicts the main features of the observed data. There is evidence, however, of an effect due to relative motion between the grains and the fluid.

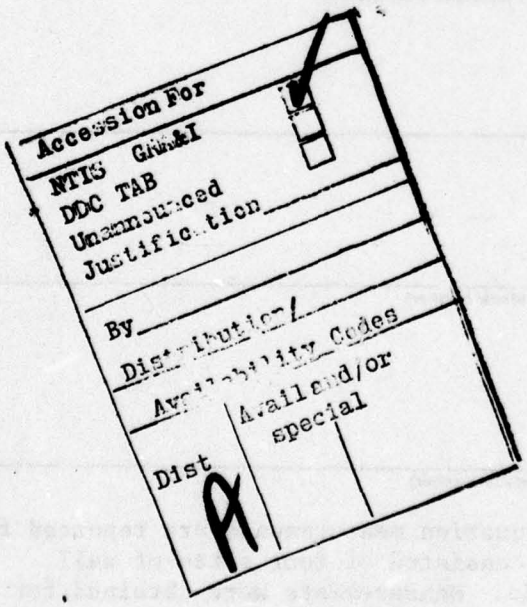

TABLE OF CONTENTS

L I S T O F I L L U S T R A T I O N S

C H A P T E R I

INTRODUCTION

Interest in underwater sound transmission has led to the study of the acoustic properties of marine sediments. Extensive experimental work has established useful empirical relationships which characterize compressional wave propagation in such materials. However, compressional wave parameters alone are inadequate for a complete description of acoustic interactions at the ocean floor. Almost all natural sediments exhibit sufficient rigidity to support transverse oscillations excited by compressional wave conversion. The shear wave properties of marine sediments, however, are poorly known. The shear modulus is normally so small that direct measurement of shear wave properties has been difficult. Although scattered data exist, a general experimental characterization of the viscoelastic shear wave properties of fully saturated, unconsolidated media has been lacking. Recently, the development of new transducers has overcome the barriers to shear wave detection in low rigidity materials (Shirley and Hampton, 1978; Shirley, 1978). Such transducers were utilized

in the present study to obtain shear wave speed and attenuation in several laboratory sediments.

A review in Chapter II of previous experimental determinations of sediment shear wave properties reveals insufficient data to test the various theoretical models of shear wave propagation reviewed in Chapter III. Measurements of shear wave speed and attenuation as functions of frequency in the same sediment sample are required for a decisive comparison of theoretical predictions. Various physical properties, notably the permeability, are also required. Chapters IV through VII detail the acquisition of such data in the present study. Chapters VIII and IX present the results.

Although little experimental work has been done in surficial marine sediments, interest in shear wave propagation in porous media is not confined to underwater acoustics. The dynamic shear modulus of loose soil is a determining factor in the design of foundations subject to vibratory loads (Wu, 1971). Combined shear and compressional wave measurements can potentially provide the petroleum industry with a direct indication of hydrocarbon accumulations (Tatham and Stoffa, 1976). Changes in shear wave propagation caused by the reaction of microcracks to

abnormal stress are a possible means of earthquake prediction (Nur, 1972). Theories of acoustic propagation in two-phase fluid and solid media have been applied to interior portions of the earth wherein the pore fluid is molten rock (Walsh, 1968; Gliko, 1976).

Numerous experimental and theoretical studies of shear wave propagation applicable to the above interests have been made. These cannot always be directly applied to the study of saturated sediments. Partial saturation, large vibration amplitudes, and large confining pressures are all inappropriate for surficial marine sediments. Nevertheless, important insights into shear wave propagation can be gained from such studies. These will therefore be reviewed along with the available sediment measurements in Chapter II.

C H A P T E R I I

EXPERIMENTAL BACKGROUND

Review of Techniques

Several experimental procedures have been developed to measure the dynamic properties of porous media. Taken as a group, these techniques provide for stress cycles from less than a hertz to several megahertz. However, the individual methods have limited resolutions and frequency sensitivities. It is therefore necessary to understand the limitations of the various experimental arrangements before comparison of their results are undertaken.

Since the properties of a grossly homogeneous medium are desired, the size of the available sample places the first restrictions on the measurement of its acoustic parameters. The concept of a porous substance as a single entity is invalid when the wavelength approaches the pore size. Thus, the maximum frequency of interest is determined by the medium itself. The lowest frequency available to an investigator with a finite sample, either in the field or the laboratory, depends on the validity of

techniques that account for the impedance contrasts at the boundaries.

Laboratory Pulse Transmission

Direct laboratory measurement of the acoustic properties of a porous media is easily obtained from the propagation of an acoustic signal through a sample large in comparison to the wavelength. Generally, the transmission path lies between a projector and one or more receivers. The transit time of a pulse or the phase change of a continuous signal allows determination of the speed. A change in signal amplitude with separation indicates the energy loss. Other arrangements place both projector and receiver on one edge of a sample and monitor the arrival times and amplitudes of multiple reflections from the opposite boundary. This provides a change in path length for a single fixed receiver.

If broadband transducers are used, the variation of amplitude with frequency may be monitored by either of two common methods. The ratio of the Fourier spectra of an impulsive input recorded at two receivers gives the relative amplitude loss over a set propagation distance.

Alternatively, one or more cycles of a sine wave may be used as the input. A narrow bandpass filter centered on the oscillator frequency is applied to the received signal to eliminate frequencies introduced by gating the input. The frequency resolution is determined by the filter setting and the number of cycles present in the pulse. Ideally, perfect frequency discrimination could be obtained from a continuous input. However, this is normally impractical due to interference from reflections present in the wave train. Reflections can also limit the application of spectral analysis. In any case, the responses of the measuring devices and the geometric divergence of the energy must be determined for a valid measurement of the attenuation. Depending on the system, velocities reported in the literature may be group velocities or phase velocities.

The transducers used for laboratory compressional wave measurements are normally piezoelectric crystals or polarized ceramics. The useful frequency output depends on the type of material, the size of the element, and the method of coupling. Some experimental arrangements use broadband elements, others use highly resonant devices. Gregory (1975) gives a short discussion of the advantages and disadvantages of each technique. The narrowband signal offers

better time resolution and is less subject to frequency distortion in materials with high attenuation. The choice of a particular ceramic material is sometimes dictated by the ambient pressures encountered in the experiment. If the element is not isolated from pressure changes, materials are chosen which are relatively insensitive to the pressure. These normally are low Q devices (Shirley and Bell, 1978).

Laboratory shear waves can be generated by a ceramic element polarized perpendicular to the applied field or by quartz crystals cut in either the Y or AC planes (e.g., Simmons, 1964). Alternatively, compressional waves may be converted to shear waves at an interface (King, 1966; Gregory and Podio, 1970). The second method provides a shear wave pulse free from the compressional wave precursor that is often generated by shear elements. Both of these techniques have allowed successful measurements of shear wave properties of rocks. However, such instruments often do not have sufficient sensitivity to detect a shear wave in unconsolidated materials.

In the absence of external pressure, unconsolidated sediments display large shear wave attenuations which increase rapidly with frequency. Relatively low

frequencies are required if the signal-to-noise ratio is to remain tolerable over even short propagation distances. The resonance frequency of a ceramic shear element is high unless the length to thickness ratio is small. Additionally, the ceramic material is not nearly as compliant as the sediment. A large impedance mismatch exists between the transducer and the sample. This limits the amount of energy transferred to the sediment. Most of the laboratory pulse experiments reported in the literature for shear wave propagation in unconsolidated materials have required the application of external frame pressure to increase the rigidity to a point where a signal could be detected. Although such pressures may exist at depth in a sediment column, they are not representative of conditions at the sediment surface. Comparison of experimental results therefore requires specification of the overburden pressure. Values of shear wave speed and attenuation obtained with minimal external pressure can be quite different from measurements where the vertical stress is due only to self-weight.

Shirley and Anderson (1975a) conducted a series of tests designed to develop a transducer capable of making measurements in materials with shear moduli in the range of natural ocean sediments. Continued development (Shirley

and Hampton 1978, Shirley 1978) has resulted in a bender element capable of detecting shear wave speeds as low as 2 m/sec in saturated clays with a bulk density of 1.38 g/cm^3. This represents a shear modulus of 5.5 x 10^3 N/m^2. This may be compared with a shear modulus of approximately 10^{10} N/m^2 for saturated sandstones (King, 1966). The implementation of the bender elements for routine measurement of sediment shear wave properties will be discussed in a later section of this report.

Laboratory transmission of an acoustic pulse is limited to relatively high frequencies (short wavelengths) by the finite size of the test chamber, although the restriction is not as severe for low speed shear waves as it is for compressional wave measurements. For frequencies below 100 Hz, the shear wavelengths for sands are over a meter. The same wavelength for the compressional wave exists at approximately 2 kHz.

Resonant Column Techniques

The forced vibration of a cylindrical rod is a common laboratory means of determining dynamic properties at low frequencies. Speeds can be calculated from the

length of the sample and the resonance frequency. Both the shape of the resonances in steady state motion and the decay of the amplitude with time for free vibration yield a measure of the internal damping.

If the length of the cylinder is large compared to its diameter, both torsional and longitudinal vibrations are approximately one dimensional. For a perfectly elastic rod fixed at one end and free at the other, the resonance frequencies depend on the length L, through

$$\omega_n = (n/2L)\sqrt{c/\rho} \quad n = 1,3,5,\ldots, \qquad \text{II-1}$$

where c is respectively the shear modulus and Young's modulus for torsional and longitudinal vibrations (Wu 1971, p. 127). The integer n gives the number of 1/4 wavelengths within the cylinder. The expression will change for different boundary conditions.

If the damping is small, the quality factor Q is obtained from the steady state amplitude versus frequency curve by

$$Q = (\omega_n/\Delta\omega)\,(A_{max}^2 - A^2)/A^2 , \qquad \text{II-2}$$

where A_{max} is the amplitude at ω_n and A is the amplitude at $1/2\omega$ on either side of the resonance (Hall and Richart,

1963). Conventionally,

$$Q = f/\Delta f \ , \qquad \text{II-3}$$

where Δf is taken at the half-power points, that is, $.707\ A_{max}$.

If the cylinder is driven at resonance and then allowed to decay, the natural logarithm of the ratio of successive peak amplitudes gives the logarithmic decrement δ.

The attenuation a in nepers/unit distance measured in pulse experiments is related to the decay per wavelength δ and the sharpness of the resonance Q, for small damping, by

$$\delta = aV/f = \pi/Q \ , \qquad \text{II-4}$$

where V is the velocity of the appropriate wave type. The attenuation for shear waves in the bulk medium and the decay of torsional vibrations of a cylinder are directly related by Eq. II-4 when V is the shear velocity. However, for longitudinal vibrations, δ and Q as determined by resonant column experiments strictly refer to Young's modulus waves rather than the bulk compressional wave measured by pulse transmission. This distinction is not always made

when comparing pulse measurements with resonant column results. In the present report, dilational wave parameters referring to one dimensional Young's modulus waves are termed longitudinal, whereas bulk dilational waves are called compressional. The differences are often negligible (White, 1965).

The wave equations for a perfectly elastic medium are based on the assumption that the stress can be expressed as a linear combination of the strains. If the medium is driven by a sinusoidal force, then the stress and strain will be in phase. In a lossy medium, a steady state oscillation will still result in a stress that is proportional to the strain, but the two will be out of phase (White, 1965). The shape of the closed curve representing a stress-strain cycle can thus be used to measure the damping properties of the material.

In the case of a simple shear stress cycle, the points of maximum stress define a line whose slope is the shear modulus. The area within the loop is proportional to the energy dissipated in the cycle and is related to the maximum stored energy by the damping ratio D,

$$D = A/2\pi A_m \quad , \qquad \text{II-5}$$

where A is the area of the loop and A_m is the area beneath the line defining the shear modulus (Hardin and Drnevich, 1972). For small damping, $\delta = 2\pi D$.

The condition of simple shear stress is obtained in the laboratory by application of a reversible torque to the end of a hollow cylinder of the material under investigation. The ratio of the wall thickness to the radius of the cylinder must be small enough that radial variations of stress are insignificant. The cylindrical shape of the specimen avoids problems with boundary conditions which would exist if a shear stress was imposed on a finite block of material (Hardin and Drnevich, 1972).

The application of the techniques discussed above present several practical problems for unconsolidated materials. Since sediments lack sufficient cohesion to maintain themselves in cylindrical shapes, a container must be used. The resonance frequencies will depend not only on the sediment properties but also on those of the container. Additionally, the packing of particles in such a cylinder may differ from packings in pulse experiments on loose material. Analysis of the boundary conditions is involved and will vary from one apparatus to another. Often the effects of external stress are studied. This causes

additional modification of the simple cases discussed above. The reader may refer to the articles cited or to any of the many texts on soil mechanics if additional detail is desired, e.g., Wu (1971).

Since investigators may report the damping properties of a material in terms of a, δ, Q, or D, the relationships between these quantities have been summarized in Fig. II-1. The formulas are valid only if the damping is small. Small will be defined in a later section.

Laboratory Simulation of In Situ Conditions

Sediments in the field are often subject to stresses not found in small laboratory samples. The weight of overlying material will cause the rigidity to vary with depth. Sediments at the surface of the ocean floor are subjected to hydrostatic pressure not found in a core sample. Much of the work reported in the literature has been concerned with the variation of acoustic parameters with stress in an effort to simulate in situ conditions. These studies often give an acoustic property, such as the speed, as a function of pressure. However, since stress is a tensor inadequately defined by the term pressure, the

TORSIONAL VIBRATION OF SOLID CYLINDER

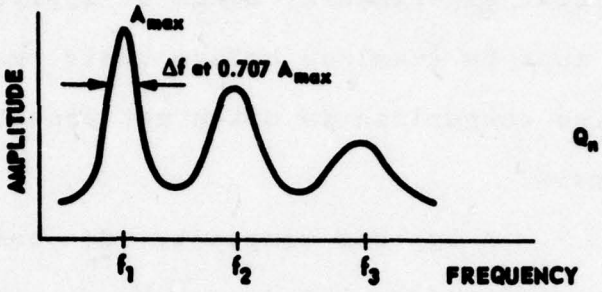

VARIATION OF AMPLITUDE WITH FREQUENCY, QUALITY FACTOR Q OBTAINED FROM SHARPNESS OF RESONANCE.

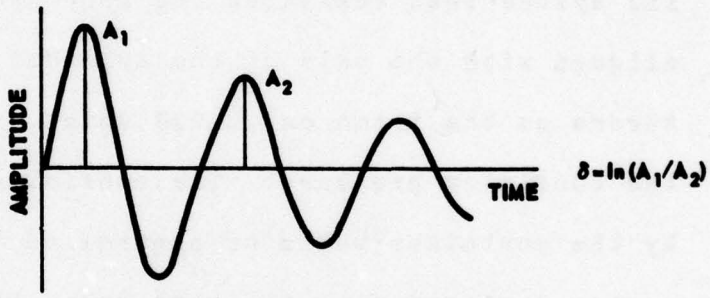

FREE VIBRATION DECAY AT RESONANCE, LOG DECREMENT δ OBTAINED FROM RATIO OF SUCCESSIVE AMPLITUDES.

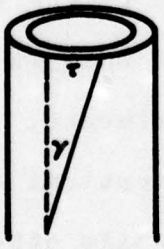

TORSIONAL VIBRATION OF HOLLOW CYLINDER

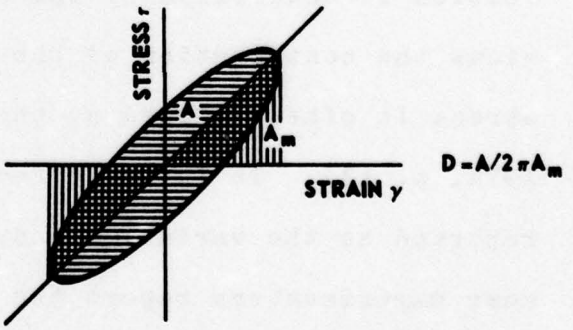

STRESS-STRAIN RECORD ANALYSIS, DAMPING RATIO D OBTAINED FROM AREA WITHIN CURVE DIVIDED BY AREA AT MAXIMUM.

FIGURE II-1

COMPARISON OF DAMPING COEFFICIENTS DETERMINED BY CYLINDER VIBRATION

FOR SMALL DAMPING, $\delta = aV/f = \pi/Q = 2\pi D$

different experimental means of applying external compaction must be examined before their results are compared. A precise comparison is often not possible without detailed analysis.

A typical composite of a compression device can apply three different forces to a cylindrical sample. The fluid in the pore space is connected to an external hydraulic system that regulates the pore pressure. A piston aligned with the axis of the cylinder exerts a vertical stress on the frame and fluid which is opposed laterally by the confining pressure. The confining pressure is supplied by the container walls or controlled by a second hydraulic system isolated from the pore space by a flexible membrane.

The compression of the sample in a particular direction is determined by the total stress in that direction minus the contribution of the pore pressure. The effective stress is often defined as the difference of the two (Wu, 1971, p. 13). It is the effective stress that is normally reported as the variable in dynamic experiments. However, some experimenters report the effective vertical stress, often called the differential pressure, while others report the effective confining pressure. The two are not equivalent (Hamilton, 1976c). The relationship between the

two depends on the elastic moduli of the material and on the experimental control of both. No effort will be made in the present report to connect the two.

Several additional terms arise in the discussion of stress within natural sediments. For uniform layers of sediment, the total vertical stress at a given depth, called the overburden or geostatic pressure, is determined by the weight of the sediment and fluid above that depth. The hydrostatic or pore pressure is given by the weight of the water column. The effective stress obtained from the overburden pressure minus the pore pressure is sometimes called the frame or skeleton pressure and corresponds to the differential pressure applied in the laboratory.

The above discussion implies that a given parameter dependent on the compression is a constant for a particular effective pressure regardless of the combinations of total stress and pore pressure involved. This is strictly true only for special cases. Modifications to the definition of effective stress given above are sometimes employed (Robin, 1973).

The laboratory control of physical conditions such as the pressure makes possible a detailed study of the effects of various parameters on acoustic propagation in

porous media. However, even when environmental conditions are simulated as closely as possible in the laboratory, the exact duplication of in situ characteristics is doubtful. In situ measurements are therefore required for a complete acoustic description of natural unconsolidated materials. Additionally, lower frequencies can be used in situ than are possible in laboratory pulse techniques.

In Situ Pulse Transmission

The most direct measurements of in situ acoustic properties are obtained from extensions of the transmission techniques discussed above. A signal can be sent between probes inserted to shallow depths in loose sediments. This has been done in the ocean by divers at shallow water depths and from research submersibles approximately 1,000 m below the ocean surface (Hamilton et al., 1970). Additionally, the ocean bottom has been probed by transducers attached to the cutting head of a geologic corer (Shirley and Anderson, 1975c). The propagation path is as near the end as possible to minimize disturbance of the sediment. Signals have also been sent between two or more boreholes, between the surface and a source or receiver in a single

borehole, or between source and receiver in the same borehole. Since the propagation path lengths are often orders of magnitude greater than those in the laboratory, the compressional wave sources for large scale transmission measurements are normally explosive charges or other high energy devices. The detectors are often moving coil geophones sensitive to velocity changes rather than pressure.

Accurate compressional wave measurements are easily obtained by the above procedures, although special corrections must be applied for certain geometries. The generation and detection of shear waves, however, is sometimes more difficult. Shear waves are normally excited during an explosion (Geyer and Martner, 1969) and can be enhanced by special shaping of the charge. Ohta and Shima (1967) found a charge detonated in an iron pipe to be an effective generator of S waves. Warrick (1974) tested Primacord on the side of a shallow pit. However, these techniques also generate compressional waves which, due to greater speed, often obscure the shear wave arrival. If both source and receiver are near the surface, additional interference will be caused by surface waves whose speeds are slightly less than those of the shear wave.

In their study of a contained explosion, Ohta and Shima (1976) found that vertically polarized shear waves could easily be generated by striking the casing pipe of a shot hole with a hammer. Stokoe and Woods (1972) used a hammer blow on a rod inserted in a shallow borehole as a shear wave source for small scale in situ tests. White and Sengbush (1953) found that a weight dropped into a container spiked to the borehole wall was an adequate generator of vertically polarized shear waves.

Horizontally polarized shear waves can be generated by a blow to the end of a wooden beam held in place by the weight of a truck (Kudo and Shima, 1970; Warrick, 1974). A greater impulse can be applied by shooting water or heavy weights from an iron pipe fixed to the beam (Jolly, 1956; Shima and Ohta, 1967). If the direction of the blow applied to the beam is reversed, the received shear wave pulse will change polarity. However, compressional wave noise will not. Thus the received signal can be enhanced by recording signals from oppositely directed impulses and subtracting one from the other. Mechanical vibrators can be used to impart lateral motion to a plate for the production of shear waves at a given frequency (Cherry and Water, 1968).

Indirect measurement of shear properties has sometimes been more feasible than the design of a shear wave source. Cunny and Fry (1973) derived shear wave speeds from Rayleigh wave velocities. Hamilton et al. (1970) did the same for Stoneley waves on the ocean floor. The effective depth of such an estimate is approximately one half the wave length of the boundary wave.

In Situ Reflection/Refraction Profiles

In situ placement of measuring devices at great depths, either in the sea or beneath the sediment surface, is not economically viable for surveys of large areal extent. However, routine surveys are conducted by standard reflection and refraction techniques that yield profiles tens of kilometers in length and several kilometers in depth. The typical exploration survey is a vertical profile with signals near normal incidence. Variable incident angle records are also commonly obtained by the use of expendable sonobuoys. A detailed analysis of these techniques is beyond the scope of this paper, but a review of the main features is necessary for an evaluation of the data in the literature. The reader who desires further

detail may consult one of the texts on exploration geophysics (e.g., Dobrin, 1976). A summary of the techniques as applied to marine geophysics is given by several articles in The Sea, Vol. 3 (Hill, ed., 1963). Also useful are papers by Le Pichon et al. (1968) which discusses both vertical and variable angle profiling and by Rutherford (1976) which emphasizes analytical techniques for determining velocity profiles in unconsolidated sediments.

Compressional wave speeds derived from reflection returns, either by simple geometric techniques (Grant and West, 1965) or by detailed analysis of multifold data (Taner and Koehler, 1969), refer to average interval velocities between discontinuities. Such values are accurate to approximately 100 m/sec in ocean sediment surveys (Le Pichon et al., 1968). For deep sea sediments the earliest returns are usually 50 to 100 m below the sediment surface (Hamilton et al., 1977). The results are useful for determining the structural relationships of sediment layers and for establishing velocity profiles with depth. They do not yield detailed information on the surface acoustic properties. Unconsolidated sediments are found to depths over a 1,000 m (Houtz and Ewing, 1963).

Although deep sea sediments do not return signals of significant strength from the sediment surface, it is sometimes possible to relate an observed phase change with the surface velocity (Fry and Raitt, 1961). This model assumes a low sediment velocity and treats the sediment as a fluid.

Conventional exploration reflection surveys provide only the gross properties of bottom sediments. However, this is due in part to intentional design specifications. That is, the normal seismic profiling system is designed to outline the structure of reflective surfaces at great depths, not near the ocean floor. Since the transmission paths are large energy losses due to attenuation must be minimized. This requires low frequency, long wavelength signals incapable of resolving thin layers. For ease of operation, the source and receiver are near the top of the water column. Conversely, the ideal system for study of the top sediment layers would include a high frequency source towed near the bottom. Such devices exist (Tyce, 1976). As expected, they provide excellent definition of the sediment fine structure. It is also possible to obtain estimates of the speed and attenuation if certain simplifying assumptions are made.

Acoustic energy can be returned from the subsurface by mechanisms other than simple reflections. The classical refraction method of seismic exploration is based on the return of energy from a head wave traveling at grazing incidence to a boundary between isovelocity layers. The wave speeds and depths of these layers can be obtained from simple geometric considerations provided the interval velocities increase with increasing depth. In some applications, the refraction returns arise from a turning point associated with a continuous velocity gradient rather than from a boundary wave between layers. Curved ray path models based on assumed velocity gradients allow the velocities at greatest penetration to be inferred. Generally, refraction surveys provide better velocity information but less structural definition than do reflection profiles.

A conventional refraction profile contains both direct arrivals and head wave returns. At short source-receiver offsets the direct wave will arrive first. At larger offsets, the head wave, which travels at the greater speed of the lower medium, will overtake the direct wave. Identification of the head wave is difficult until this crossover distance is reached. The method is most useful when the source to receiver distance is large compared to

the depth of the discontinuity. It is an excellent technique for obtaining interval velocities to shallow depths on land. It will not, however, reveal a low velocity layer. Since marine sediments often have speeds lower than the overlying water, conventional refraction techniques will not sample the surface of the deep ocean floor. For greater sediment depths, the refraction record will be dominated by the reflections unless the offset distance is large compared to the depth below the water surface or the velocity contrasts are small (Kennet and Orcutt, 1976).

The interpretation of head wave returns is based on the assumption of isovelocity plane layers. If the planes are dipping, profiles in two directions are required for correct interpretation. If the layer velocity is an increasing function of depth, then the travel path between source and discontinuity will be curved. Analysis in such a case is possible (Grant and West, 1965). However, it is not always possible to differentiate between a straight line head wave record and one that is slightly curved due to a moderate velocity gradient (Kenneth and Orcutt, 1976).

It is theoretically possible to use curved path refractions to determine the velocity profile within a single layer with a positive velocity gradient (Hanna, 1973).

However, refractions near grazing incidence are hard to separate from the surface reflections. Houtz (1978) presents a method for travel time inversion of water multiple refractions that is useful in certain shallow water environments and postulates that attenuation can also be successfully measured. Case studies show that the technique is not reliable at sediment depths of less than 200 m.

Shear wave reflection and refraction profiles are similar to compressional wave records (Jolly, 1956). A simple traction source as discussed above is adequate for near-surface records on land. Multichannel shear wave seismograms comparable in quality to compressional wave profiles can be obtained with vibrator arrays as sources. The method however is not commonly used. It is also possible to observe shear wave events that arise from compressional wave conversion at an interface. Ricker and Lynn (1950) delineated subsurface structure from observations of waves that traveled as compressional waves to the interface and returned as shear waves after reflection.

Since transverse oscillations are not supported by water, shear wave determinations from marine profiles must be made on the basis of converted waves. Compressional wave arrivals that travel as shear waves in the ocean

floor have been observed and verified (Helmberger and Morris, 1970). Recent reports have studied the interpretative possibilities of these events (Tatham and Stoffa, 1976; Wood, 1978). However, they have not yet proven useful for the determination of sediment properties.

The reflection coefficient of marine sediments as a function of incident angle can be computed from theoretical models. A detailed match with observations is possible only when finite sediment rigidity is assumed. Although the agreement is often excellent, the inversion of the process to infer sediment properties from synthetic records is expensive and inefficient as well as non-unique (Kennett, 1976).

Compressional Wave Measurements

Although the present research is mainly concerned with shear wave propagation, it is necessary to review briefly the established features of compressional wave propagation in porous media in order to understand restrictions placed upon the various theoretical models that include both types of waves.

Speeds

The absolute value of the compressional wave speed in a given medium depends upon the elastic moduli, particularly on the compressibility. Porous sedimentary rocks have speeds ranging from roughly 3,000 to 8,000 m/sec at zero confining pressure (Gregory, 1975). Unconsolidated, water saturated sands have typical speeds of approximately 1,700 m/sec. Water itself has a compressional wave speed near 1,500 m/sec. High porosity saturated clays have been found to have speeds a few percent lower than water. Uncompacted dry sands have speeds as low as 100 m/sec.

Once typical values of compressional wave speed have been established for the various media, the variation of the speed with a change of one or more parameters can be studied. Parameters investigated in the literature include pore fluid, frequency, grain size, porosity, density, pressure, and temperature.

The variation in speed caused by a change in pore fluid has been of considerable interest to the petroleum industry. Several of the references cited in this paper, e.g., Wyllie et al. (1962), include measurements with various organic liquids. The observed speeds depend both on

the density and compressibility of the fluids (Brown and Korringa, 1975). In general, only results for water, including brine, and air or other gases will be reviewed here. The results for water are most applicable for natural unconsolidated marine sediments. Results for dry materials are included for comparison of theoretical predictions attendant upon liquid saturation. Three-phase systems, that is, a combination of gas and liquid in the pores, have also been extensively studied but will not be considered in the present paper. The introduction of even small amounts of air into an otherwise saturated sediment can cause pronounced changes in acoustic propagation.

There is little evidence for compressional wave dispersion in either dry or saturated porous materials. Schmidt (1954) found a constant longitudinal speed for dry sand samples from 30 to 500 Hz. His resolution appears to have been approximately 10 percent of his reported speeds. Hunter et al. (1961) measured compressional wave speeds in three well sorted dry sands. They note a maximum deviation of 4 percent from the mean value for measurements from 7 to 73 kHz. Neither Nolle et al. (1963) nor McLeroy and DeLoach (1968) report any variation of compressional wave speed for respective ranges of 400 to 1,000 kHz in

saturated sands and 15 to 1,500 kHz in natural marine sediments. However, neither paper presents the original data nor resolution limits. Hampton (1967) reports a change of 4 to 6 percent of the velocity of water in fine grained saturated sediments between 3 and 200 kHz. Hamilton (1972) was unable to measure dispersion in situ over the narrow range of 3.5 to 14 kHz.

Grain size appears to have little effect on the compressional wave speed. Hunter et al. (1961) noted a slight increase in speed with an increase in particle size for three samples of dry sand subject to a slight frame pressure. Wyllie et al. (1956) found a constant speed of 1,850 m/sec for seven samples of saturated glass beads ranging in size from .028 to .6 mm. Nolle et al. (1963) observed no change in a compressional wave speed of 1,740 m/sec for four samples of well sorted sand with different mean diameters.

In the above studies, the porosity was essentially constant regardless of the grain size. This is expected for uniform spherical particles such as glass beads since the volume of a sphere inscribed in a cube remains in constant proportion to the volume of the cube regardless of the sphere radius. Rogers and Head (1961) have shown that

the porosity of natural sands is similarly independent of grain size for well sorted samples. However, differences in porosity with grain size are observed in natural sediments due to differences in compaction, sorting, and grain shape.

Sutton et al. (1957) present an empirical formula for sound speeds taken from cores that includes grain size, porosity, and percent carbonate. The coefficient of the porosity term is an order of magnitude greater than that of the grain size. The relative amount of carbonate is a minor correction. Brandt (1959) compares the influence of various parameters on compressional wave speed and concludes on the basis of data presented by Hamilton et al. (1956) that sediment porosity is the most important factor affecting velocities in water saturated sands. Akal (1972) plots 8,287 values of compressional wave speed for marine sediments and finds a range of velocities relative to water from 1.30 to .95 for porosities from .25 to .90. He concludes that not only is porosity the most important factor influencing the speed but also that variations in the density of natural sediments are closely correlated to the porosity. Most of 15,124 samples lay between closely spaced lines representing linear variations of density with

porosity based on grain densities of 2.60 and 2.75 g/cm^3. The density of the common minerals are within this range (Hurlbut, 1971).

The above reports compare velocity variations with porosity among sediment samples of different composition. It is also possible to study porosity changes within a single specimen. This removes the effects of grain size or shape. Hardin and Richart (1963) studied porosity variations in several sorted sands with different packings. Shirley (1977) reports speed variations with porosity for three different sands, including two of the samples considered in the present study. He notes a uniform change in speed from 1,750 to 1,680 m/sec for a porosity change from .38 to .45 in a fine Panama City beach sand.

Velocity-density relationships are often given as a means of determining acoustic impedance (Hamilton, 1978). However, since porosity and density are linearly related for unconsolidated marine sediments, the two parameters represent essentially the same variable.

Compaction of a porous material by application of external pressure can result in significant changes of porosity, particularly for clays, which influence the density and wave speed. However, external stresses also influence

the elastic moduli of the sediment components. This leads to velocity variations independent of the porosity. Sands subject to pressures encountered at shallow depths show little change in porosity with compaction (Hamilton, 1976c).

The incremental change in compressional wave speed for a given change in pressure has been observed to decrease as the total pressure in increased. This change is often represented by a simple power equation, $V = kP^n$. However, there is considerable variation in the value of the exponent.

Laughton (1957) found the compressional wave speed for fine grained marine sediments to vary approximately as the square root of the frame pressure to 100 MPa with atmospheric pore pressure (1 MPa=10^6 N/m^2=145 psi). He found only minor changes of speed with changes in fluid pressure to 40 MPa at constant frame pressure. Hamilton (1976c) quotes a value of n = .013 supplied by Shell Development Company for longitudinal waves in fine St. Peter's sand from .14 to 2.8 MPa. Domenico (1977) found the compressional wave speed in brine saturated Ottawa sand and glass beads to be proportional to the .056 power of differential pressure to 35 MPa. This represents a change for the Ottawa sand from 1,910 m/sec at 2.8 MPa to 2,220 m/sec

at 35 MPa. Elliott and Wiley (1975) present similar data for a coarser Ottawa sand saturated with distilled water. They exerted pressures from 7 to 63 MPa. Their speeds are noticeably higher than Domenico's at the same pressure. However, their porosities were lower due to prior compaction. Elliott and Wiley do not fit a curve to their data, but an exponent of approximately .06 seems to satisfy the data. The discrepancy between the minor variation of speed with pressure in sand and the large change in fine sediments found by Laughton can be attributed to a change in porosity in Laughton's measurements.

The variation of compressional wave speed with pressure is greater in dry than in saturated sands. The difference in speed between dry and saturated samples is therefore most pronounced at low pressures. Gardner et al. (1964), Hamilton (1976c), and Domenico (1977) all report that the speed for dry sands and glass beads varies as the 1/4 power of the differential pressure. Schmidt (1954) was able to measure a change in longitudinal velocity from 105 to 170 m/sec presumably caused by a change in static pressure due to an increase in sand thickness from 3 to 11 cm. He also gives values of 98 and 113 m/sec respectively for dry glass bead samples 3 and 5 cm in height. Part of this

change may, however, be caused by porosity changes induced by the boundaries of the experiment. Both Wylie et al. (1956) and Hunter et al. (1961) found the speed in pulse experiments to vary until the distance between transducer faces was larger than approximately 100 grain diameters. Wylie et al. estimate a speed of 400 m/sec for dry glass beads loaded only by self-weight. When water saturated, the same beads had a velocity of 1,850 m/sec. The difference is 80 percent of the saturated speed. For similar beads under pressure, Domenico gives values which differ by 60 percent at 2.8 MPa to 30 percent at 35 MPa.

The pronounced difference between dry and saturated velocities at low pressures is not unique to unconsolidated materials. The same behavior to a lesser degree has been observed in low porosity rocks (King, 1966; Nur and Simmons, 1969).

In situ measurements relate velocities to depth of overburden. An analysis of well data by Faust (1951) indicated a variation in speed as the 1/6 power of the depth and the duration of burial for sands and shale. The age can be replaced by a formation resistivity that depends on porosity (Grant and West, 1965). The velocity is not a simple function of depth because lithification depends on

time. White and Sengbush (1953) note a smooth increase in speed with depth in surface sands to the top of the water table that is consistent with a variation proportional to the 1/6 power. They measured a horizontal compressional wave velocity at the surface of 300 m/sec.

An accurate determination of a similar velocity profile with depth in natural marine sediments is lacking. Normally, interval velocities from 50 to 100 m below the sediment surface are combined with surface measurements or estimates to project a linear velocity gradient (Nafe and Drake, 1957; Hamilton et al., 1977). The method is sufficient to distinguish between different sediment environments, but is unable to determine a detailed relationship between overburden pressure and velocity. Normal gradients are approximately 1 to 2 m/sec/m. These have been confirmed for the first few meters by direct measurements made while coring (Shirley and Bell, 1978).

Precise comparison of compressional wave velocities in saturated sediments requires specification of the temperature (Brandt, 1960). Shumway (1958) measured longitudinal speeds in five sediments as a function of temperature and found the variation to be proportional to that in water alone. Values for a quartz sand ranged from

1,600 m/sec at 0°C to 1,800 m/sec at 70°C. A decrease of velocity with an increase of temperature is sometimes observed in rocks. Timur (1977) measured the effect of temperature on compressional wave velocity in two sandstones and seven carbonates saturated with brine and subjected to substantial pore and frame pressures. He found an average decrease of 1.7 percent per 100°C temperature change. For Boise sandstone the decrease was from 3,350 m/sec at 20° to 3,260 m/sec at 120°. The decrease was postulated to arise from development of microcracks within the rock caused by differential expansion of the rock matrix.

Attenuation

The variation of compressional wave attenuation with frequency, as a first approximation, can be expressed by a simple power equation $\alpha = kf^n$. For fine grained sediments and rocks over a wide frequency range, $n \simeq 1$. For well sorted sands, there is a variation in reported values of n which suggests that a simple power law may be an oversimplification.

Wood and Weston (1964) measured attenuation between probes in tidal mud flats. They found the attenuation to vary as f^1 from 4 to 50 kHz. Cole (1965) compared

observed reflection returns from in situ marine sediments with theoretical predictions of bottom loss. He found that an assumed f^1 dependence of attenuation of frequency gave a reasonable fit between .1 and 1 Khz. Bennet (1967) found attenuation proportional to f^1 between 40 and 900 Hz by comparison of surface and subsurface reflection returns from a natural wedge of sediments. Tullos and Reid (1969) obtained a linear dependence from 50 to 400 Hz from down-hold shooting through layers of sediment. McLeroy and DeLoach (1968) measured attenuation in a number of natural sediment samples in the laboratory and found n = 1 from 15 to 1,500 kHz. McCann and McCann (1969) give f^1 for mud and $f^{1.26}$ for sand between 5 and 50 Hz. Nolle et al. (1963) found an $f^{1/2}$ dependence between 400 and 1,000 kHz in four well sorted sands. Hampton (1967) gives $f^{1.37}$ for clay and $f^{1/2}$ for sand from 4 to 600 kHz. Busby and Richardson (1957) found the variation of attenuation with frequency to change with grain size for several samples of sand and glass beads from .5 to 3 MHz. The beads exhibited an f^4 dependence. For these frequencies, the wavelength becomes comparable to the grain size. Kuster and Toksoz (1974) found that a linear dependence of attenuation on frequency was inadequate for measurements in suspensions of glass and plastic beads in various liquids from 100 to 500 kHz.

The values given above pertain to measurements in specific samples over a fairly wide frequency range. Numerous measurements of attenuation at discrete frequencies in different sediment samples are available in the literature, e.g., Hamilton et al. (1956), Shumway (1960). Hamilton (1972) has compiled the data available from numerous sources and presented the result as a graph of attenuation versus frequency for unconsolidated sediments from approximately 1 Hz to 1 MHz. Even though the measurements represent sediments with a wide range of porosity and grain sizes, a definite trend in the data exists. This trend is adequately represented as an f^1 dependence of attenuation on frequency. However, measurements in a single sediment, such as those above, can show considerable deviation from f^1 behavior over approximately a decade of frequency and still fall within the scatter of the overall data. The detailed behavior of attenuation with frequency over several decades is still not established, particularly for sand size particles. A recent version of Hamilton's graph (Hamilton, 1976a) is reproduced in Fig. II-2.

Wyllie et al. (1962) summarize the attenuation data then available for consolidated sediments. Included are measurements by Born (1941) from 1 to 4 kHz which imply

a constant log decrement for extensional vibrations, and measurements by McDonal et al. (1958) in Pierre shale that yield an f^1 dependence from 1 to 600 Hz. Attwell and Ramana (1966) present a plot similar to Fig. II-2 for measurements in rock samples. There is a single trend from 1 to 10^7 Hz in agreement with a linear dependence of attenuation with frequency. Considerable scatter exists, however, when different rock samples are compared. Recently, Toksoz et al. (1978) report a linear increase of attenuation with frequency from .1 to 1.5 MHz for both dry and saturated rock samples.

Studies of compressional wave attenuation versus frequency in dry unconsolidated materials are not prevalent. Kottonski and Malechi (1958) measured attenuation to vary as $f^{.23}$ from 300 dB/m at 30 kHz to 1,650 dB/m at 90 kHz. Nyborg et al. (1950) give values in sand at 10, 18, and 26 kHz which are not adequately represented by a simple power equation. Pilbeam and Vaisnys (1973) found constant Q values from 1 to 20 kHz for glass bead samples at low confining pressure.

The expected magnitude of compressional wave attenuation in surficial marine sediments can be obtained from the data shown in Fig. II-2. Hamilton (1976b)

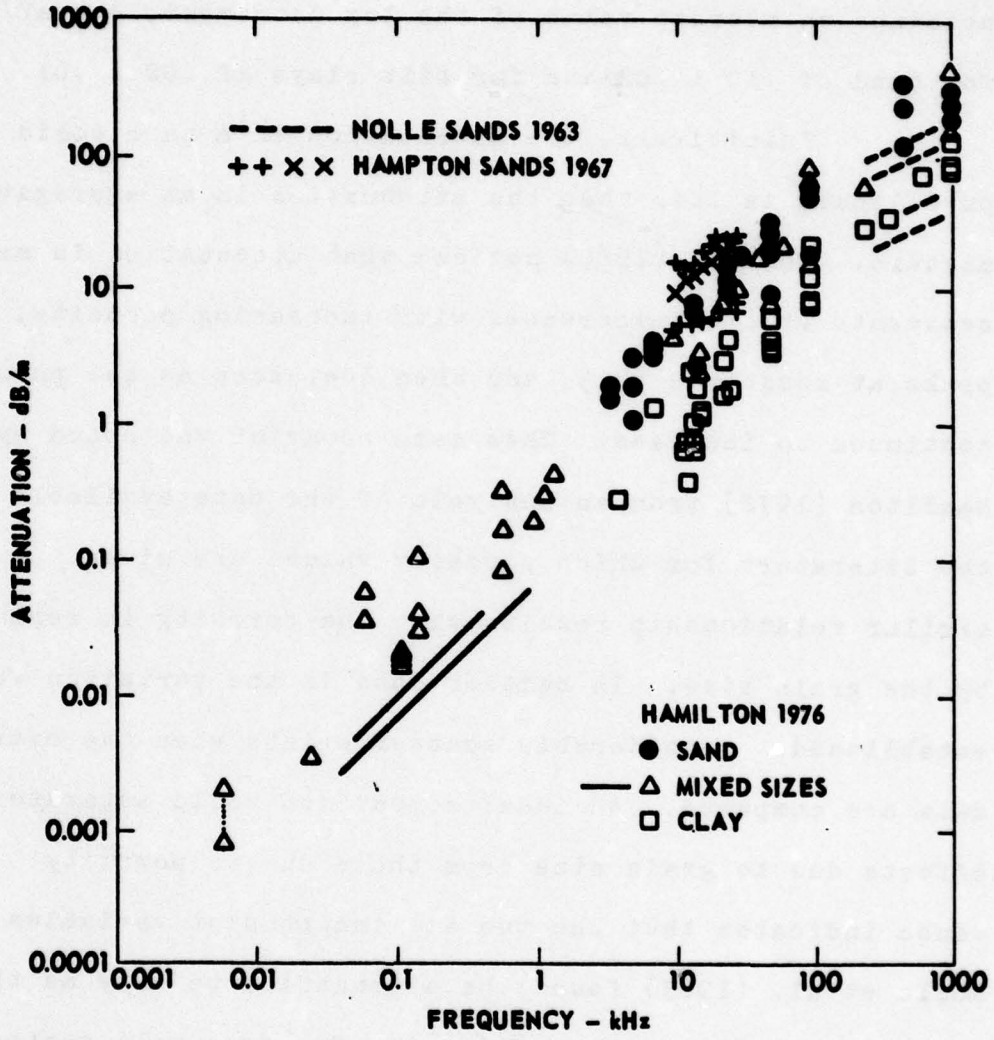

FIGURE II-2
COMPRESSIONAL WAVE ATTENUATION versus FREQUENCY
(after Hamilton 1976)

obtained an average value of the log decrement, $\delta = aV/f$, for sand of .10 ± .03 and for silt clays of .02 ± .01.

Intuitively, the attenuation in a pure solid or pure liquid is less than the attenuation in an aggregate mixture. Shumway (1960) noticed that attenuation in marine sediments at first increases with increasing porosity, peaks at roughly $\beta = .5$, and then decreases as the porosity continues to increase. This same behavior was noted by Hamilton (1972) from an analysis of the data available in the literature for which porosity values are given. A similar relationship results when the porosity is replaced by the grain size. In neither case is the variation well established. Considerable scatter exists when the overall data are compared. An ideal comparison would separate the effects due to grain size from those due to porosity. Evidence indicates that the two are independent variables. Nolle et al. (1963) found the attenuation to vary as the square root of the mean grain size for four well sorted sands having essentially the same porosity. Compressional wave attenuation has also been reported to decrease with gravitational compaction in laboratory sediments (Shirley and Bell, 1978), that is, for a constant grain size and decreasing porosity.

Compared with the study of pressure effects on compressional wave speed, there is little data available on attenuation versus pressure in unconsolidated materials. Hunter et al. (1961) found the attenuation in dry sand to decrease with an increase of frame pressure. Hardin and Richard (1963) found the decrement for longitudinal vibrations to decrease with increasing confining pressure for both dry and saturated samples of Ottawa sand and glass beads. The damping was greater in the saturated samples than in the dry. The measured decrement for the dry materials showed considerable variation with both pressure and amplitude of vibration. Gardner et al. (1964) found the log decrement in dry sands to decrease as the 1/6 power of the overburden pressure. Pilbeam and Vaisnys (1973) found the damping in samples of dry glass beads to decrease with increasing confining pressure from approximately zero to one atmosphere as the .3 to .8 power of the pressure.

Toksoz et al. (1978) and Johnson and Toksoz (1978) have studied compressional wave attenuation versus pressure in porous rocks. They found the attenuation to decrease with increasing differential pressure for both dry and saturated samples. The attenuation was greater in saturated than in dry specimens.

Shear Wave Results

Speeds

The available data on shear wave speeds in fully saturated unconsolidated sediments at small confining pressure are sparse, both for in situ and laboratory measurements. Warrick (1974) measured a speed of 90 m/sec near the top of a bore hole in a mud flat. Shirley and Anderson (1975) observed a smooth increase in speeds from 8 to 24 m/sec in kaolinite clay which was allowed to settle under the influence of gravity and interparticle forces. Shirley (1977) reports speeds of 60 to 110 m/sec, depending on porosity, for three sand samples. Shirley and Bell (1978) measured speeds of 100, 40, and 16 m/sec, respectively, for sand, silt, and clay with probes 9 cm below the sediment surface. The speeds were observed to vary as much as 50 percent with porosity changes affected by stirring the sediments.

Davies (1965) calculated shear wave speeds from Stoneley waves excited on the ocean floor by explosive charges. The speeds varied from 50 to 190 m/sec with depth to 16 m. Hamilton et al. (1970) also obtained in situ shear wave speeds from Stoneley wave observations. They

obtained speeds of approximately 100 m/sec in silt clays at an effective depth of 2 m. Their results in sands varied from 100 to 200 m/sec with an increase in effective depth from 2.2 to 3.4 m.

As can be inferred from the data given above, shear wave speeds in unconsolidated materials are very dependent upon the compaction, both in terms of porosity changes and overburden pressure. Schmidt (1954) noted a change in speed from 76 to 98 to 120 m/sec for dry sand samples 3.2, 6.4 and 11 cm in height. Laughton (1957) measured speeds in dry red clay of 1,370 and 1,110 m/sec transverse and parallel to the axis of compaction at 136 MPa. Hardin and Richart (1963) measured shear wave speeds in both dry and saturated sands and silts subjected to torsional vibrations at confining pressures from 1.4 to 70 MPa. They found the shear wave speed to vary as the 1/4 power of confining pressure for both dry and saturated sands at relatively high pressures (>14 MPa). At lower pressures the variation was between 1/2 and 1/4 powers depending on the sample. The total variation for saturated Ottawa sand was from approximately 90 to 340 m/sec. Pilbeam and Vaisnys (1973) found the speed in dry glass beads to vary as the 1/3 power of pressure between 0 and .1 MPa. The samples were evacuated such that the effective

confining pressure was exerted by the atmosphere. Hamilton (1976c) reviewed torsional vibration data obtained from Shell Development Company for dry and brine saturated St. Peters sand. The shear wave speed was observed to vary as the 1/4 power of the differential pressure from approximately 280 m/sec at 70 kPa to 900 m/sec at 7 MPa. Domenico (1977) obtained a similar 1/4 power variation of shear wave speed with differential pressures from 3 to 35 MPa for both Ottawa sand and glass beads.

Hamilton (1976c) recommends a depth exponent of 1/4 for prediction of shear wave velocities in sand based on available in situ data. There is, however, considerable scatter in the data with bounds of 1/3 to 1/6 suggested by Hamilton. Much of the data reviewed by Hamilton was obtained from land measurements. In some cases the water table was less than 2 m below the surface; in others it was beyond the depth of the measurements. Since the measurements were obtained in natural soils in the field, it must be assumed that the sediments above the water table exhibited various degrees of partial saturation.

The review of compressional wave propagation in porous media showed a significant difference between compressional wave speeds in dry and saturated materials.

Three-phase systems were not considered, but data in the literature indicate that major changes in propagation occur when only small amounts of either gas or liquid are added to an otherwise single phase pore fluid (e.g., Gardner et al., 1964). In particular, the variation of attenuation with frequency is definitely nonlinear (Anderson, 1974). In comparison, shear wave speeds show smaller variations with percent saturation. Hardin and Richart (1963) found that the shear modulus for mature sands decreases as much as 15 percent with increasing saturation, with most of the change occurring at the onset of liquid introduction. Angular sands showed smaller variations. Domenico (1977) reports a change in speed from 691 m/sec at total brine saturation to 640 m/sec at total gas saturation for a differential pressure of 7 MPa. The decrease is smooth for intermediate saturations. The error introduced in Hamilton's analysis by consideration of partially saturated sands is probably smaller than the scatter in the data. However, care must be exercised in applying the data to other situations.

In each of the above studies, i.e., Hardin and Richart (1963), Hamilton (1976c), and Domenico (1977), the shear wave speed was always less in the saturated than in

the dry material. The same general behavior is found in consolidated samples although at high differential pressure the closure of microcracks in rocks sometimes leads to a greater speed in the dry material (Wyllie et al., 1962; Gregory, 1976; Johnson and Toksoz, 1978).

The effects of grain size and shape on shear wave speeds were studied by Hardin and Richart (1963). They found the velocity to be independent of grain size and gradation for sands except for associated changes in porosity. Results for fine grained silts were dependent on time and precompression. Angular sands had higher speeds than rounded sands. This is also supported by Pilbeam and Vaisnys (1973).

The variation of shear wave speed with frequency in unconsolidated sediments has received little attention. Schmidt (1954) found no evidence of dispersion in dry samples of sand and glass beads between 50 and 200 Hz. His resolution appears to have been within 10 percent. Kudo and Shima (1970) measured a constant phase velocity between 30 and 90 Hz in soil. Pilbeam and Vaisinys (1973) found no variation in speeds derived from torsional vibrations of dry glass beads between 1-20 kHz.

Shear wave velocity measurements are available over a larger frequency range in rocks. Simmons (1964) compared speeds obtained from pulse experiments at 1-5 MHz with torsional velocities measured by Birch and Bancroft (1938) in the same rock samples at a few kHz. The results differed at most by 2 percent. Peselnick and Outerbridge (1961) used three different experimental techniques to measure shear wave velocities in a sample of Solenhofen limestone. No dispersion was found between 3 Hz and 10 MHz.

Attenuation

Damping in unconsolidated materials has been found to depend on the confining pressure, the amplitude of vibration, the frequency, the degree of saturation, and the porosity. There are, however, much less data available on shear wave damping than for compressional waves.

Schmidt (1954) found the shear wave decrement to decrease with an increase of sample length for dry sands. Hardin and Richart (1963) found the decrement of torsional vibrations to decrease with an increase of confining pressure for both dry and saturated samples. However, they also found the decrement to decrease as the 1/4 power of

decreasing vibration amplitude. The amplitude curves were not parallel for different confining pressures. Gardner et al. (1964) found the torsional decrements for dry sand and glass beads to decrease as the 1/6 power of the pressure below 7 MPa and to approach a constant value above 35 MPa. Their measurements were independent of amplitude at the levels used. Pilbeam and Vaisnys (1973) found the torsional decrements for several sizes of dry glass beads to vary between the .3 and .8 power of confining pressure below .1 MPa. Their results were independent of vibration amplitudes differing by a power of 10.

Schmidt (1954) found that the damping was independent of frequency for dry sands between 100 and 2,000 Hz. Barkan (1962) reports a constant damping ratio for soils between .6 and 1.8 kHz. Kudo and Shima (1970) made borehole measurements of attenuation with a surface shear wave source. They report that the attenuation is approximately proportional to the first power of the frequency from 10 to 90 Hz. Their results are reproduced in Fig. II-3. A linear variation with frequency is a better fit for fine grained soils than for the sand. The materials should be considered as partially saturated. Also, since the measurements were made between the surface and a

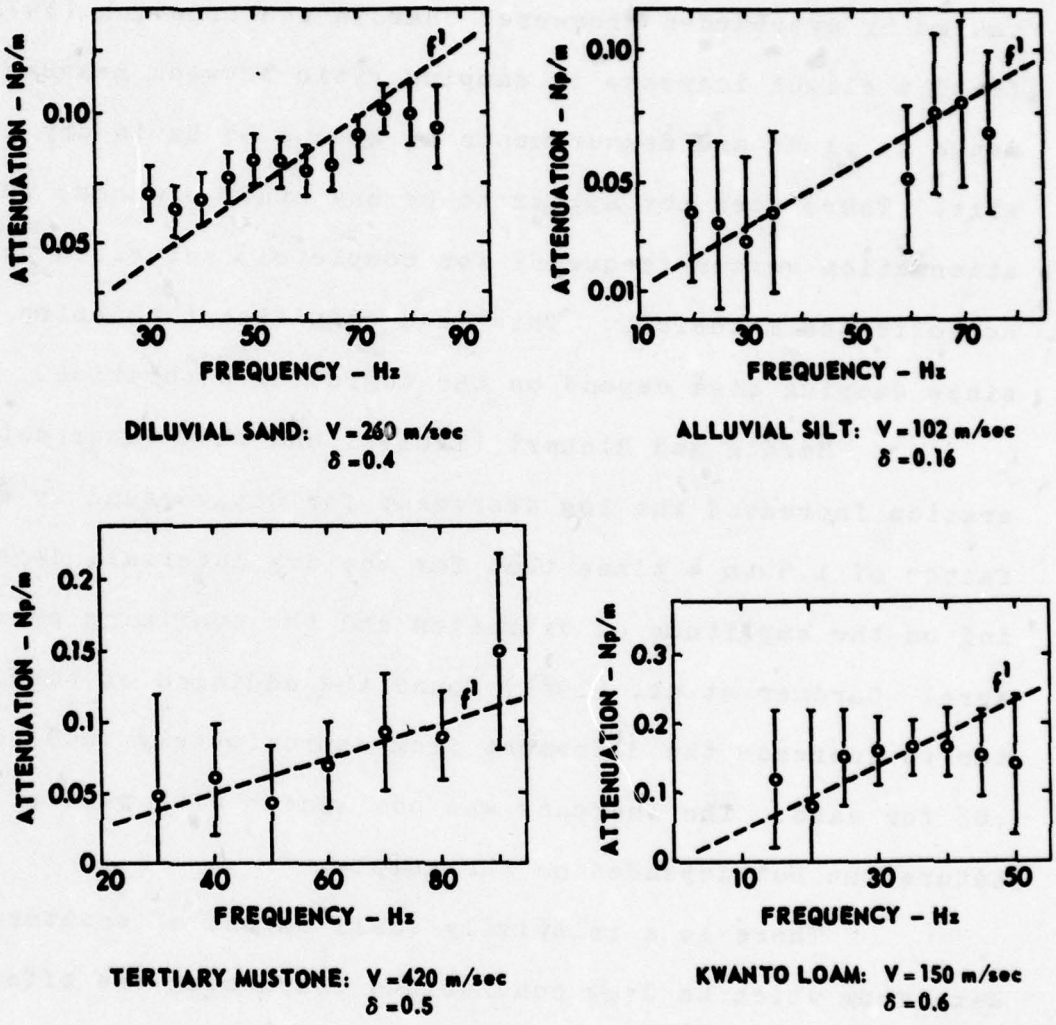

FIGURE II-3
INSITU MEASUREMENTS OF SHEAR WAVE ATTENUATION versus FREQUENCY
(after Kudo and Shima 1970)

depth of 40 m, the results are averages over any changes caused by overburden pressure. Hardin and Drnevich (1972) found a slight increase in damping ratio between measurements at .1 Hz and measurements at 25 and 38 Hz in dry silt. There does not appear to be any study of shear wave attenuation versus frequency for completely saturated unconsolidated materials. This is a significant omission since damping does depend on the degree of saturation.

Hardin and Richart (1963) found that water saturation increased the log decrement for Ottawa sand by a factor of 1.5 to 4 times that for the dry material, depending on the amplitude of vibration and the confining pressure. Gardner et al. (1964) found the addition of pore water to increase the decrement from approximately .005 to .06 for sand. The increase was not linear with partial saturation but depended on the sample.

There is a relatively small amount of scattered data from which to draw conclusions concerning the effects of grain size and porosity on shear wave damping. Hamilton (1976b) reviews the available literature and concludes that most values of the log decrement corresponding to near-surface pressures are between .1 and .6 for both sands and clays. He recommends approximate values for saturated sand

of .30 ± .15 and for saturated silt-clays of .2 ± .1. That is, decrements in high porosity, fine grained materials appear to be slightly lower than in relatively low porosity, coarser sands. Gardner et al. (1964) found the damping to be independent of grain size and porosity for sand. Pilbeam and Vaisnys (1973) note a slight change in log decrement for different size dry glass beads. Hardin and Drnevich (1972) found a decrease in damping ratio with an increase in porosity for undisturbed cohesive soils.

Shear wave attenuation in unconsolidated sediments may be compared with measurements obtained in consolidated materials. In situ shear wave attenuation measurements in Pierre shale (McDonald et al., 1958) were approximately linear with frequency from 25 to 150 Hz although a definite change in slope was apparent from 100 to 150 Hz. Gardner et al. (1967) obtained measurements of the damping in dry Solenhofen limestone from 10 Hz to 20 kHz. They found a constant decrement of .0043 for all frequencies. They compared this with a value of .005 at 3.59 Hz (Peselnick and Outerbridge, 1961) and of .0167 at 1 MHz (Peselnick and Zietz, 1959) obtained in similar samples. Toksoz et al. (1978) and Johnson and Toksoz (1978) report that shear wave attenuation is linearly proportional to

frequency from approximately 100 kHz to 1 MHz in both dry and saturated samples of sandstone and limestone. The attenuation decreased with increasing differential pressure and was smaller when the rocks were dry rather than saturated.

Summary of Known Properties

The following salient features of acoustic propagation in porous media may be stated.

1. Dispersion of either compressional or shear waves, if present, is small.

2. Compressional wave speeds in saturated materials are substantially higher than in dry materials. Shear wave speeds in saturated materials are slightly lower than in dry materials.

3. Compressional wave attenuation varies roughly as the first power of the frequency over a wide frequency range, although for sands the variation may differ somewhat over narrow frequency bands. Shear wave attenuation appears to follow the same pattern. There is, however, a lack of shear wave data, particularly for unconsolidated, saturated media.

4. Both compressional and shear wave speeds increase with increasing effective pressure, with a corresponding decrease in attenuation. Shear wave parameters appear to be more sensitive to small changes in stress at low pressures than do the compressional wave properties.

C H A P T E R I I I

THEORETICAL BACKGROUND

General Review

Numerous attempts have been made to fit the above observations into the framework of a mathematical theory. These attempts can be divided into two broad categories depending upon the extent a porous medium is considered to be homogeneous. One approach models the medium as a continuum with viscoelastic properties pertaining only to the bulk material. The system can be described by complex moduli and creep or relaxation functions chosen to fit empirical relationships. A second approach assumes a definite loss mechanism based on the interactions of the constituents of the material. This allows the effects of observable macroscopic properties of the system, such as porosity or fluid compressibility, to be predicted by the model.

Perhaps the simplest viscoelastic model of a continuum is obtained by modeling the substance as the parallel addition of an ideal spring and an ideal dashpot. The combination is known as a Voigt element (Bland, 1960).

Mathematically, this adds a term proportional to the rate of strain to the elastic, or Hookean, stress-strain relation. The resulting equation of motion is linear and contains two constants, the normal elastic modulus and a coefficient of viscosity. A harmonic solution at low frequencies yields attenuation proportional to the square of the frequency with a velocity independent of frequency. At high frequencies both the attenuation and velocity become proportional to the square root of the frequency (White, 1965; Grant and West, 1965).

The response of a Voigt element to a constant stress is called a creep function since, in general, the extension, or strain, is a function of time. The ratio of the coefficient of viscosity and the elastic modulus represents the time required for the creep function to reach a certain proportion of its final value. This ratio is known as the retardation time (Bland, 1960). Thus the coefficient of viscosity may be replaced by a constant with units of time. The simple Voigt model contains one such time constant in addition to the elastic modulus.

If the Voigt model is modified by an additional term proportional to the rate of stress, then two time constants are required. Proper selection of these constants

allowed Horton (1959) to successfully apply such a model to the attenuation data of the Pierre shale supplied by McDonal et al. (1958). Four time constants and two moduli were required to fit both the compressional and shear wave data over the given frequency range. However, an approximately linear variation of attenuation with frequency over an extended frequency range would have required the addition of higher order time derivatives to the stress strain equation. These in turn would have introduced a predicted dispersion not in accord with the general observations (White, 1965).

If the number of Voigt elements added to the viscoelastic model increases indefinitely, then it is possible to define a distribution function of retardation times. Chae (1968) assumed a distribution function for the viscoelastic properties of sand which gives a reasonable fit to the shear wave data of Kudo and Shima (1970). The latter authors, however, were able to obtain slightly better agreement by assuming a different distribution function. Neither predicts a strictly constant log decrement or phase velocity. Indeed, it has been shown (Collins and Lee, 1956; Knopoff and MacDonald, 1958) that a constant

decrement and phase velocity for all frequencies cannot be obtained by a linear model.

White (1965) reviews briefly models which contain nonlinear stress-strain relations. However, as emphasized by Collins and Lee (1956), the available data are not sufficiently precise to require an exact first power dependence of attenuation on frequency, and therefore linear models that can approximate the observed behavior over a finite frequency band should not be arbitrarily discarded. Indeed, a linear variation of shear wave attenuation with frequency for saturated unconsolidated media has not been adequately demonstrated.

A simple linear viscoelastic model that yields a constant phase velocity and log decrement in the limit of small damping is suggested by the schematic stress-strain diagram given in Fig. II-1. The area within the stress-strain curve is directly proportional to the damping ratio. If the stress-strain cycle defines a smooth curve, e.g., an ellipse, then the area is related to the ratio of the minor and major axes of the curve. A vector at an angle ϕ to the major axis allows this ratio to be expressed as the tangent of ϕ. Since the major axis defined the shear modulus, tan ϕ is mathematically equivalent to the ratio of the

imaginary and real parts of a complex shear modulus. That is, the damping is proportional to $\tan \phi = \mu'/\mu$ where $\bar{\mu} = \mu + i\mu'$. Thus a viscoelastic model results if the shear modulus is regarded as complex. If the damping is small, $|\bar{\mu}| \approx \mu$ and the frequency independent elastic expression for the velocity, $v = (\mu/\rho)^{1/2}$, is recovered.

The above model is favored by Hamilton (1976b) since it is able to satisfy the two main tenets of acoustic propagation in porous media, namely that dispersion is negligible and that attenuation varies linearly with frequency. Further, the model indicates how well the viscoelastic parameters can be approximated by the elastic equations. However, there is no provision for the determination of the real and imaginary parts of the complex modulus apart from direct measurement of the speed and attenuation in the bulk medium. A theory would display greater utility if these parameters could be estimated from the physical properties of the medium.

Three main mechanisms have been considered as probable causes of attenuation in porous materials. These are scattering, frictional forces at grain contacts, and viscous flow of pore fluid relative to the frame. The total observed attenuation is probably a combined effect of

all three mechanisms. However, under certain conditions, one or two mechanisms may dominate.

In a suspension, grain contacts are absent. Urick (1948) presents a formula for the attenuation in a suspension that includes both scattering from the individual particles and viscous loss due to relative motion of the particles and the liquid. At low frequencies, the viscous term predominates; at high frequencies, scattering makes the major contribution (Anderson, 1974). In a granular material, scattering is again important at high frequencies, that is, when the wavelength approaches the particle size. Plona and Tsang (1979) use scattering theory to predict that attenuation in a porous material is proportional to the cube of the grain size and the fourth power of the frequency. They present experimental confirmation in saturated glass beads at frequencies near 1 MHz. This same dependence was observed by Busby and Richardson (1957).

A necessary concept in the comparison of contact losses and viscous dissipation is the existence of a "frame." Wood (1930) developed a formula for compressional wave speed which related the individual compressiblities and densities of the constituents of a suspension to a bulk

compressibility and density. The relative contributions of the fluid and the particles depended on the porosity. The Wood equation correctly predicts that the speed in high porosity marine sediments will be lower than the speed in water (Anderson, 1974). However, predicted values are lower than observed values (Shirley and Bell, 1978). This can be attributed to a finite rigidity in the sediment that arises from the grain to grain contacts. This is not the rigidity of the material comprising the grains, which is quite high, nor the rigidity of the fluid, which has none. Rather, it is a property of the arrangement of the particles, that is, the frame.

Gassman (1951) derived expressions for the bulk moduli of a porous material in terms of the moduli of the fluid, the grains, and the frame. The formula reduces to that of Wood (1930) when the frame moduli are zero. Gassman suggested that the frame moduli could be measured in the absence of the pore fluid. The theoretical characterization of the frame is difficult.

Gassman studied the contact areas of an hexagonal array of perfect spheres under the influence of self-weight. Tangential stress was neglected. He predicted that the speed should vary as the 1/6 power of the depth.

Other authors have considered different packings of idealized spheres. White (1965) reviews much of this work. Walton (1975, 1977) calculates the moduli of a fluid saturated cubic array. He predicts that the velocity in the dry material should vary as the 1/3 power of the depth at shallow depths and as the 1/6 power at larger depths. He also predicts the existence of two compressional waves, one associated with the frame and one with the fluid.

Attenuation in the frame can be introduced through conjectural frictional forces at the grain contacts. White (1965) reviews the work, both theoretical and experimental, which has been done with arrays of spherical particles. He concludes that both static and dynamic friction must be considered in the displacement cycle if the predicted attenuation is to agree with experimental evidence. In consolidated materials, the possibility exists of friction between crack surfaces as well as at grain boundaries (Walsh, 1966). Johnston et al. (1978) review this subject. Although the important features of the frame attenuation can be predicted qualitatively, quantitative results are hampered by several unknown parameters. Therefore the relative importance of frame attenuation to viscous attenuation must be based on observation.

Numerical values of the attenuation due to relative movement of the fluid and frame can be calculated. Biot (1956a, 1956b) developed a general theory of acoustic propagation in porous media based on the earlier work of Zwikker and Kosten (1949) and Morse (1952). When no relative movement between frame and fluid exists, Biot's equations reduce to Gassman's (1951) formulation (Geertsma and Smith, 1961). When relative movement is allowed, the predictions depend upon frequency. At low frequencies, the flow in the pores is laminar, the speed is essentially constant, and the attenuation varies as the square of the frequency. At high frequencies, the flow pattern is complex, the speed is again approximately constant although different, and the attenuation varies as the square root of the frequency. At intermediate frequencies, a transition zone exists. The details of the transition depend upon the compressibility and viscosity of the fluid and the moduli and permeability of the frame. The theory assumes a narrow distribution of pore sizes.

The above observations apply to both the compressional wave and the shear wave. However, the theory also predicts the existence of a second dilational wave of low velocity and extremely high attenuation. This second type

of compressional wave has not been observed in liquid saturated porous media (Yew and Jogi, 1976). Even in materials where the viscous effect is expected to be large, the attenuation of the second wave is expected to make direct observation extremely difficult. It is conceivable, however, that the presence of the second wave could be deduced from a change in reflection coefficient with frequency since mode conversion should exist at a boundary. The second wave has been considered a prominent mechanism of energy loss in gas saturated acoustic absorbers (Zwikker and Kosten, 1949; Ferrero and Sacerdote, 1951).

The viscous interaction model correctly predicts that the compressional wave speed increases and the shear wave speed decreases with fluid saturation. However, the lack of experimental observations supporting a general f^2 or $f^{1/2}$ dependence of attenuation on frequency and the apparent lack of dispersion have been cited as evidence that viscous loss is of minor importance to overall sediment attenuation (Hamilton, 1972). Although such a conclusion may be correct, the available experimental data are inadequate to dismiss the theory in all cases.

Several factors must be considered when comparing the theoretical predictions with observations. First the

attenuation will be a combination of both the contact losses and the viscous term. The contact losses are difficult to calculate, but are known to exist since the attenuation does not vanish when the fluid is removed. Since the viscous attenuation depends on the permeability, the frame loss can be expected to dominate in low permeability clays and rocks. If the frame loss is linear with frequency, then, to first approximation, so will be the bulk attenuation. Second, the theory is based on a uniform pore size. If the sediment is poorly sorted, then the transition zone between the f^2 and $f^{1/2}$ dependence may extend over a wide band of frequencies. Third, only measurements in the same sample can be compared since permeability changes between slightly different particle sizes will obscure the predicted effects. A study in a single sand over an extended frequency range is lacking. However, as noted earlier, attenuation in well sorted sand samples has been observed to vary as $f^{1/2}$. An observation of the small amount of dispersion implied by the theory will require accurate measurements over a frequency band that includes the transition zone. Most measurements have been made at either very low or very high frequencies.

Biot (1962) recognized that losses due to the frame must be included in a general theory of acoustic propagation in porous media. He suggested that the elastic moduli be replaced by complex operators and outlined the form of possible distributions of retardation times. Stoll (1974, 1977) and Stoll and Bryan (1970) have made extensive quantitative studies based on the simplifying assumption that the operators can be approximated by complex constants independent of frequency. In effect, this adds a constant frame log decrement to the viscous loss.

Several authors have studied special aspects of the general viscous interaction model. Geertsma and Smit (1961), Deresiewicz and Rice (1962, 1964), and Horton (1978) have considered the effects of boundaries. Brutsaert (1963) has studied partially saturated systems. Smith and Greenhorn (1972, Smith et al., 1974) have considered thermal conductivity as well as viscous dissipation in a rigid frame. Mengi and McNiven (1977, 1978) have studied the response of porous media to a transient pulse and the influence of anisotrophy on acoustic wave shapes. Chase (1979) has applied the theory to saturated foam.

The next section presents a simplified derivation of the equations that govern shear wave propagation in

in porous media. The end result is equivalent to Stoll's (1977) formulation of the theory.

Viscous Loss Model

The displacement of a damped harmonic oscillation is given by

$$u = e^{i(\omega t - \bar{\ell} x)} , \qquad \text{III-1}$$

where Real $(\bar{\ell}) = \ell = \frac{1}{\lambda} = \frac{\omega}{v}$

Img $(\bar{\ell}) = \ell' = a$ (attenuation in nepers/unit distance) .

The elastic wave equation for shear waves, that is, displacements perpendicular to the direction of motion, is

$$\mu \frac{\partial^2 u_y}{\partial x^2} = \rho \frac{\partial^2 u_y}{\partial t^2} . \qquad \text{III-2}$$

Substitution of Eq. III-1 into Eq. III-2 yields

$$\mu \bar{\ell}^2 = \omega^2 \rho \qquad \text{III-3}$$

which, in the absence of dissipation, gives the familiar expression for the shear wave speed in terms of the shear modulus and the density,

$$v^2 = \mu/\rho \ . \qquad \text{III-4}$$

However, if Eq. III-3 is applied for $\ell' \neq 0$, then either μ or ρ, or both, must be considered as complex operators.

If μ is arbitrarily assigned an imaginary component, then Eq. III-3 implies

$$\mu = \rho V^2 \frac{(1-r^2)}{(1+r^2)^2} \ , \qquad \text{III-5}$$

$$\mu' = \rho V^2 \frac{2r}{(1+r^2)^2} \ , \qquad \text{III-6}$$

$$\delta = \frac{2\ aV}{\omega(1-r^2)} \ , \qquad \text{III-7}$$

where $r = aV/\omega$.

When the damping is small, $r^2 >> 1$ and Eqs. III-5 and III-7 reduce to

$$V^2 = \mu/\rho \ ,$$
$$\delta = aV/f \ . \qquad \text{III-8}$$

Equation III-8, which is independent of the frequency, corresponds to the elastic expression for the speed. Equation III-9 yields a constant log decrement if a varies as the first power of the frequency. This is the viscoelastic model favored by Hamilton (1976b). The equation given in

Fig. II-1 are valid when Eq. III-7 can be approximated by Eq. III-9.

The above expressions pertain to the properties of the bulk system. However, since water has vanishing rigidity, Gassman (1951) concluded that

$$\mu(\text{bulk}) = \mu(\text{frame}) \ . \qquad \text{III-10}$$

Rigorously, the properties of the frame are defined only in terms of the total sediment. However, it is often assumed in laboratory studies that values obtained from the dry sediment can be used to approximate the frame parameters when the sediment is saturated (e.g., Gardner et al., 1964; Gregory, 1976; Domenico, 1977). It is then possible to predict the effects of fluid saturation.

From small damping, application of Eq. III-10 to Eqs. III-8 and III-9 implies

$$V^2(\text{bulk}) = \frac{V^2(\text{frame})\rho(\text{frame})}{\rho(\text{bulk})} \qquad \text{III-11}$$

and

$$\delta(\text{bulk}) = \frac{V(\text{bulk})}{V(\text{frame})}\delta(\text{frame}) \ , \qquad \text{III-12}$$

where V(frame) is the shear speed in the dry material.

Equation III-11 states that the bulk shear speed is less than that of the frame in proportion to the square

root of the ratio of the two densities. Since dissipation has been introduced only through the imaginary part of the shear modulus, which, for the moment, is assumed equal for both the frame and the bulk sediment, the attenuation in each case is the same. This leads to Eq. III-12 which states that the bulk log decrement is less than that of the frame.

Data in the literature, in contradiction to Eq. III-12, indicate that attenuation increases with saturation. This implies an additional loss mechanism due to the presence of the fluid. Conceivably, the fluid could influence the frictional losses at the grain boundaries. That is, the frame loss in the dry sediment could be different from the frame loss in the saturated sediment. Alternatively, the additional attenuation could arise from viscous drag caused by the relative movement of the frame and the pore fluid.

Equation III-11 was obtained with the assumption that the entire mass of the fluid was perfectly coupled to the frame (Gassman's "closed system"). However, if the coupling is due to viscous interaction, then the possibility exists that only a portion of the fluid will move with the frame. The ρ(bulk) in Eq. III-11 should then be

replaced by an "effective density" which in general will depend upon the frequency. If the coupling is less than perfect, then a smaller change between the dry frame and the bulk velocities is indicated than that predicted by Eq. III-11. This has been observed by Hardin and Richart (1963) in Ottawa and crushed quartz sand and by Domenico (1977) in pressurized sand and glass bead specimens.

Ament (1953) obtained an equation for the effective density based on a simple consideration of viscous, incompressible flow. He found

$$\rho(\text{effective}) = \rho(\text{static}) + \frac{i\omega(K/\eta)(1-\beta)^2\beta\Delta^2}{\beta - i\omega(K/\eta)(1-\beta)(\rho_f+\beta\Delta)} \quad \text{III-13}$$

where K is the absolute permeability, η the fluid viscosity, β the porosity, and $\Delta = \rho_s - \rho_f$ is the difference between the grain and fluid densities.

The imaginary part of Eq. III-13 will introduce an additional attenuation due to the relative movement of fluid and frame that at first increases as the square of the frequency and then becomes almost constant. In order for the permeability measured at steady flow rates to be appropriate, Ament states that the frequency should be less than approximately

$$\omega = 2\eta/\rho_f a^2 \ ,$$

where a is the pore "size."

In a detailed study of relative frame-fluid movement caused by acoustic stress, Biot (1956b) obtained an expression similar to Eq. III-14. The assumption of Poiseuille flow is invalid above this frequency. He derived a complex correction factor for the viscosity that allows consideration of higher frequencies. His result, in terms of zero order Kelvin functions, was

$$F(\kappa) = \frac{1}{4} \frac{\kappa T(\kappa)}{1 + 2T(\kappa)i/\kappa} \ , \qquad \text{III-15}$$

where

$$T(\kappa) = \frac{\text{ber}'(\kappa) + i\text{bei}'(\kappa)}{\text{ber}(\kappa) + i\text{bei}(\kappa)} \qquad \text{III-16}$$

and

$$\kappa = a(\omega\rho_f/\eta)^{1/2} \ . \qquad \text{III-17}$$

The pore size a is strictly the radius of a circular tube. However, Biot found that the analytic solution for flow between two infinite parallel plates gave essentially the same correction if a was adjusted by a scale factor. Thus a may be regarded as a pore size parameter

that will vary with pore shape and sinuosity. However, a large variation in pore size is not allowed in the theoretical formulation.

Replacing the viscosity in Eq. 13 by $\eta F(\kappa)$ as defined in Eq. III-24 results in a viscous loss term that increases as the square of the frequency at lower frequencies and as the square root of the frequency at high frequencies.

With both $\bar{\mu}$ and $\bar{\rho}$ regarded as complex, Eq. III-3 gives

$$\ell^2 = \frac{\omega^2}{2} \frac{\rho\mu + \rho'\mu'}{\mu^2 + \mu'^2} \left[1 + \sqrt{1 + \left(\frac{\rho'\mu+\rho\mu'}{\rho\mu+\rho'\mu'} \right)^2} \right] \quad \text{III-18}$$

and

$$\ell'^2 = \frac{-\omega^2}{2} \frac{\rho\mu + \rho'\mu'}{\mu^2 + \mu'^2} \left[1 - \sqrt{1 + \left(\frac{\rho'\mu+\rho\mu'}{\rho\mu+\rho'\mu'} \right)^2} \right] . \quad \text{III-19}$$

If $\bar{\mu}$ is taken as an empirical complex constant determined by the frame, and $\bar{\rho}$ is Ament's effective density, Eq. III-13, modified by Biot's frequency correction to the viscosity, Eq. III-15, then, with the appropriate choice of parameters, Eqs. III-18 and III-19 are equivalent to Stoll's (1978) application of Biot's theory for shear wave propagation in porous media. This is not unexpected

since Geersma and Smit (1961) showed that Ament's equation can be derived from Biot's equations of motion. The only difference between Eqs. III-18 and III-19 and similar formulas used by Stoll is the number of parameters which must be specified. Stoll's formulation includes not only the pore size parameter discussed above, but also an additional "structure constant."

The structure constant in effect adds an additional term to the effective density of Eq. III-13 to account for the possibility of mass coupling between the frame and fluid not due to viscous interaction, such as would exist in isolated cavities oriented perpendicular to the pressure gradient (Zwikker and Kosten, 1949). For the highly permeable sediments considered in the present study, stagnant pockets of fluid can be neglected. This amounts to setting Stoll's structure constant to unity or Biot's (1956a) mass coupling parameter, ρ_{12}, to zero. Slight variations of these parameters cause only minor changes in the shape of the resulting attenuation versus frequency curves.

Figure III-1 illustrates the relative theoretical effects of the various alterations to the elastic solution of the shear wave equation of motion. The values are

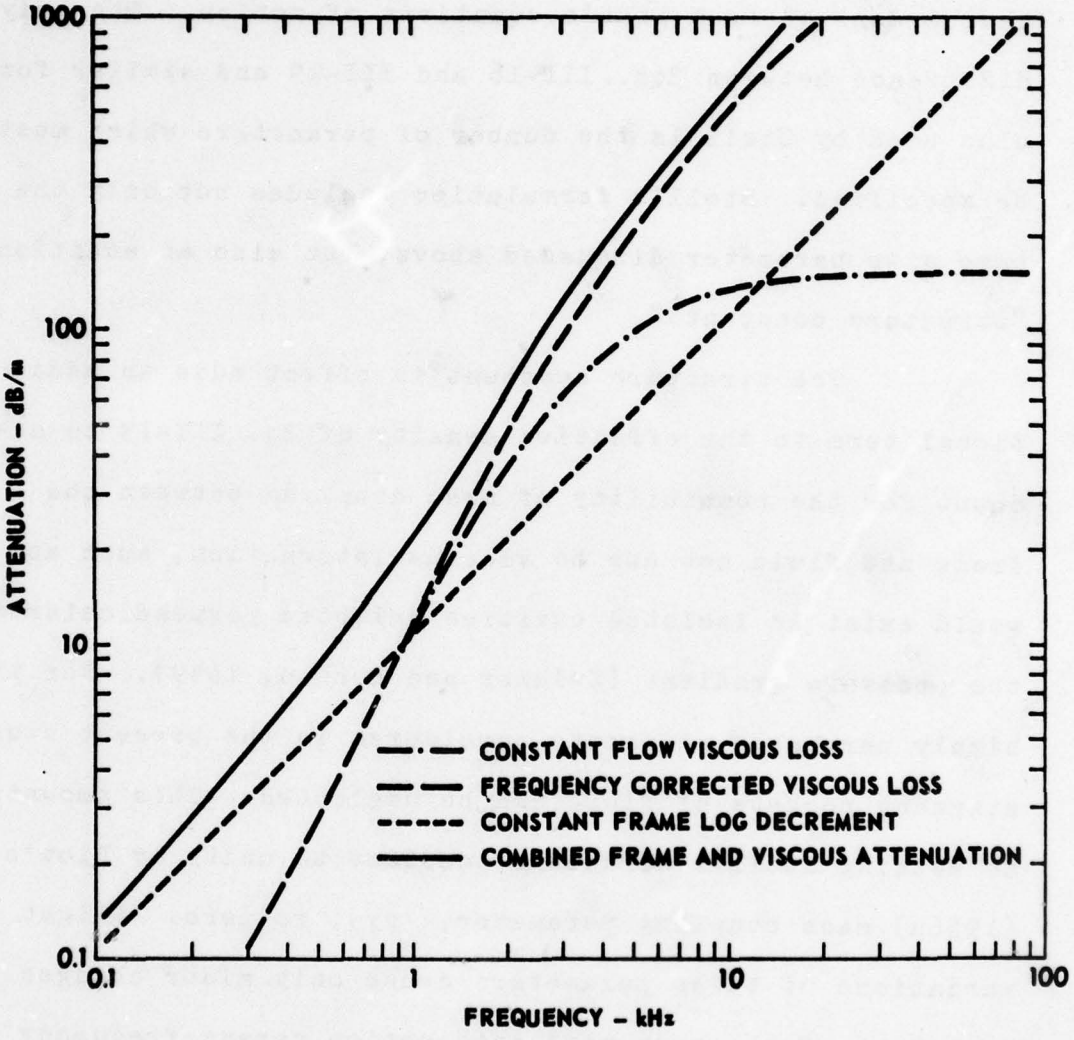

FIGURE III-1
RELATIVE CONTRIBUTIONS OF THEORETICAL FRAME LOSS
AND VISCOUS DISSIPATION TO SHEAR WAVE ATTENUATION

appropriate for glass beads .18 mm in diameter. With $\bar{\rho} = \rho(\text{dry})$, a constant log decrement for the frame, given by μ', yields a straight line with unity slope. With $\mu' = 0$, the viscous loss for constant flow resistance obtained from Ament's effective density gives a constant attenuation at high frequencies. Introduction of Biot's frequency correction to the viscosity causes the viscous loss at high frequencies to vary as the square root of the frequency. The total predicted attenuation when all parameters in Eq. III-19 are finite is the sum of the individual frame and viscous losses.

Figure III-2 shows the variation of the predicted viscous loss with changes of grain size and permeability. The input parameters correspond to expected values for four sizes of glass beads near the surface of the sample. The transition region between the asymptotic f^2 and $f^{1/2}$ dependence of attenuation on frequency is seen to depend upon the permeability, which in turn is controlled by the grain size. The transition occurs at lower frequencies for larger grain sizes, in accord with Eq. III-14. At low frequencies the viscous attenuation is expected to increase with grain size. At higher frequencies, a simple statement of the relation between grain size and attenuation is no

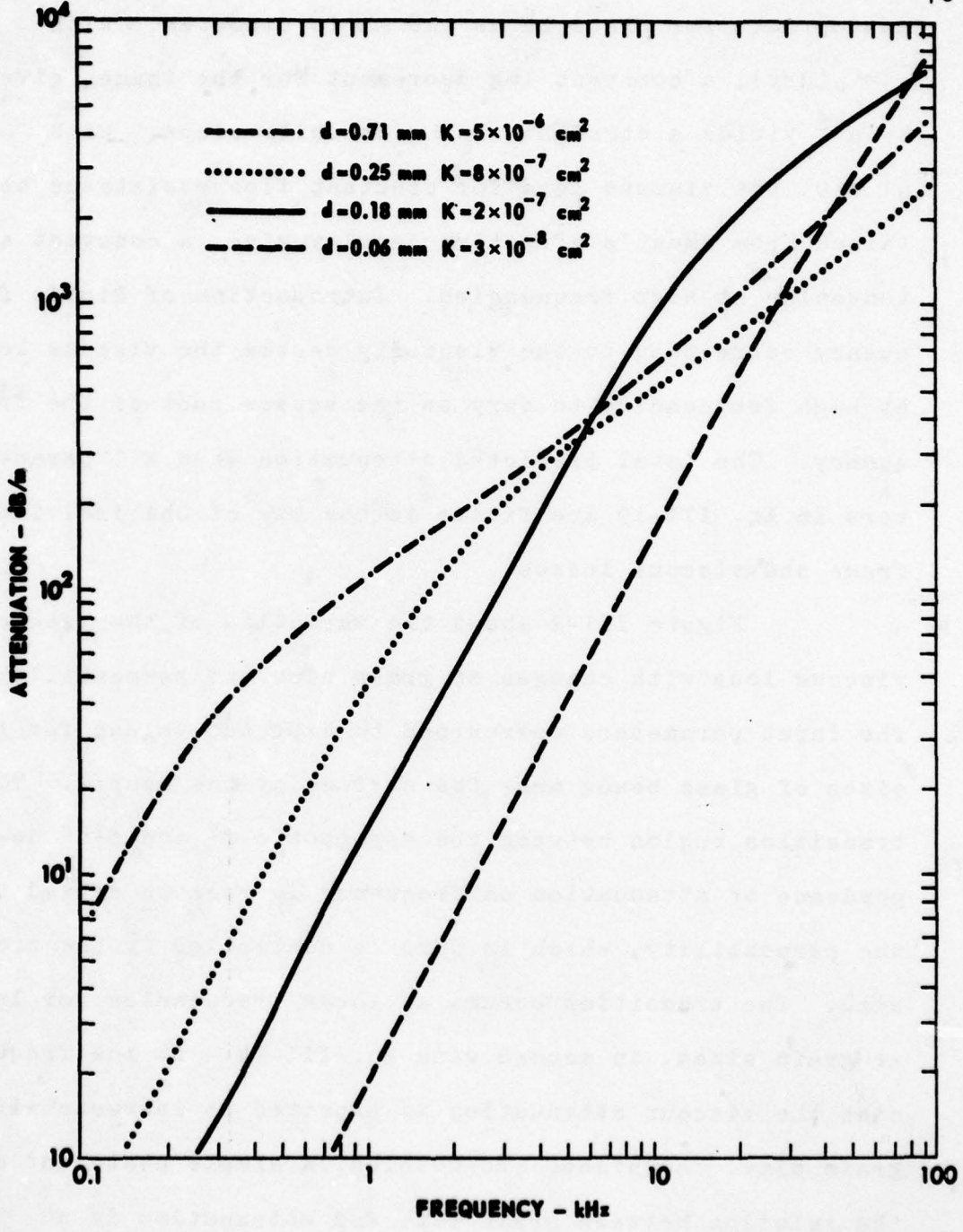

FIGURE III-2
VARIATION OF PREDICTED VISCOUS LOSS WITH GRAIN SIZE AND PERMEABILITY

longer possible since the frequency dependent breakdown of Poiseuille flow causes the curves to overlap.

Figure III-3 illustrates the theoretical dependence of shear wave speed on frequency. The input parameters correspond to the four sizes of glass beads considered in Fig. III-2. The absolute value of the speed depends on the value assigned to the real part of the shear modulus. This value was purposely varied with grain size in order to simplify the display. Therefore the variation with grain size of the absolute magnitude of the phase velocity shown in the figure is not a prediction of the theory. The relative change in speed with frequency is the quantity of interest. For a given grain size, the speed at low frequencies corresponds to perfect coupling between the fluid and the frame. That is, the density term in the expression $V^2 = \mu/\rho$ is the total density of the sediment. At infinite frequency, the fluid no longer moves with the frame. The limiting value of the speed is then given by the density of the frame alone. The overall change in speed between high and low frequencies depends upon the porosity, that is, the ratio of the volume of the fluid to the total volume. Typical values of porosity represent a predicted dispersion of

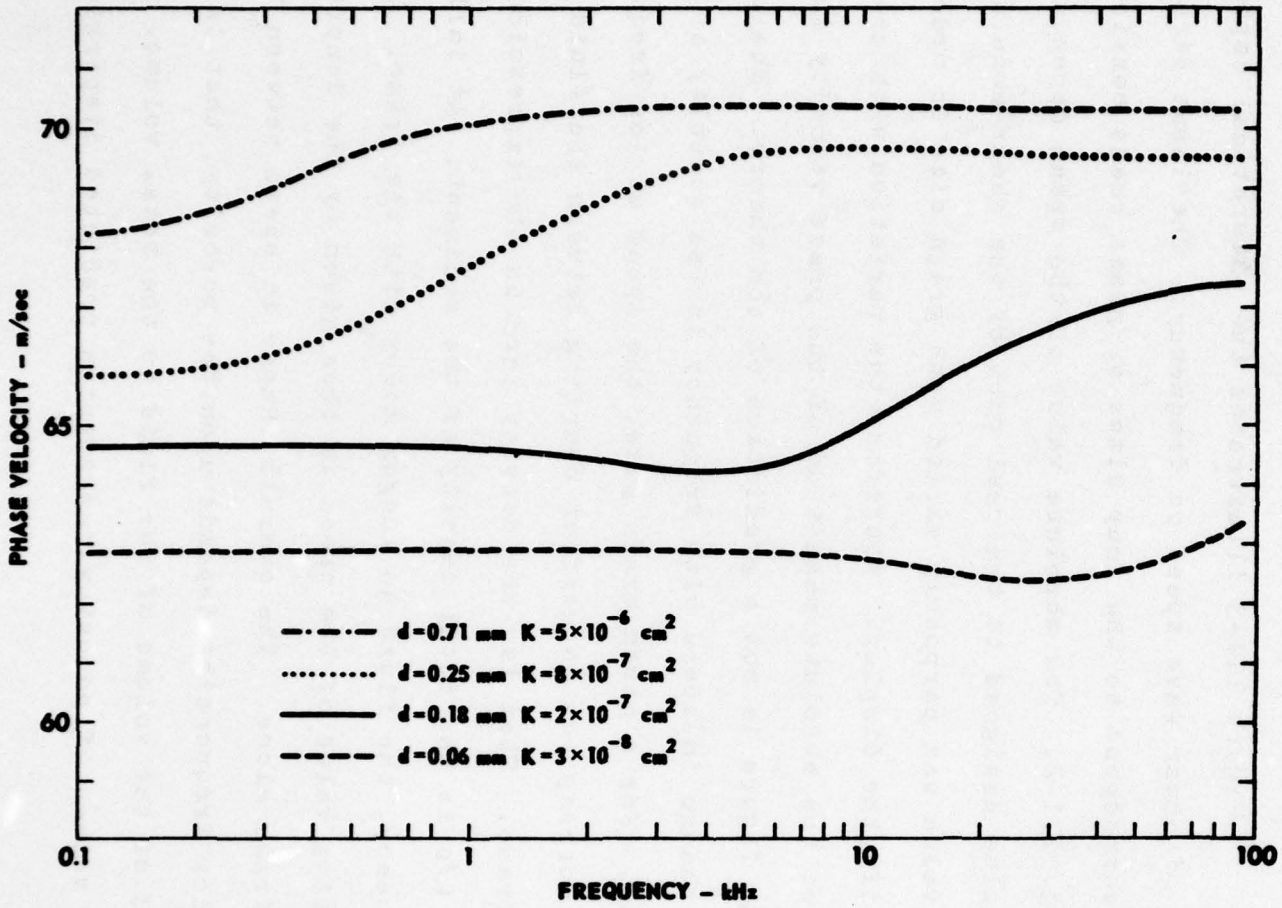

FIGURE III-3
PREDICTED SHEAR WAVE DISPERSION FOR VARIOUS GRAIN SIZES

a few percent from zero to infinite frequency. Figure III-3 shows, however, that most of the change occurs in a relatively narrow frequency band, and that this region depends upon the grain size and permeability.

C H A P T E R I V

SEDIMENT PHYSICAL PROPERTIES

The review presented in Chapter II of the shear wave data available in the literature reveals a scarcity of measurements, particularly of attenuation in unconsolidated porous media. There are sufficient data to suggest trends in the variations of shear wave parameters with changes in sediment physical properties, but the empirical relations so established are inadequately determined. Much of the current knowledge of shear wave propagation in marine sediments is based on measurements performed in partially saturated soils or in rocks. While these are expected to parallel approximately the acoustic behavior of completely saturated unconsolidated sediments, the possibility exists that the mechanisms responsible for attenuation may differ significantly. It is possible to predict theoretically the effects of certain loss mechanisms. However, the available data are inadequate to test the models proposed. Supplementary data are supplied in the present study.

In order to monitor the relationships between an acoustic parameter, such as the wave speed, and a physical

characteristic, such as grain size, several sediments are required, ideally identical except for the properties of interest. Artificial sediments provide the easiest means of ensuring such uniformity. Four sizes of spherical glass beads were chosen for the present investigations. Additional measurements have been made in three natural sands. This allows the effect of grain shape to be assessed, as well as providing values more representative of natural sediments. Highly permeable sands were considered the sediments most likely to provide discrimination among theoretical models.

The grain size distributions of the sediments as determined by sieve analysis are shown in Figure IV-1. The beads are commercial glass shot abrasives obtained from the Cataphote division of Ferro Corporation, Jackson, Mississippi. They are referred to by the last letters of the manufacturer's designations with the following nominal sizes in microns - L, 74-44; MH, 210-105; XHX, 420-210; XPX, 710-350. The beads are spherical with not more than 15 percent irregularly shaped particles and less than 1 percent angular grains. The density of the glass itself is given as 2.5 g/cm^3 with a sound speed of 5,300 m/sec at room temperature and a modulus of elasticity of 10^{11} N/m^2.

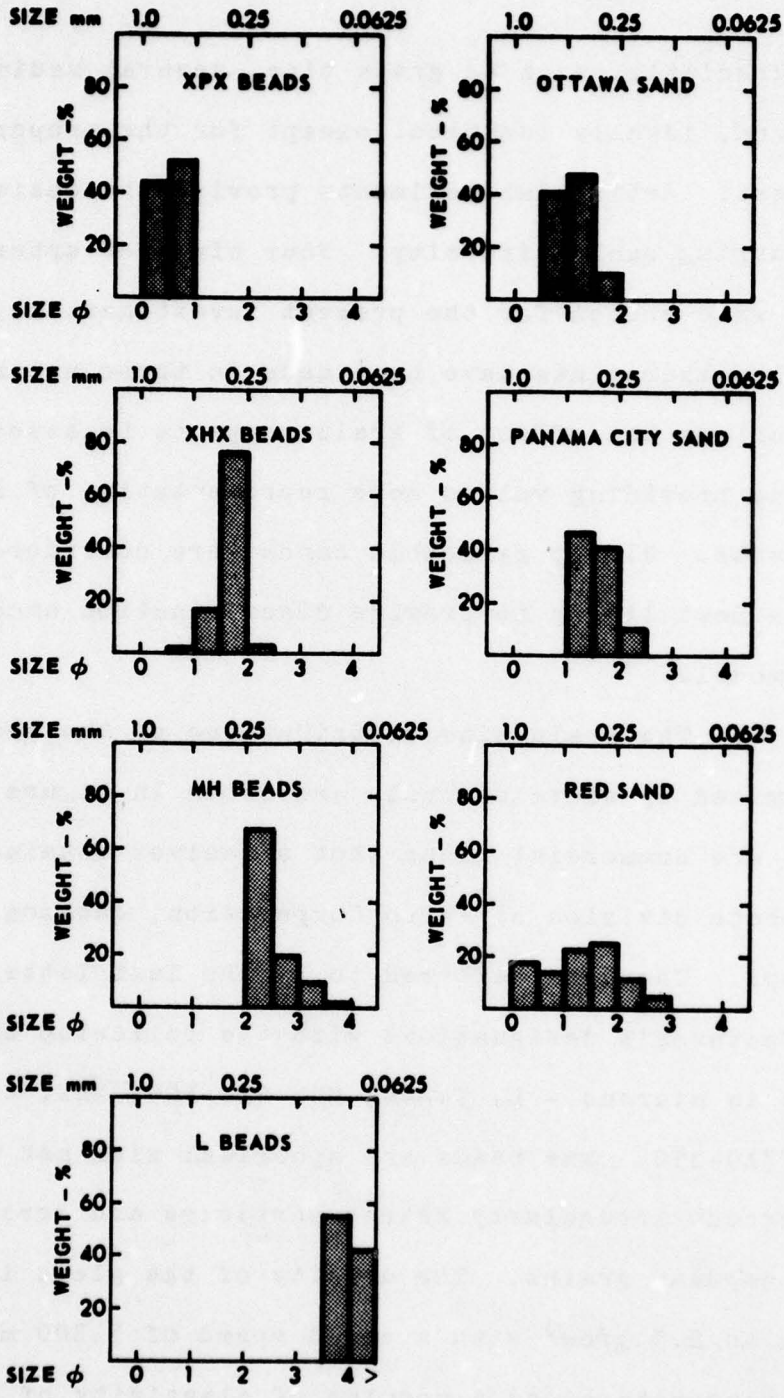

FIGURE IV-1
SEDIMENT GRAIN SIZE DISTRIBUTIONS

The Panama City, or PC, sand is a mature, medium white quartz beach sand from Panama City, Florida. The Ottawa sand is a supermature, medium to coarse quartz sand sold as a standard for field tests of soil density. Textural maturity reflects the sorting and smoothness of the grains. The Ottawa grains are fairly well rounded, the PC grains are more angular. The Red sand is a submature, coarse, riverbed sand of mixed quartz and fledspar grains. Values of the density and bulk modulus of pure quartz are 2.65 g/cm^3 and 3.8×10^{10} N/m^2 (Gregory, 1975).

The viscous interaction model outlined in the previous section requires specification of several physical parameters. These are the frame and fluid densities, the porosity, the permeability, and the fluid viscosity. Water was used as the pore fluid. It has a density of 1 g/cm^3 and a viscosity of approximately .001 $nsec/m^2$ depending on the temperature (CRC, 1963). The densities, porosities, and permeabilities of the sediments as measured in the laboratory are given in Table I.

The density and porosity of a regular packing of identical spheres should not change with grain diameter. The expected value of porosity for a random packing of like spheres is .38 (Carman, 1956). The fluctuation of the

TABLE I

SEDIMENT PHYSICAL PROPERTIES

Sediment	Grain Size (mm)	Porosity	Dry Density (g/cm^3)	Saturated Density	Permeability (m^2)
L	.0625	.389 ± .004	1.42 ± .008	1.81	2.58×10^{-12}
MH	.177	.365 ± .008	1.55 ± .02	1.92	1.70×10^{-11}
XHX	.250	.369 ± .007	1.55 ± .01	1.92	7.76×10^{-11}
XPX	.707	.373 ± .006	1.53 ± .009	1.90	4.63×10^{-10}
RED	--	.383	1.64	2.02	5.71×10^{-11}
PC	.354	.386 ± .014	1.60 ± .03	1.99	3.79×10^{-11}
OTT	.50	3.56 ± .005	1.69 ± .01	2.05	1.39×10^{-10}

measured values about the ideal porosity reflect variations in grain size and shape. However, to first order, the porosities are the same. The densities and porosities were determined by adding a known volume of water to a weighted volume of sediment packed by vibration. The standard deviations of four separate measurements are given in the table.

A constant head permeameter was constructed according to ASTM standards (ASTM D2434-68) to obtain values of the permeability. Figure IV-2 is a scale drawing of the apparatus. A differential pressure gauge was used to measure the pressure drop, h, due to the flow resistance of the sediment. The coefficient of permeability, k, is related to the quantity of water, Q, that flows in time, t, by

$$k = QL/thA \quad , \qquad \text{IV-1}$$

where L is the sample length and A the cross-sectional area. Figure IV-3 is a sample plot of flow rate, Q/At, versus the pressure gradient, h/L. The slope of the line is the permeability, k, in cm/sec at the temperature T of the experiment. The ratio of the viscosity of water at T to that at 20°C was used to reduce the measurements to a standard temperature-viscosity reference.

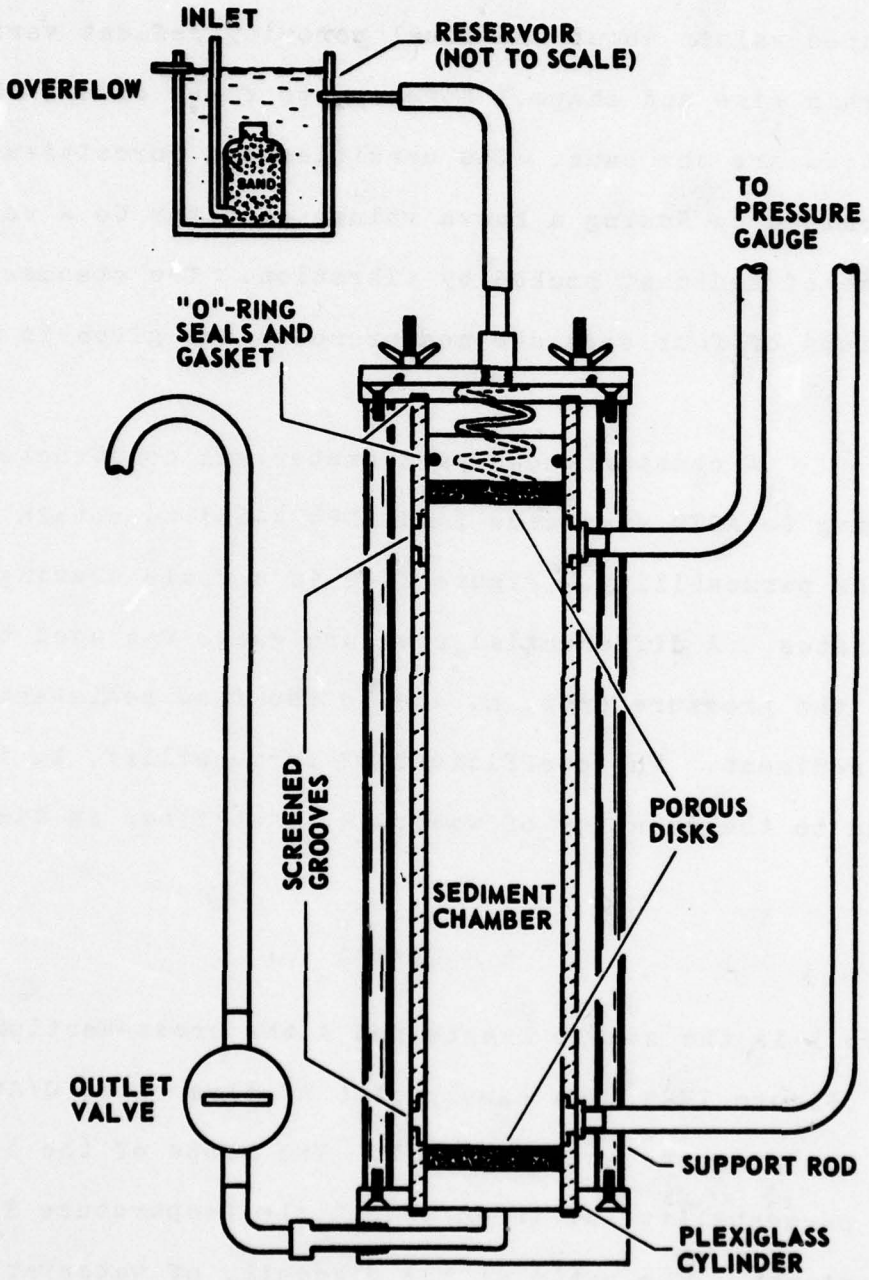

FIGURE IV-2
CONSTANT-HEAD PERMEAMETER

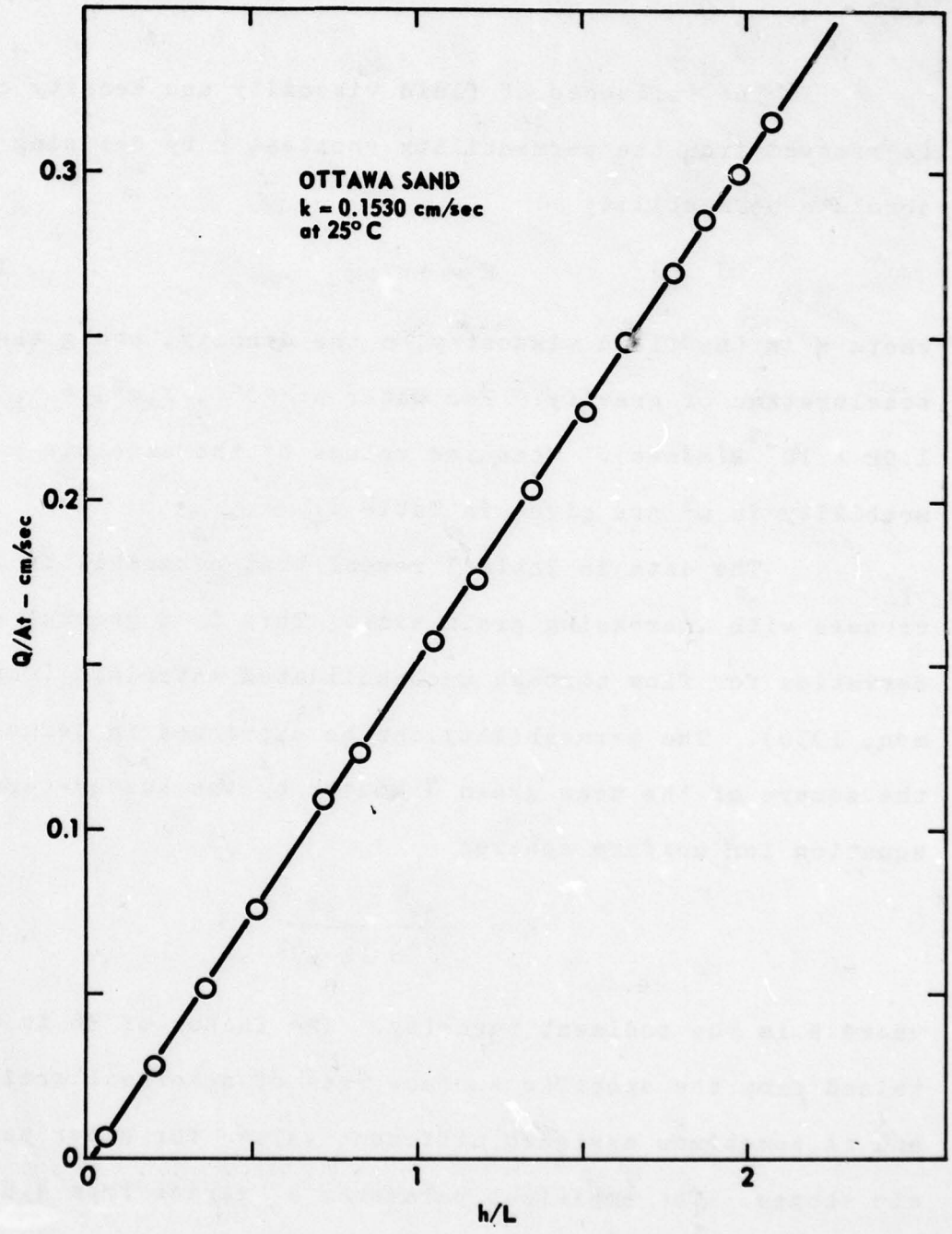

FIGURE IV-3
DETERMINATION OF SEDIMENT PERMEABILITY

AD-A072 867 TEXAS UNIV AT AUSTIN APPLIED RESEARCH LABS F/G 20/1
SHEAR WAVE PROPAGATION IN UNCONSOLIDATED FLUID SATURATED POROUS--ETC(U)
MAY 79 D W BELL N00014-76-C-0117
UNCLASSIFIED ARL-TR-79-31 NL

2 OF 2
ADA
072867

END
DATE
FILMED
9-79
DDC

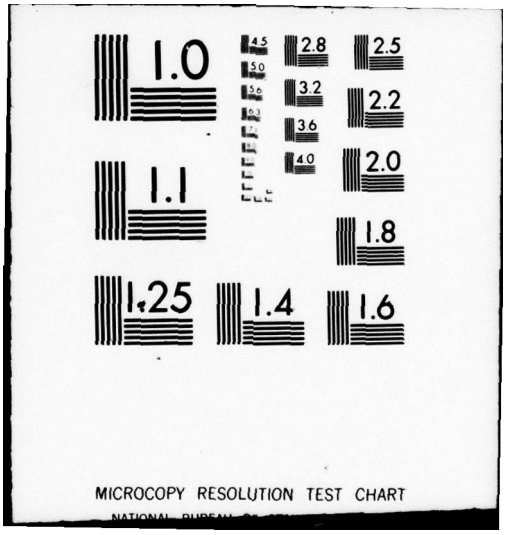
1.0
1.1
1.25
1.4
1.6
1.8
2.0
2.2
2.5
2.8
3.2
3.6
4.0
4.5
5.0
5.6
6.3
7.1
MICROCOPY RESOLUTION TEST CHART

The influence of fluid viscosity and density can be removed from the permeability constant k by defining an absolute permeability

$$K = k\eta/\rho g \quad , \qquad \text{IV-2}$$

where η is the fluid viscosity, ρ the density, and g the acceleration of gravity. For water at 20°C, $K(m^2) = 1.02 \times 10^{-3} k(m/sec)$. Measured values of the absolute permeability in m^2 are given in Table I.

The data in Table I reveal that permeability increases with increasing grain size. This is a general observation for flow through unconsolidated materials (Carman, 1956). The permeability can be expressed in terms of the square of the mean grain diameter by the Kozeny-Carman equation for uniform spheres

$$K = \frac{d^2}{36k_o} \frac{\beta^3}{(1-\beta)^2} \quad , \qquad \text{IV-3}$$

where β is the sediment porosity. The factor of 36 is obtained from the specific surface area of spherical grains and is sometimes assigned different values for other particle shapes. The empirical parameter k_o varies from 4.5 to 5.1 for gas flow through packings of spheres (Carman, 1956). The value obtained from the present data is 4.0 for

the beads and 5.6 for well sorted sands (Fig. IV-4). Additional sand data were obtained from Nolle et al. (1963).

Both the specific surface area, represented by the value 36, and the parameter k_o are necessary to adapt equations established for flow in parallel tubes of constant cross-section to the irregular pore shapes found in a loose aggregate. The flow resistance depends on the surface area exposed to the fluid and the rate at which the fluid moves past the surface. The flow rate measured in a permeability test is actually less than the fluid speed in the medium due to the sinuosity of the pores. That is, the path followed by the fluid is longer than the length of the sample. A constant value of k_o for the various sediments under consideration implies that the effects of sinuosity can be characterized by a single number.

Biot (1956) obtained a high frequency correction to the viscous resistance in a porous media induced by acoustic stress by consideration of the velocity pattern within a uniform circular tube. His formula included the tube diameter (Eq. III-17). It was suggested that the value of the diameter could be empirically adjusted to account for the effects of pore shape and sinuosity. The Kozeny-Carman equation allows Biot's pore size parameter to be

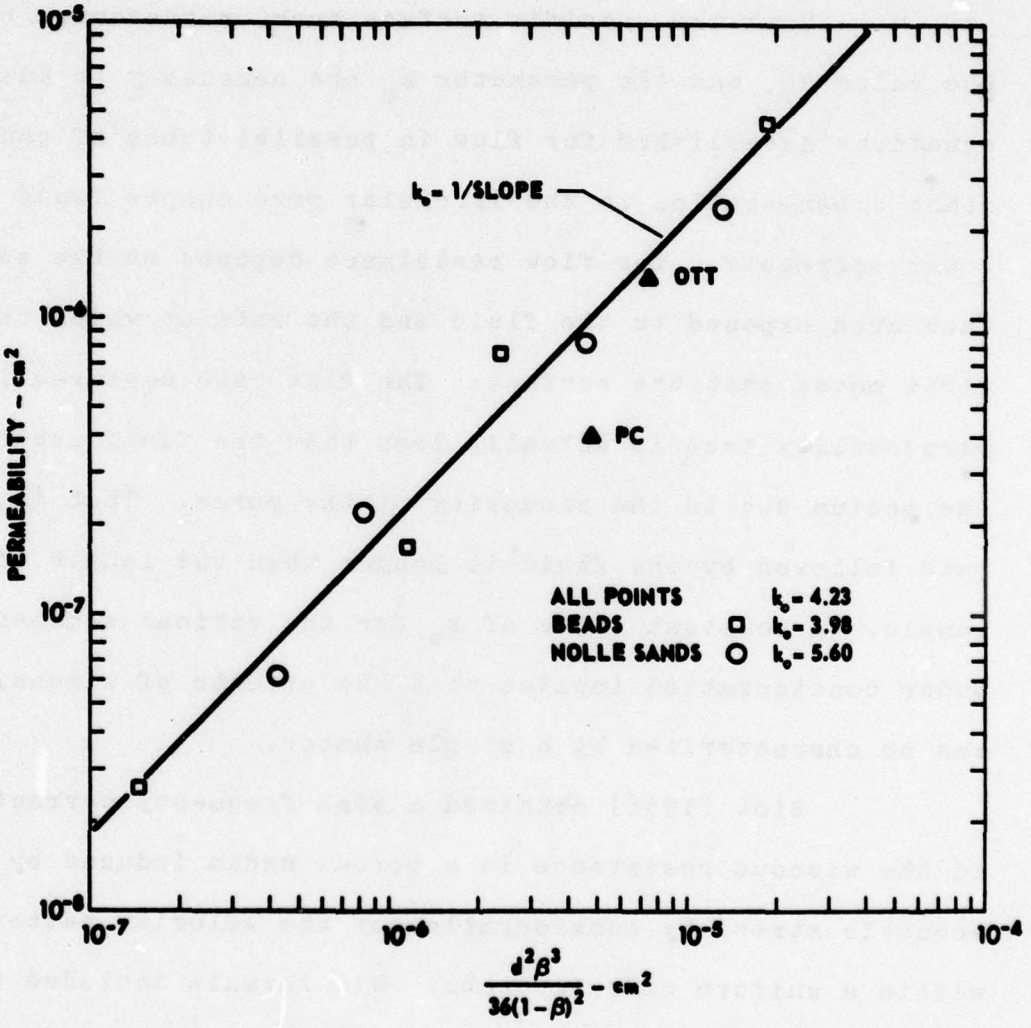

FIGURE IV-4
DETERMINATION OF KOZENY-CARMAN CONSTANT
RELATING PERMEABILITY TO GRAIN SIZE

expressed in terms of the mean grain diameter determined by permeability measurements at low flow rates. Hovem (1979) concluded that

$$a = \frac{d}{3} \frac{\beta}{(1-\beta)} \quad , \qquad \text{IV-4}$$

where a is the pore size parameter in Eq. III-17 and d is the mean particle size in Eq. IV-3. This compares favorably with Stoll's (1976) suggested value of 1/6 the particle size.

The usefulness of Eq. IV-4 depends upon the validity of the Kozeny-Carman equation. For certain materials, including many rocks (Carman, 1956), k_o is not a constant. That is, the effects of pore shape and sinuosity are not easily related to a grain or pore size. For unconsolidated sands, however, Eq. IV-4 provides a value of the pore size parameter independent of acoustic measurements.

C H A P T E R V

TRANSDUCER CHARACTERISTICS

A primary reason for the scarcity of shear wave measurements in marine sediments has been the lack of a source-receiver combination capable of detecting such waves in low rigidity media. The use of bender elements has overcome this difficulty (Shirley and Anderson, 1975a; Shirley and Hampton, 1978). A bender element consists of two ceramic plates cemented back to back but oppositely polarized. An applied voltage causes one plate to contract while the other expands. This causes the assembly to bend in a manner similar to the action of a bimetal strip in a thermostat (Fig. V-1). Displacement of the sediment perpendicular to the length of the element causes a shear wave to propagate parallel to the axis of the transducer. Bender elements are commercially available.

Previous laboratory work (Shirley and Anderson, 1975b; Shirley, 1977) has been conducted with transducer arrays of from one to six bender elements separated by compliant spacers. Only the ends of the elements were directly coupled to the sediment. The present research has

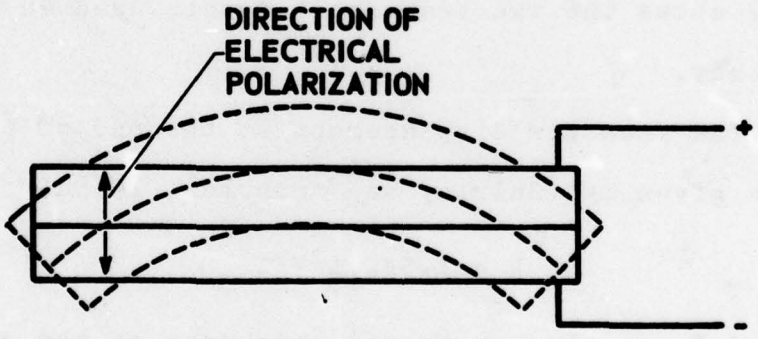

FIGURE V-1
OPERATION OF A CERAMIC BENDER TRANSDUCER

(after Shirley 1978)

utilized an improved laboratory design (Shirley, 1978) in which the entire length of the element drives the sediment. This significantly increases the signal amplitude for a given flexion of the transducer. The bender elements are suspended beneath a thin stainless steel plate by a semi-flexible urethane potting compound. The casting material provides both support and electrical insulation, but is pliable enough to allow the elements to vibrate freely. Figure V-2 shows the two transducer mounts used in the present study.

The free air displacement at the end of a bender element is given by (Shirley and Anderson, 1975a)

$$D = 1.5 d_{31} L^2 V / T^2 \ , \qquad \text{V-1}$$

where L and T are the length and thickness of the element, V is the applied voltage and d_{31} is the piezoelectric constant of the ceramic material. The individual ceramic plates are operated in the length extensional mode, that is, the applied voltage is across the thickness of the plate while the resultant mechanical strain is parallel to the length of the plate. The subscripts 3 and 1 simply indicate that the strain is perpendicular to the direction of polarization.

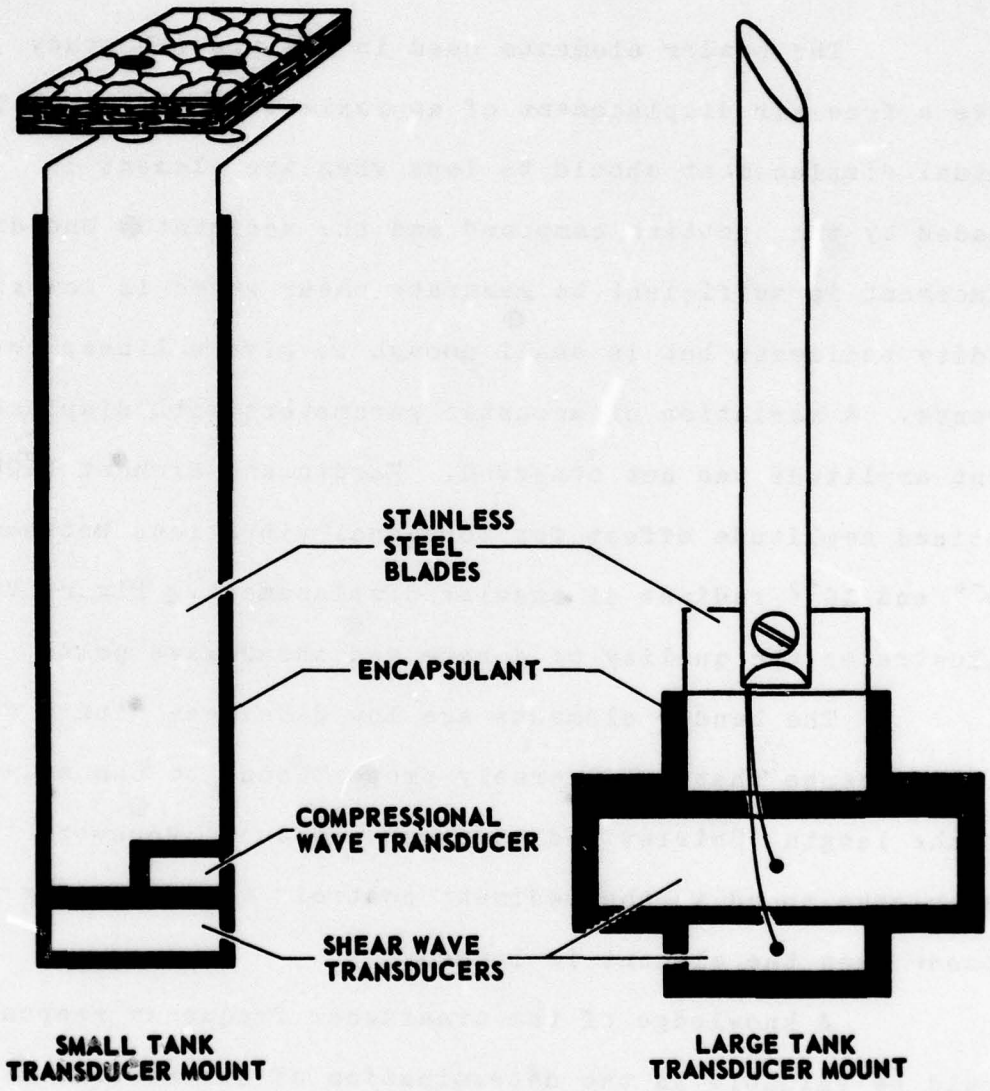

FIGURE V-2
TRANSDUCER MOUNTS

The bender elements used in the present study have a free air displacement of approximately 10^{-4} cm. The actual displacement should be less when the element is loaded by the potting compound and the sediment. The displacement is sufficient to generate shear waves in low rigidity sediments but is small enough to give a linear response. A variation of acoustic parameters with displacement amplitude was not observed. Hardin and Richart (1963) noticed amplitude effect for torsional vibrations between 10^{-4} and 10^{-2} radians of angular displacement. Figure V-3 illustrates the quality of a received shear wave pulse.

The bender elements are low Q devices with a free air resonance that is inversely proportional to the square of the length (Shirley and Anderson, 1975a). However, the shear wave speed in the sediment controls the frequency response when the element is loaded.

A knowledge of the transducer frequency response would be valuable in the determination of attenuation as a function of frequency. An accurate characterization requires the transducer to be mounted in the sediment since the response depends upon the load. This in turn requires the frequency response of the medium to be known. However,

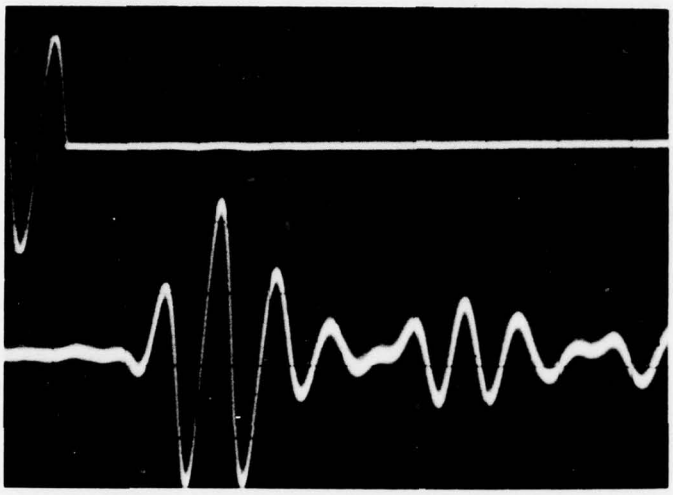

SATURATED 2.5 kHz at 3.5 cm SEPARATION
VERTICAL SCALE: 10 V/div TOP
0.2 V/div BOTTOM
HORIZONTAL SCALE: 0.5 msec/div

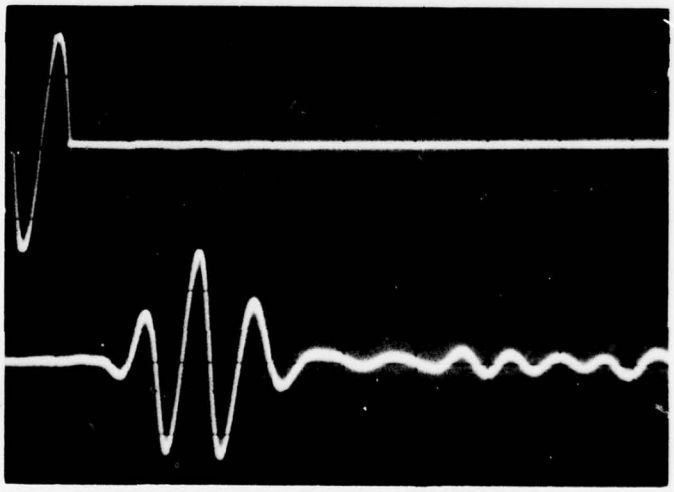

DRY 2.5 kHz at 3.5 cm SEPARATION
VERTICAL SCALE: 10 V/div TOP
0.5 V/div BOTTOM
HORIZONTAL SCALE: 0.5 msec/div

FIGURE V-3
SHEAR WAVE SIGNAL QUALITY – OTTAWA SAND

ARL:UT
AS-79-216
DWB-GA
2-7-79

the response of the sediment is the goal of the present research. There has not yet been sufficient work done to establish a reference medium whose shear wave properties are known accurately enough to allow routine calibration of the elements. It is possible, however, to solve for the transducer frequency response once the sediment attenuation has been determined.

Figure V-4 shows the measured amplitude response of a 2.54 cm bender element in three different sediment types. The attenuation in each sediment was first determined from the amplitude decay with transducer separation at fixed frequencies. The measured amplitudes at a single separation were then corrected to give the response of the two-element projector-receiver combination. Figure V-5 shows the variation with transducer separation of the observed output voltages in the PC sand.

Figure V-4 clearly shows the dependence of the transducer response on the wavelength excited in the sediment. The measured shear wave speed decreases from sand to clay. The figure also indicates the useful bandwidth of the transducers. The small bender elements generate measurable signals over approximately a decade of frequency.

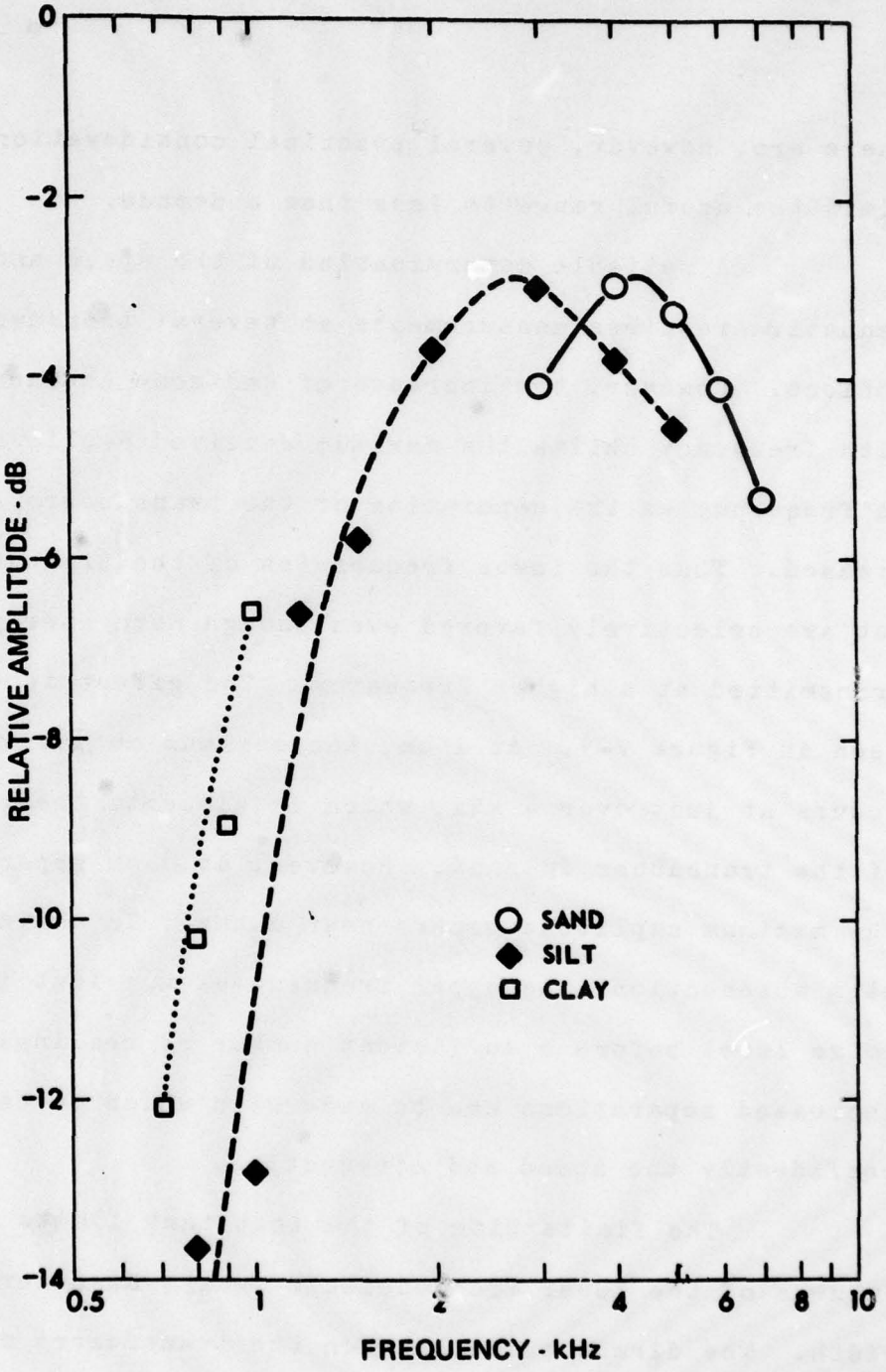

FIGURE V-4
AMPLITUDE RESPONSE OF SHEAR WAVE TRANSDUCER

There are, however, several practical considerations which limit the useful range to less than a decade.

A reliable determination of the speed and the attenuation requires measurements at several transducer separations. However, the increase of sediment attenuation with frequency shifts the maximum received amplitude lower in frequency as the separation of the transducers is increased. Thus the lower frequencies of the transducer output are selectively favored even though more energy may be transmitted at a higher frequency. The effect is easily seen in Figure V-5. At 1 cm, the maximum output voltage occurs at just over 4 kHz, which is close to the resonance of the transducer in sand. However, at 8 cm separation, the maximum amplitude occurs near 3 kHz. In sediments with high attenuation, the upper frequencies are lost in the noise level before a sufficient number of readings at increased separations can be made with which to calculate confidently the speed and attenuation.

The finite size of the test tank limits the usefulness of the lower frequencies of the transducer bandwidth. The direct pulse between the transducers must be relatively short in order to distinguish the direct arrival

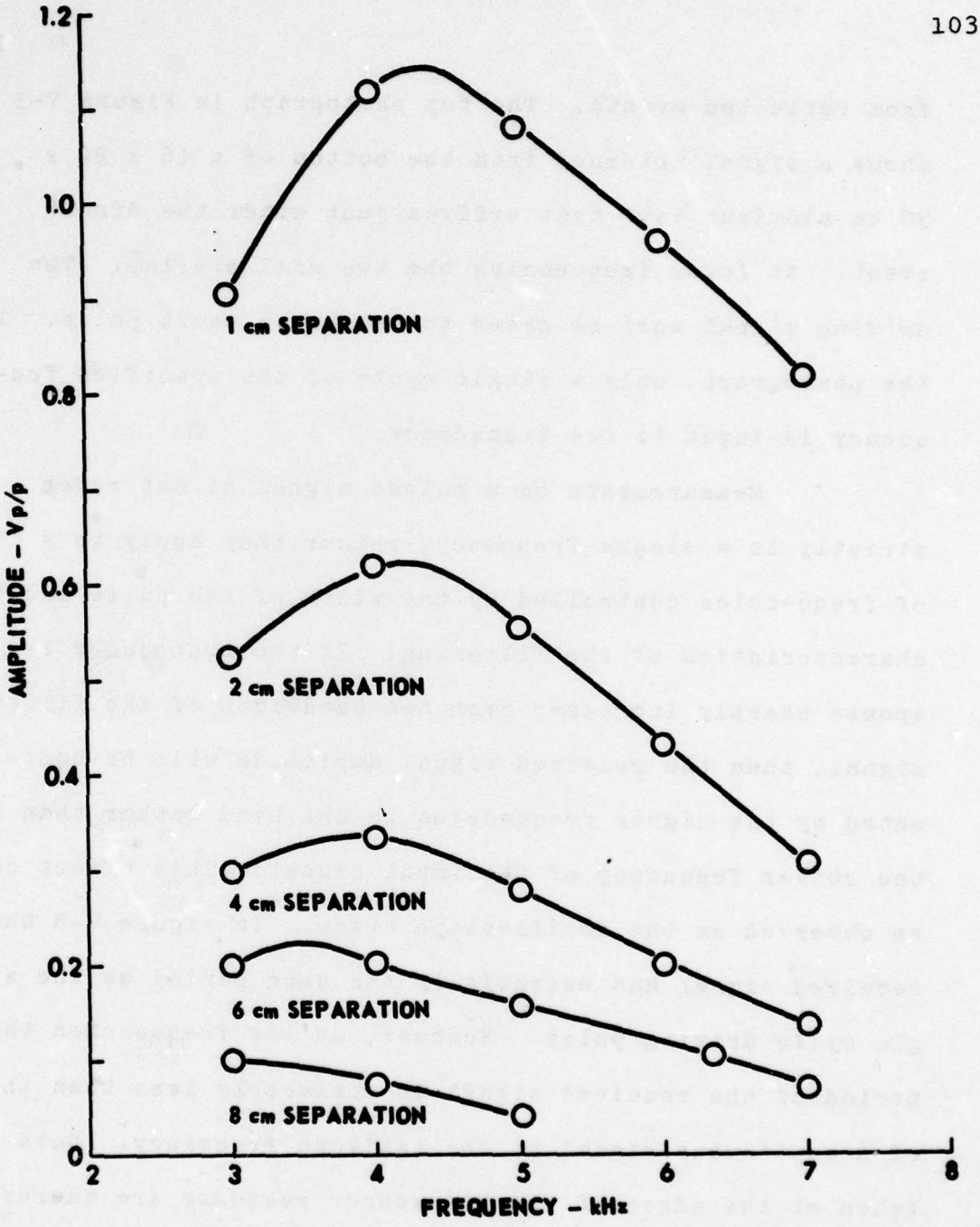

FIGURE V-5
VARIATION OF AMPLITUDE WITH SEPARATION OF RECEIVED SHEAR WAVES

from reflected events. The top photograph in Figure V-3 shows a signal returned from the bottom of a 16 x 20 x 30 cm aluminum tank that arrives just after the direct event. At lower frequencies the two will overlap. The driving signal must be gated to produce a short pulse. In the photograph, only a single cycle of the specified frequency is input to the transducer.

Measurements on a pulsed signal do not refer strictly to a single frequency; rather they apply to a band of frequencies controlled by the width of the pulse and the characteristics of the filtering. If the transducer response sharply increases over the bandwidth of the filtered signal, then the received signal amplitude will be dominated by the higher frequencies in the band rather than by the center frequency of the input signal. This effect can be observed on the oscilloscope trace. In Figure V-3 the received signal has essentially the same period as the single cycle driving pulse. However, at low frequencies the period of the received signal is noticeably less than that of a continuous signal at the assigned frequency. Data taken at the edges of the transducer response are therefore somewhat ambiguous, even though the amplitude is sufficient for a reading. Better discrimination of the signal

frequency can be obtained by adjustment of the output filter to a higher Q. This, however, also greatly reduces the received signal amplitude.

An additional problem arises at low frequencies due to the unknown radiation pattern of the bender elements. The divergence of the transmitted energy due to geometrical spreading must be removed from the observed amplitude decay before a reliable determination of the sediment attenuation can be made. If the geometrical spreading is correctly removed, then a plot of relative signal amplitude expressed in dB will vary linearly with separation. The slope is the attenuation per unit distance due to the sediment. Figure V-6 shows the relative signal amplitudes obtained from Figure V-5 after removal of assumed spherical spreading using the center to center distance between the transducers. This results in a consistent determination of the attenuation which in turn allows calculation of the transducer response shown in Figure V-4. However, an easily observed signal was obtained at frequencies less than 3 kHz. These data are shown in Figure V-7 with the same spherical divergence correction applied as in Figure V-6. The progressive curvature of the amplitude versus separation lines suggests that the

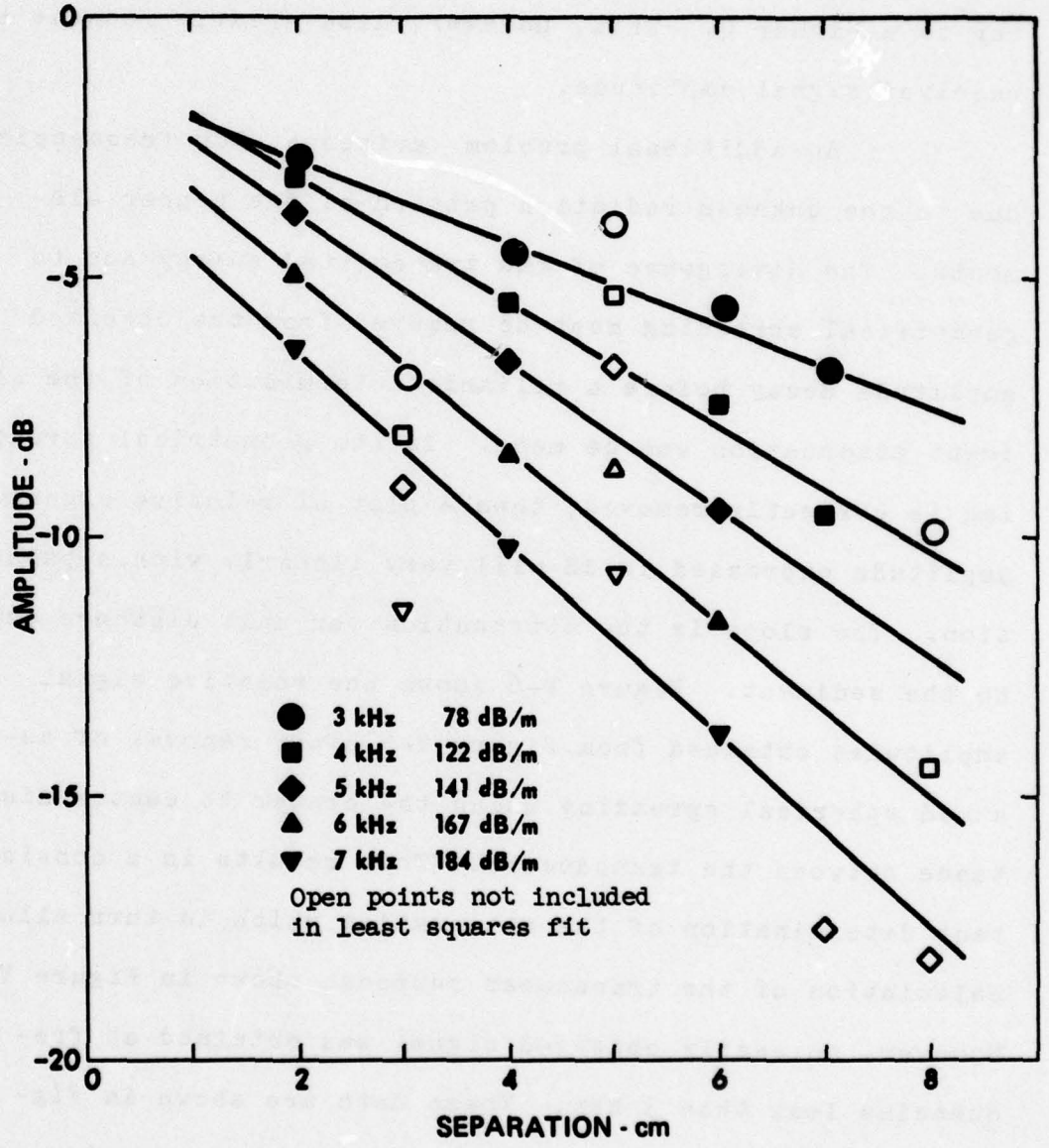

FIGURE V-6
MEASUREMENT OF SHEAR WAVE ATTENUATION AT DIFFERING FREQUENCY - SAND HIGH FREQUENCIES

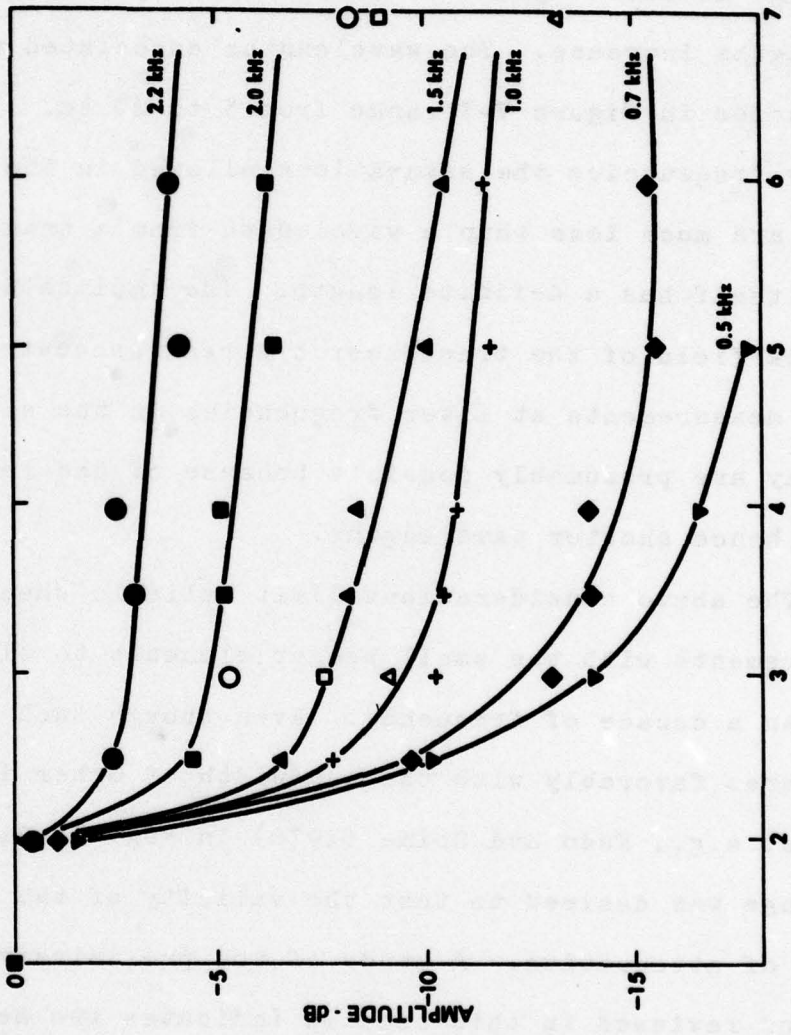

FIGURE V-7
MEASUREMENT OF SHEAR WAVE ATTENUATION
AT DIFFERING FREQUENCY - SAND
LOW FREQUENCIES

assumption of spherical spreading is no longer valid. The curves become linear at greater and greater separations as the wavelengths increase. The wavelengths associated with the frequencies in Figure V-7 range from 5 to 20 cm. That is, for low freqeuncies the separations allowed in the small tank are much less than a wavelength from a transducer which itself has a definite length. The implication is that the nearfield of the transducer has been encountered. Consistent measurements at lower frequencies in the silt and the clay are presumably possible because of the lower speeds and hence shorter wavelengths.

The above considerations limit reliable shear wave measurements with the small bender elements to slightly less than a decade of frequency. Even though such a range compares favorably with the bandwidth of other investigators, e.g., Kudo and Shima (1970) in Fig. II-3, a broader range was desired to test the validity of the viscous model of attenuation. A study of the preliminary investigations reviewed in this section indicates two means of increasing the available bandwidth. First, a larger tank would permit both a longer driving pulse and greater separations. Second, since the resonance frequency of the transducer depends on the length of the element, an array

of different sized elements could extend the frequency range. Both of these improvements have been implemented.

Figure V-2 shows a transducer that consists of both a 2.54 cm and a 5.08 cm bender element. These transducers were used in an aluminum tank 46 x 56 x 71 cm. The frequency of greatest sensitivity is slightly lower in the larger element than in the shorter one. However, the Q of the larger element is such that its usable bandwidth encompasses that of the smaller element. Measurements with the larger elements can be obtained over slightly more than a decade of frequency. The smaller elements serve as a consistency check.

C H A P T E R V I

LABORATORY EQUIPMENT AND PROCEDURE

Shear and compressional wave speed and attenuation were measured for each of the seven sediments described in Chapter IV, both when dry and completely water saturated. The transducer probes shown in Figure V-2 were inserted in the sediments at fixed depth and variable separation. The projecting transducers were driven by a pulsed sine wave from one to forty cycles in duration. The received signal was filtered and displayed on an oscilloscope screen. The change in arrival time with separation of a distinctive peak of the received signal, as measured by a 5-digit LED display function of the oscilloscope, was used to compute the wave speed. Attenuation was calcualted from the decay of signal amplitude with separation, as measured peak to trough on the oscilloscope screen for the shorter signals or rms with a sampling voltmeter for the longer signals. The filter was adjusted for a constant $Q = 10$ to ensure that the cycle frequency of the driving pulse was representative of the received signal frequency.

A constant Q, that is, $f/\Delta f$, rather than a constant Δf preserves the wave shape at different center frequencies.

Measurements of the saturated sediment properties were performed in a small aluminum tank, 16 x 20 x 30 cm, using the projector-receiver configuration shown in Figure VI-1. One of the transducer mounts was attached to a rigid crossbar and remained in a set location. The other mount was fixed to a threaded rod located on top of the tank. Rotation of this rod moved the second set of transducers relative to the first. Small sheets of cork placed above the transducer mounts were found necessary to prevent acoustic transmission through the support mechanism. The shear wave elements were approximately 9 cm below the sediment surface.

Careful preparation of the sediment was necessary to ensure complete water saturation. The sands could be successfully deaerated by slowly adding the sediment to the water and then vibrating the tank under vacuum. The beads, however, showed a greater affinity for entraining air. They were successfully deaerated by heating the sediment in the tank to boiling.

The compressional wave transducers mounted above the shear wave elements allowed a quantitative test of

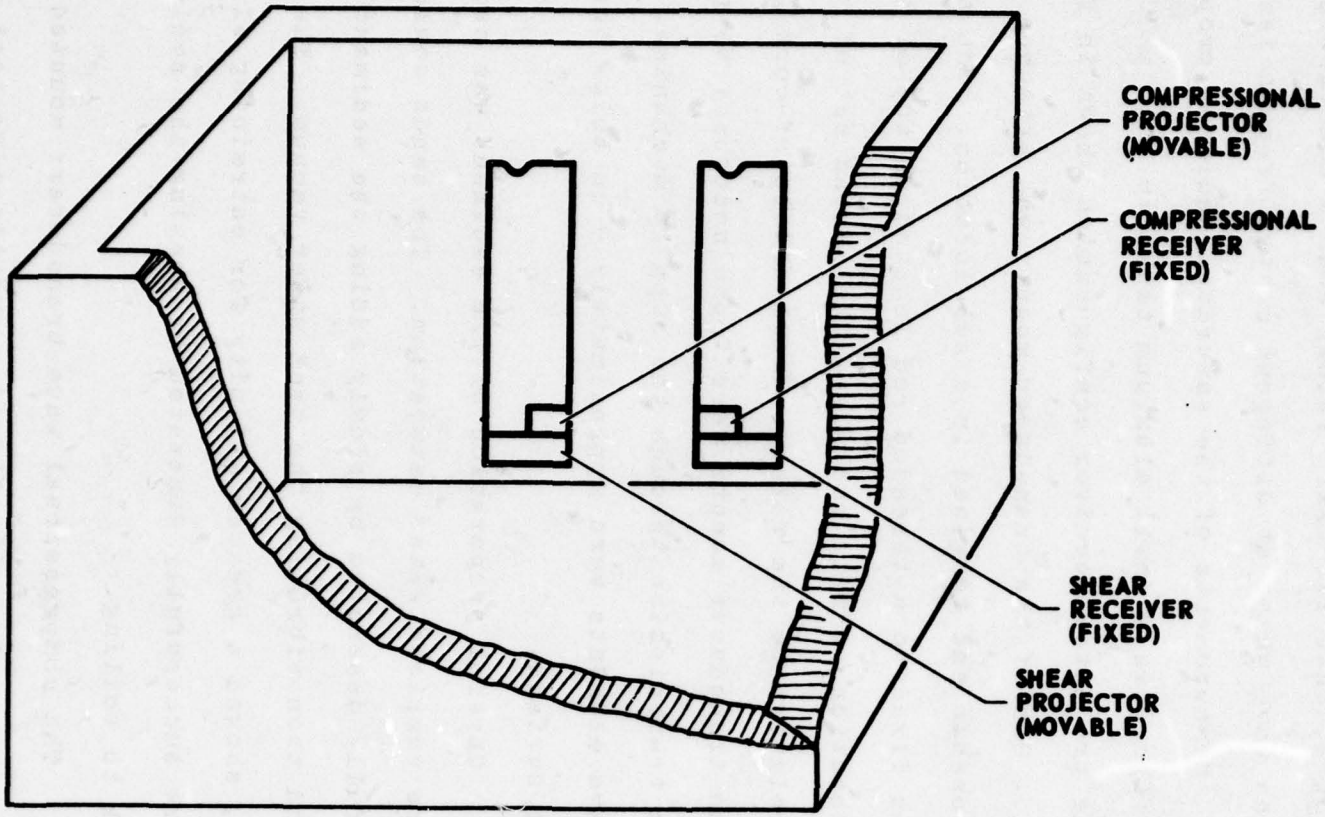

FIGURE VI-1
PROJECTOR-RECEIVER CONFIGURATION

complete saturation. Only a small amount of air trapped in the sediment would significantly reduce the transit time and amplitude of the compressional wave pulse.

The compressional wave elements were thin piezoelectric ceramics operated in the length extensional mode, highly resonant at 120 kHz. They were driven by a two-cycle pulse. A 100-140 kHz bandpass filter was applied to the compressional wave output.

Two modifications were necessary before reliable shear wave results could be obtained in the dry materials. First, the transducer mounts were coated with conducting paint to eliminate electrical feedover between the source and receiver circuits that obscured the beginning of the shear wave pulse. Second, a slightly larger tank was constructed to allow better discrimination between the direct arrival and reflection returns. This was a wood box lined with porous foam with inside dimensions of 25 x 36 x 24 cm. The same transducers and support mechanism were used for both the small aluminum tank and the wooden container. The depth of the transducer beneath the surface was the same in each.

The small tanks were used primarily to study the effects of grain size and shape on the sediment acoustic

properties. They were convenient for this purpose since it was easier to saturate the smaller sediment samples. Shear wave data were collected at only a few closely spaced frequencies near the transducer resonance. A larger tank was used to investigate the variation of shear wave parameters with frequency.

The large tank and second set of transducers are shown in Figure VI-2. Desired use of the tank as its own vacuum chamber required a wall thickness of 3/4 in. (1.9 cm). The tank volume was approximately 150 liters.

Three of the double element transducers shown in Figure V-2 were mounted in line in the large tank. The middle transducer was used as the source, the two outside transducers as receivers. The transducers could be held rigidly at any desired spacing within the tank. The depth was set at approximately 20 cm below the sediment surface.

A refraction from the bottom of the unlined tank restricted the use of a multicycle driving pulse. A lining of 3 cm thick porous foam with randomly spaced foam pyramids 6 cm in height effectively produced an anechoic chamber. The result is shown in Figure VI-3. Noise interference was still present to a noticeable extent for the large shear elements and both elements showed some pulse

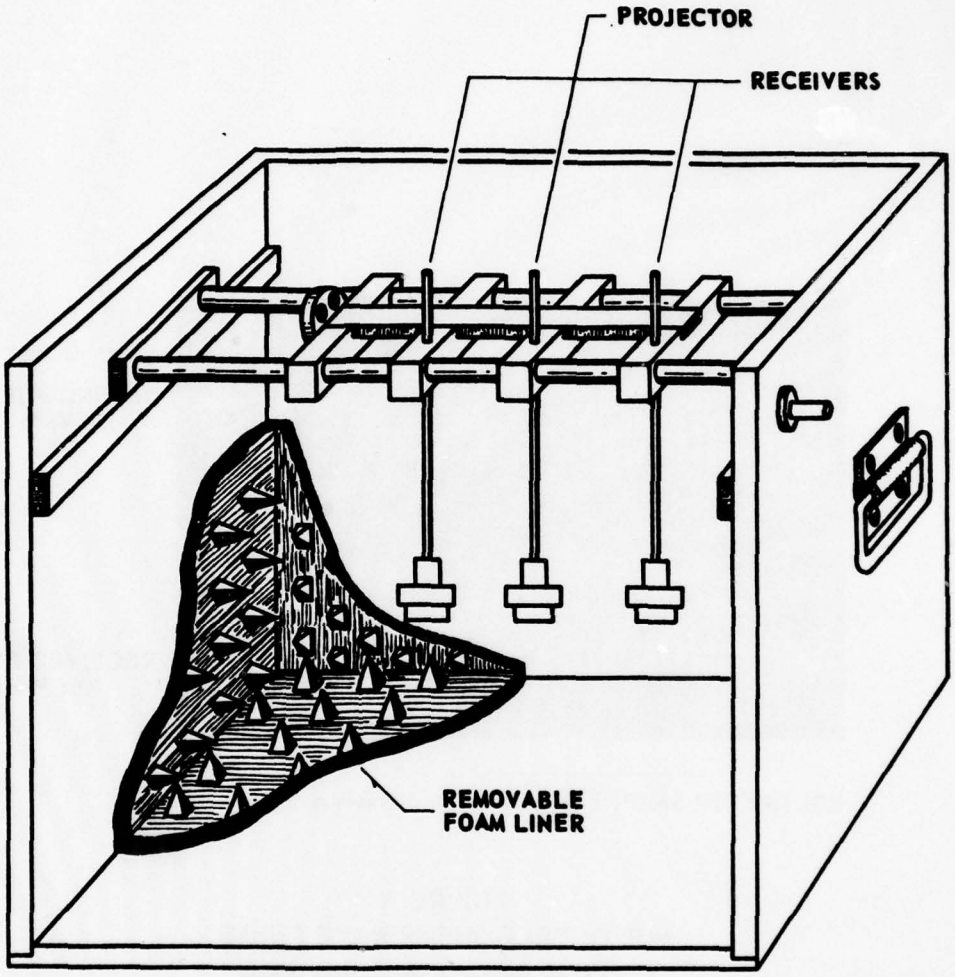

FIGURE VI-2
LARGE SEDIMENT TANK AND TRANSDUCER CONFIGURATION

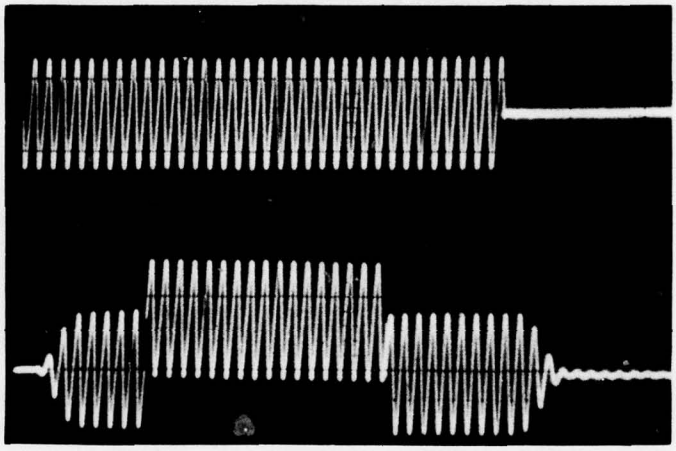

FIGURE VI-3
MULTICYCLE SHEAR WAVE PULSE
SMALL ELEMENTS IN LARGE TANK
SATURATED MH BEADS
1.5 kHz 9 cm SEPARATION

ARL:UT
AS-79-217
DWB-GA
2-7-79

distortion at short wavelengths. Most of the measurements reported herein were obtained with short driving pulses. The longer multicycle pulses were used primarily for quality estimation.

The variability of shear wave parameters with only small changes in sediment packing was of major experimental concern. Preliminary investigations (Shirley and Bell, 1978) showed that self-supporting structures were possible in the PC sand for porosities from roughly .36 to .40. The shear wave speed varied from 130 to 70 m/sec with changes in porosity. The high porosity states were not stable but settled slowly with time and rapidly with mechanical shock. Since data were taken at several transducer separations, a means of returning the sediment to a previous porosity was desired.

Considerable research on soil compaction has been conducted in association with foundation design (Barkan, 1962; Wu, 1971). Minimum porosity packing of dry cohesionless particles can be obtained by slowly pouring the material from a height into a container. The flow rate must be slow enough that each particle strikes the sediment surface independently. If such a packing is later subjected to a small amplitude mechanical shock, the porosity may

increase slightly. However, vibrations characterized by large accelerations will return the dry sediment to minimum porosity. Small external stresses have little effect on the porosity.

Each of the three tanks used for shear wave measurements had vibrators attached. The small tanks had adjustable electromechanical vibrators bolted directly to their sides. The large tank was vibrated by an eccentrically loaded, single speed motor mounted beneath the tank stand. A noticeable change in both dry and saturated sediment volume was observed upon initial vibration. Extended vibration caused no further reduction in volume. The tanks were vibrated during and after a change in transducer separation. The vibration sufficiently fluidized the sediment that the thin transducers could easily be inserted or moved.

The shear wave parameters of the sediments were found to depend not only on the porosity, but also on small internal stresses developed by the vibration process. Abrupt halt of the vibration can cause abnormal stresses within a loose aggregate, particularly at the boundaries of the container. Shear wave measurements taken just after vibration of the tanks had longer delay times and larger

amplitudes than measurements obtained after the sediment was allowed to relax. The decay in transit time was approximately exponential and reached steady values more quickly if the vibration amplitude was slowly decreased rather than abruptly stopped. Compressional wave results did not vary with time.

Measurements in the small tanks were made after a uniform settling time of one and a half hours, after fifteen minutes of low amplitude vibration. The transducers were active the last fifteen minutes of the waiting period. Data in the large tank were taken 24 hours after the transducer spacings were changed.

Noticeable changes in the shear wave amplitude and transit time could be caused by very minor disturbances of the sediment, particularly for the dry glass beads in the small tank. Gently tapping the side of the tank would cause the transit time to increase. If the disturbance was small, recovery of the waveform was rapid enough to be visible. If the disturbance was relatively large, the wave form was distorted and a repeat of the vibration cycle was necessary to recover the previous readings. This extreme sensitivity presented the greatest obstacle to reliable

shear wave measurements. The compressional wave signals were unaffected by disturbances of this magnitude.

The small compressional wave transducers used in the saturated sediments did not couple sufficiently well with the dry material for a compressional wave to be observed. To obtain estimates of the compressional wave speed and attenuation in the dry sediments, a small press was constructed from an aluminum cylinder 15 cm in diameter and 30 cm high. A projector and two receivers with surface area of approximately a square centimeter were mounted on short rods at the bottom of the press such that the propagation path was across the diameter of the cylinder. The two receivers were 4.26 and 4.97 cm from the projector as determined by calibration in three different liquids with known sound speed. The relative amplitude difference between the received signals was also measured in the fluids. Additionally, a pressure sensitive load cell was calibrated and fixed to the bottom of the cylinder. A signal of good quality was obtained for all of the sediments with only a small amount of external frame pressure. It was hoped that results for speed and attenuation could be extrapolated to zero excess pressure. However, the sensitivity was such that only order of magnitude estimates could be obtained in

that manner. Only values for those sediments in which a signal was detected without compression are included herein. Although the received signals were of poor quality, the results were repeatable to within 10 percent of one another. A filtered pulse was used with a frequency of approximately 20 kHz.

C H A P T E R V I I

DATA PRESENTATION AND ANALYSIS

Compressional and shear wave speeds were determined from a plot of time delay versus relative transducer separation. Data at several different spacings reveal the consistency of the measurement technique and eliminate the need for determining the exact beginning of the wave form or the absolute separation between the effective radiation points of the transducers. Figures VII-1, VII-2, and VII-3 present the velocity data taken in the small tank. The quoted values of speed are obtained from a least squares fit of the data. The correlations are excellent for the compressioanl wave speeds but slightly less so for the shear wave speeds in the dry materials. Not shown are points obtained in the dry sediments which were widely divergent from the mean. In such cases the vibration cycle was repeated. Shear wave speed determinations were made at several frequencies; only the center frequency data, between 2 and 4 kHz, are shown in the figures. The speeds at different frequencies differed by less than 5 m/sec in the dry sediments.

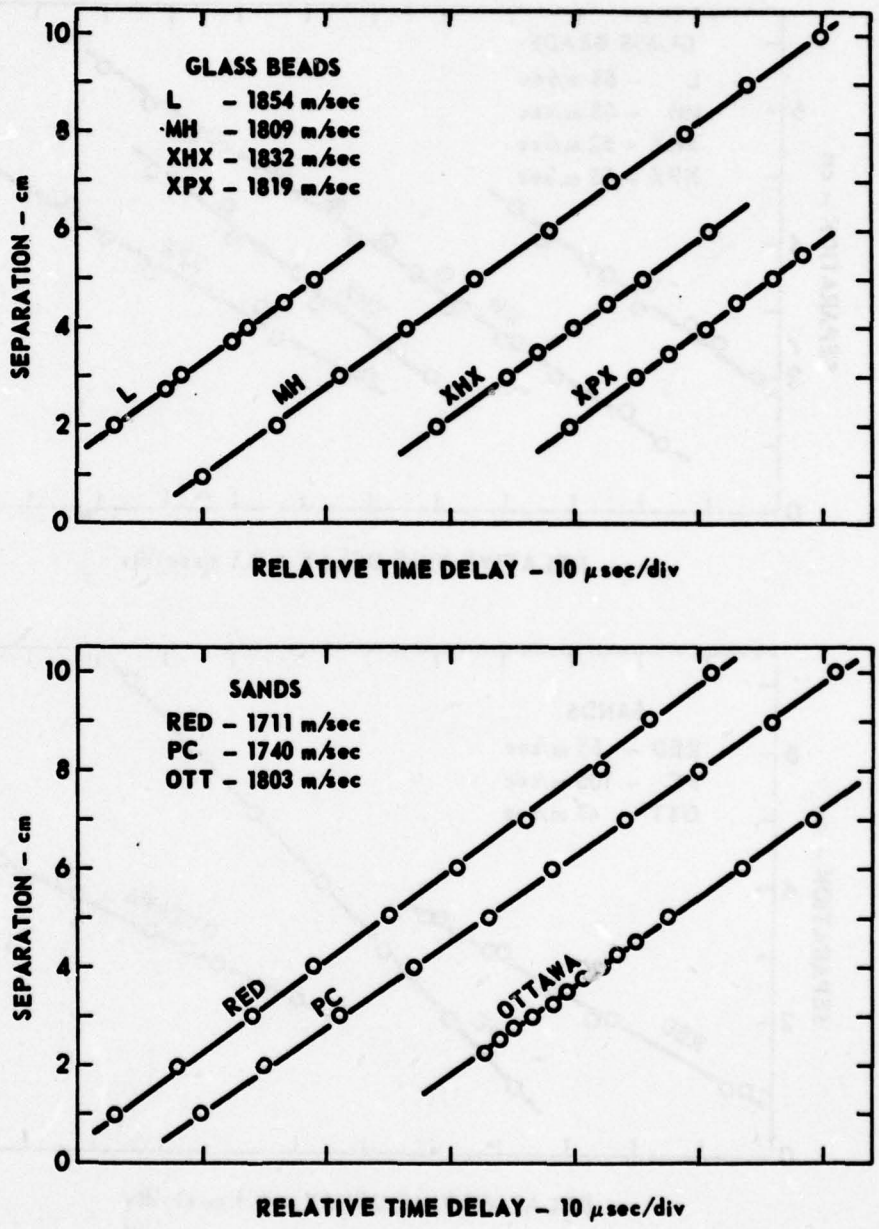

FIGURE VII-1
DETERMINATION OF COMPRESSIONAL WAVE SPEED IN SATURATED SEDIMENTS

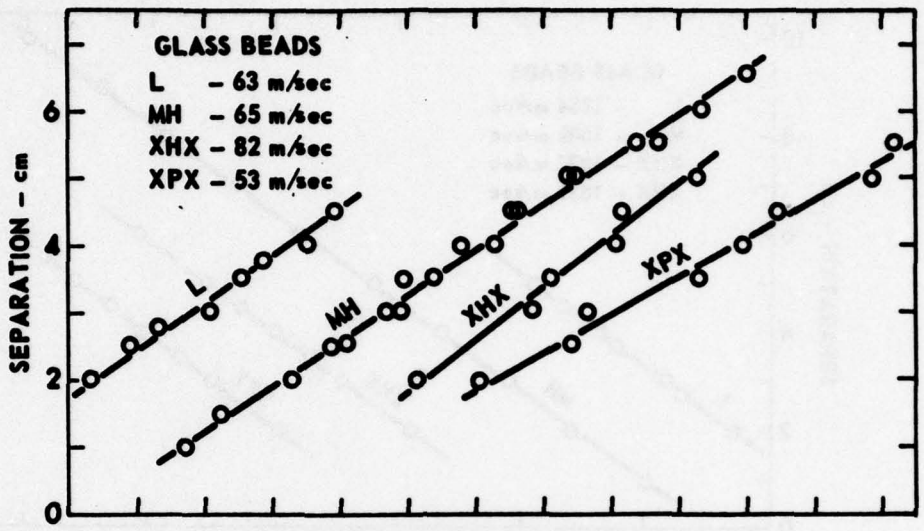

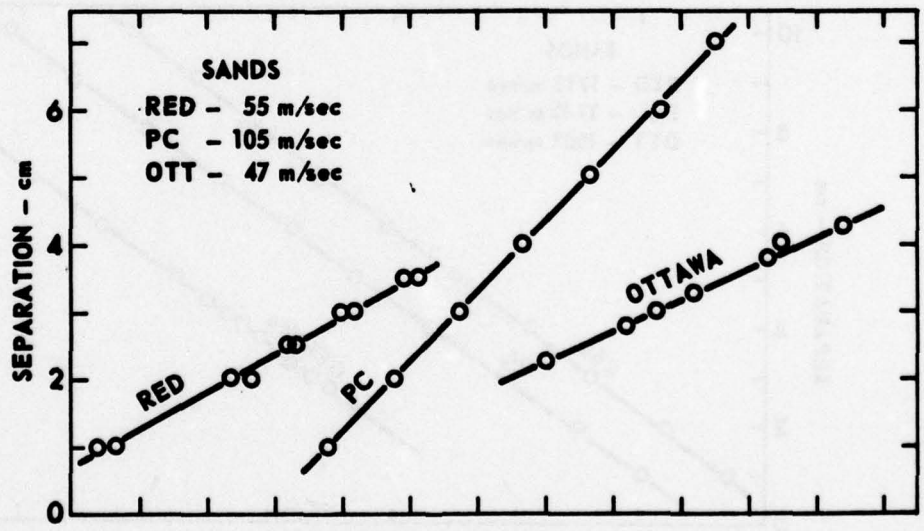

FIGURE VII-2
DETERMINATION OF SHEAR WAVE SPEED IN SATURATED SEDIMENTS

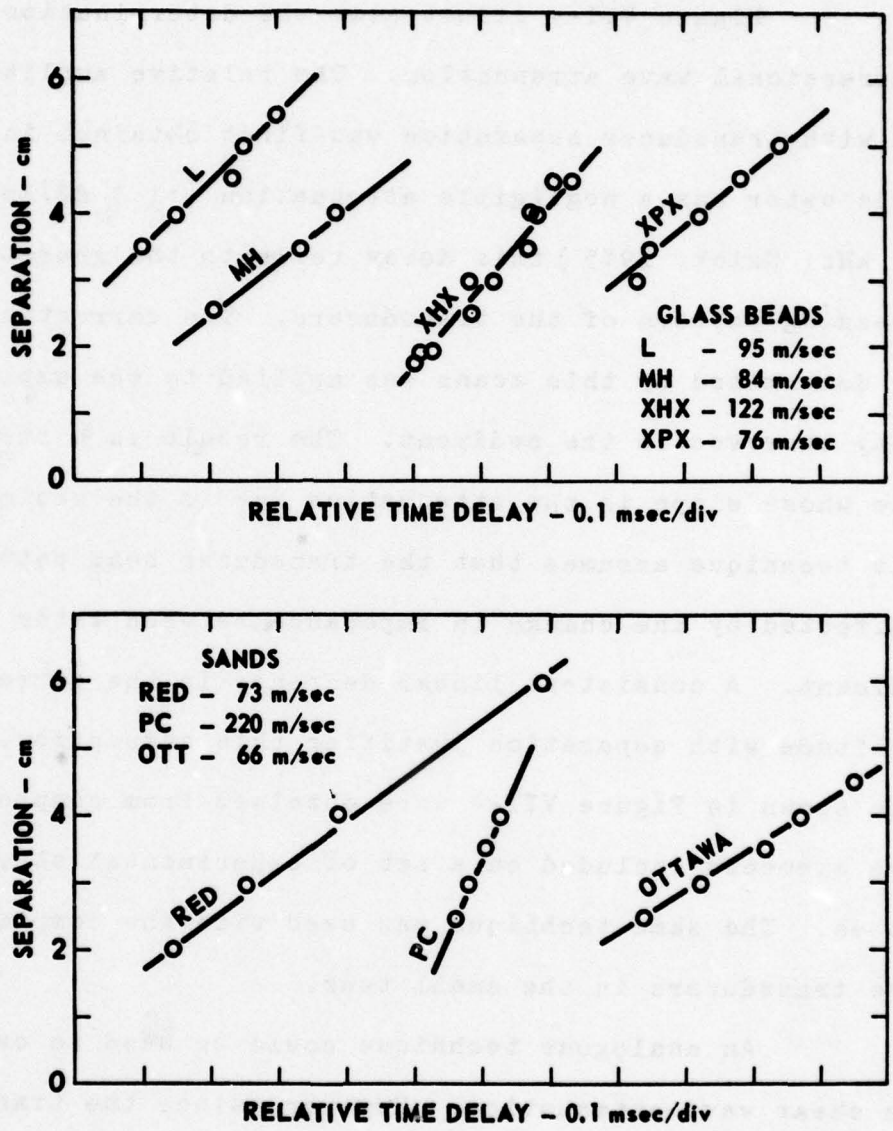

FIGURE VII-3
DETERMINATION OF SHEAR WAVE SPEED IN DRY SEDIMENTS

Figure VII-4 illustrates the determination of the compressional wave attenuation. The relative amplitude decay with transducer separation was first obtained in water. Since water has a negligible attenuation (~1.3 dB/km at 100 kHz; Urick, 1975) this decay reflects the geometrical spreading pattern of the transducers. The correction factor determined by this means was applied to the amplitude decay observed in the sediment. The result is a straight line whose slope is the attenuation due to the sediment. This technique assumes that the transducer beam pattern is unaffected by the change in impedance between water and sediment. A consistent linear decrease in the corrected amplitude with separation justifies this assumption. The data shown in Figure VII-4 were obtained from compressional wave elements included on a set of experimental shear wave probes. The same technique was used with the compressional wave transducers in the small tank.

An analogous technique could be used to calculate the shear wave attenuation. However, since the transducer response varies with the sediment load, experimental determination of the spreading loss separate from the sediment attenuation was not feasible. Spherical spreading was assumed to apply to the center to center transducer

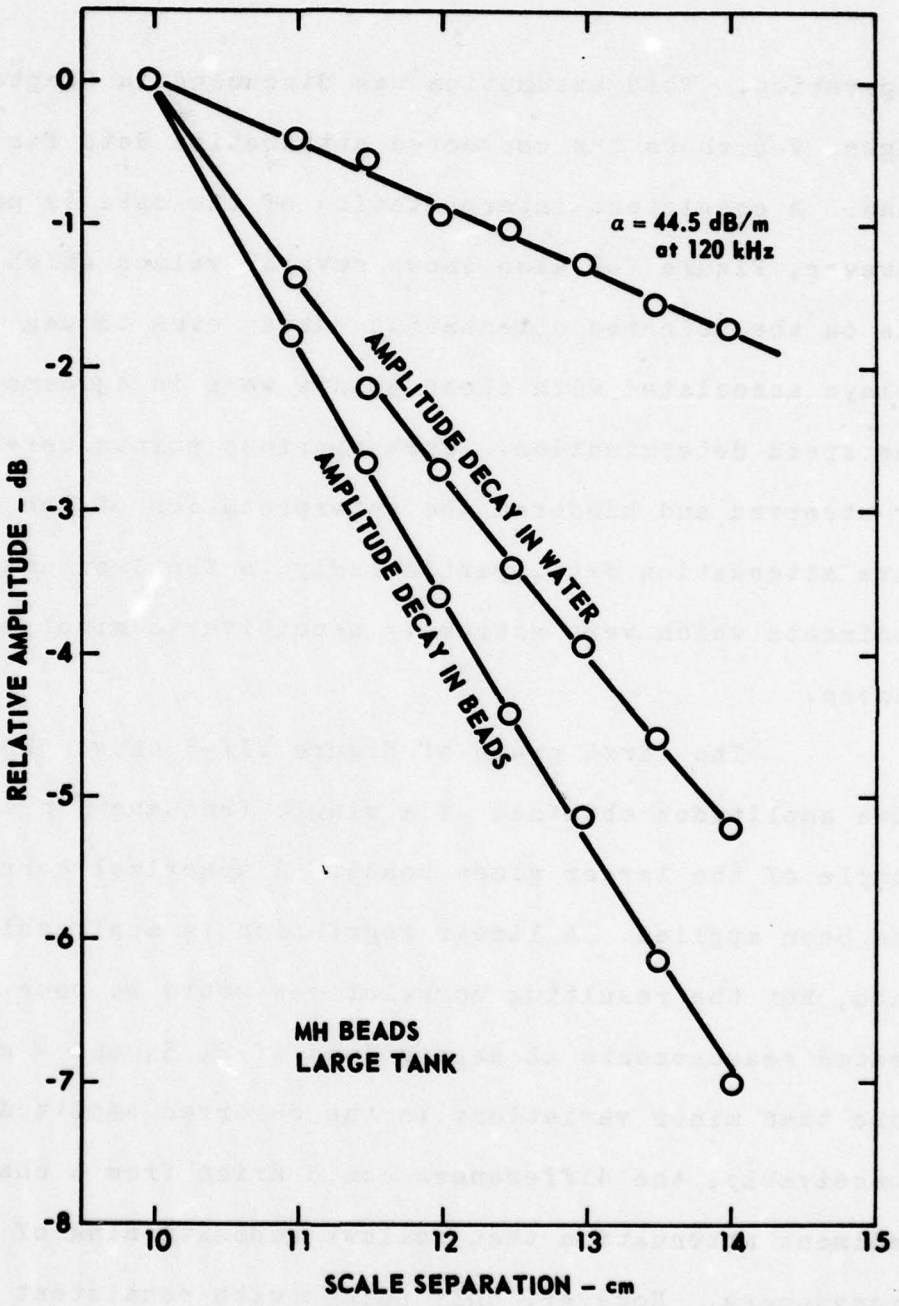

FIGURE VII-4
DETERMINATION OF COMPRESSIONAL WAVE ATTENUATION

separation. This assumption was discussed in Chapter V. Figure V-6 shows the corrected attenuation data for the PC sand. A consistent interpretation of the data is possible. However, Figure V-6 also shows several values which do not lie on the selected attenuation curves even though the time delays associated with these points were in agreement with the speed determination. Such spurious points were commonly observed and hindered the interpretation of the shear wave attenuation data, particularly in the less angular sediments which were extremely sensitive to minor disturbances.

The first graph of Figure VII-5 shows the relative amplitudes obtained at a single frequency in a dry sample of the larger glass beads. A spherical correction has been applied. A linear regression is applicable to the data, but the resulting correlations would be poor. Repeated measurements at separations of 2, 3, and 4 cm show more than minor variations in the observed amplitudes. Conceivably, the differences could arise from a change in sediment attenuation that follows repositioning of the transducers. However, only points with consistent transit times and wave shapes were considered. It is unlikely that the speed would remain constant while the attenuation

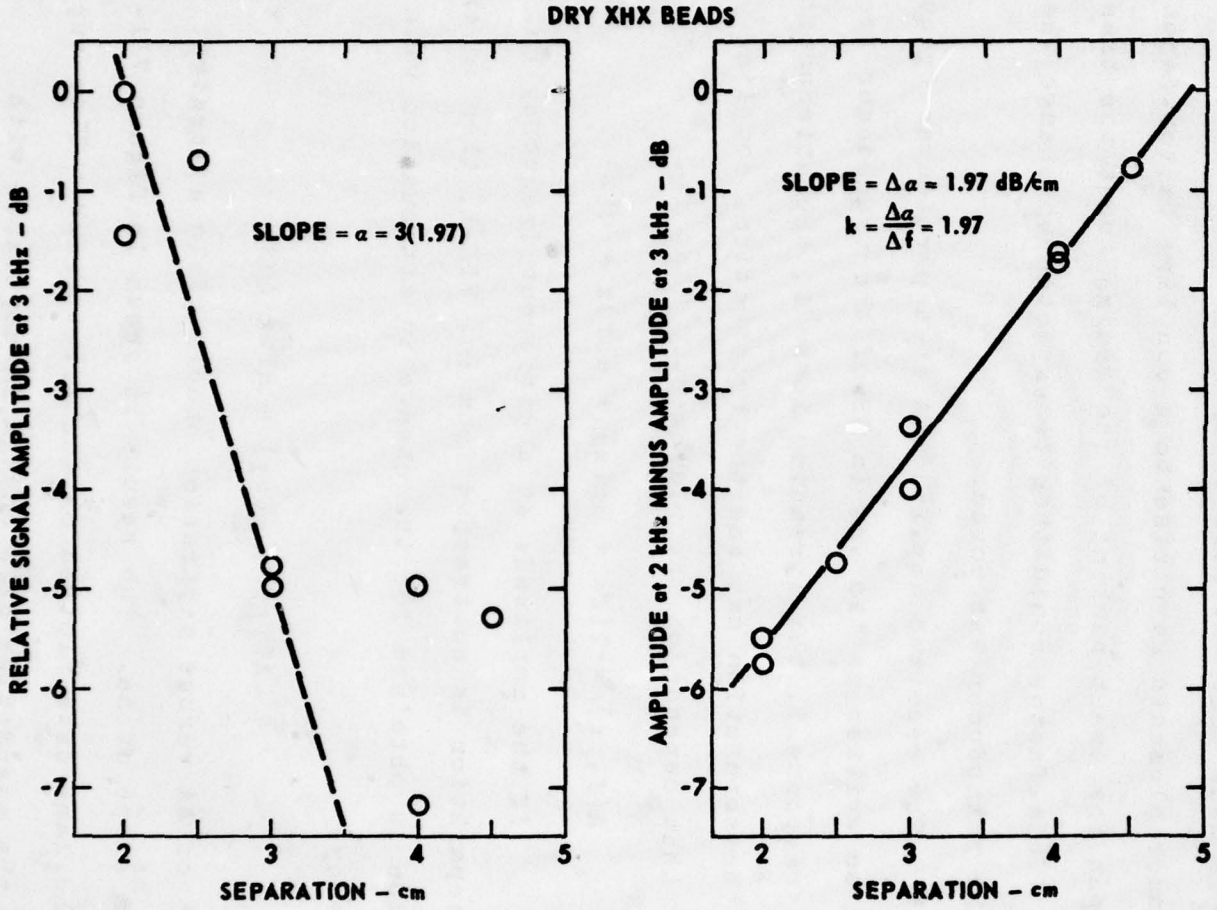

FIGURE VII-5
DETERMINATION OF SHEAR WAVE ATTENUATION FACTOR - $k = \frac{\Delta\alpha}{\Delta f}$

varied by a factor of 2 or more. The assumption was therefore made that the relatively large surface area of the bender elements gave rise to a coupling factor dependent upon the exact packing of the grains about the transducer. This factor could then be expected to change whenever the transducer was moved.

The received amplitude A at a particular frequency can be written as the sum in dB of the transducer frequency response T, the spreading loss SL, the attenuation times the separation αx, and the hypothetical coupling term C that depends on the placement. That is,

$$A(f, x) = T(f) + SL(x) + \alpha(f)x + C(x) \quad . \qquad \text{VII-1}$$

If the amplitude at a different frequency but the same separation is subtracted from Eq. VII-1, then an expression is obtained for the change in attenuation with frequency.

$$A(f_1) - A(f_2) = \Delta T + \Delta\alpha x \quad . \qquad \text{VII-2}$$

A plot of ΔA versus separation should yield a straight line with a slope of $\Delta\alpha$. The result is shown in Figure VII-5 for the same data plotted on the first graph. This supports the assumption of a change in amplitude with

separation that is independent of the sediment attenuation and the frequency.

The determination of $\Delta\alpha$ from Eq. VII-2 yields a less equivocal interpretation of the amplitude data and also eliminates the necessity of assuming spherical spreading. However, only a change in attenuation, rather than an absolute value, is obtained. Quoted values of attenuation are based on the assumption that for closely spaced frequencies the attenuation is proportional to the first power of the frequency. This assumption is shown to be valid for at least a decade of frequency by the attenuation measurements made in the large tank. The dashed line in Figure VII-5 shows how well such a determination of the attenuation fits the amplitude data at a single frequency. The log decrement is obtained from the measured change in attenuation, $\Delta\alpha$, by

$$\delta = \frac{\Delta\alpha}{\Delta f} \frac{V}{8.686} \quad , \qquad \text{VII-3}$$

where V is the shear wave velocity and 8.686 is the conversion factor between $\log_e$ and $\log_{10}$, that is, $\alpha(\text{dB/m}) = 8.686\ \alpha(\text{nepers/m})$.

Shear wave speed and attenuation were obtained as functions of frequency for two of the sediments, both when

dry and completely saturated. Neither the PC sand nor the MH beads exhibited dispersion over the total range of approximately .5 to 20 kHz. Values at different frequencies differed roughly by as much as 5 m/sec, but did not display a repeatable pattern.

The two receivers used simultaneously in the large tank would allow the attenuation to be calculated without further disturbance of the sediment, provided the responses of the transducers were known. Since no standard unconsolidated medium of known shear wave attenuation was available, and since the transducer sensitivity is dependent upon the wavelength in the medium, calibration in the sediment under investigation was required.

A successful calibration was obtained for the dry PC sand by placement of the two receivers at equal distances from the projector. At equal separations, the energy loss due to geometrical spreading and sediment attenuation should be the same for each transducer. The measured amplitude difference therefore represents the difference in transducer response. An average correction factor was obtained from readings at several equally spaced settings and at several frequencies. The transducers were then placed at different separations. The measured attenuations,

corrected for the transducer response and assumed spherical spreading, are shown in Figure VII-6. The bars on the graph are one standard deviation of the calibration measurements divided by the distance between the transducers. The open points were obtained at different relative separations than the closed points. Both the large and small transducer elements yield similar results.

A consistent calibration was not obtained in the saturated PC sand nor the MH beads. The relative amplitude difference between the two transducers depended on both the placement and the frequency and was not closely repeatable. Data for a single transducer showed the same scatter as in Figure VII-5. It was again necessary to introduce the concept of a variable transducer coupling in order to extract meaningful estimates of the attenuation.

With the amplitude of a single transducer expressed by Eq. VII-2, the combination of two receivers at distances x_1 and x_1 gives

$$\Delta A_1(x_1) - \Delta A_2(x_2) = \Delta T_1 - \Delta T_2 + \Delta\alpha(x_1-x_2) \quad , \quad \text{VII-4}$$

where Δ represents the difference between the two frequencies. Reversal of the separations gives

$$\Delta A_1(x_2) - \Delta A_2(x_1) = \Delta T_1 - \Delta T_2 - \Delta\alpha(x_1-x_2) \quad . \quad \text{VII-5}$$

Subtracting these two expressions yields the following equation for the change of attenuation between the two frequencies considered.

$$\Delta\alpha = [\Delta A_1(x_1)-\Delta A_2(x_2)-\Delta A_1(x_2)+\Delta A_2(x_1)]/2\Delta x \quad . \quad \text{VII-6}$$

The variation of $k = \Delta\alpha/\Delta f$ indicates the frequency dependence of the attenuation. A constant k would imply that the attenuation was proportional to the first power of the frequency. For the dry MH beads, a plot of k versus frequency is fairly constant. The values for the saturated sand and beads are scattered.

If a single value of the absolute attenuation was available, then the changes of attenuation calculated from Eq. VII-6 would yield a plot of attenuation versus frequency similar to Figure VII-6. A reference value of attenuation was chosen from the equation $\alpha = kf$ for a frequency pair whose calculated value of k matched the average k for all such pairs. The results are shown in Figures VII-7, VII-8, and VII-9. Each point on these graphs was determined from eight separate amplitude measurements in accordance with Eq. VII-6. Confidence limits for the curves are hard to assess, particularly in terms of

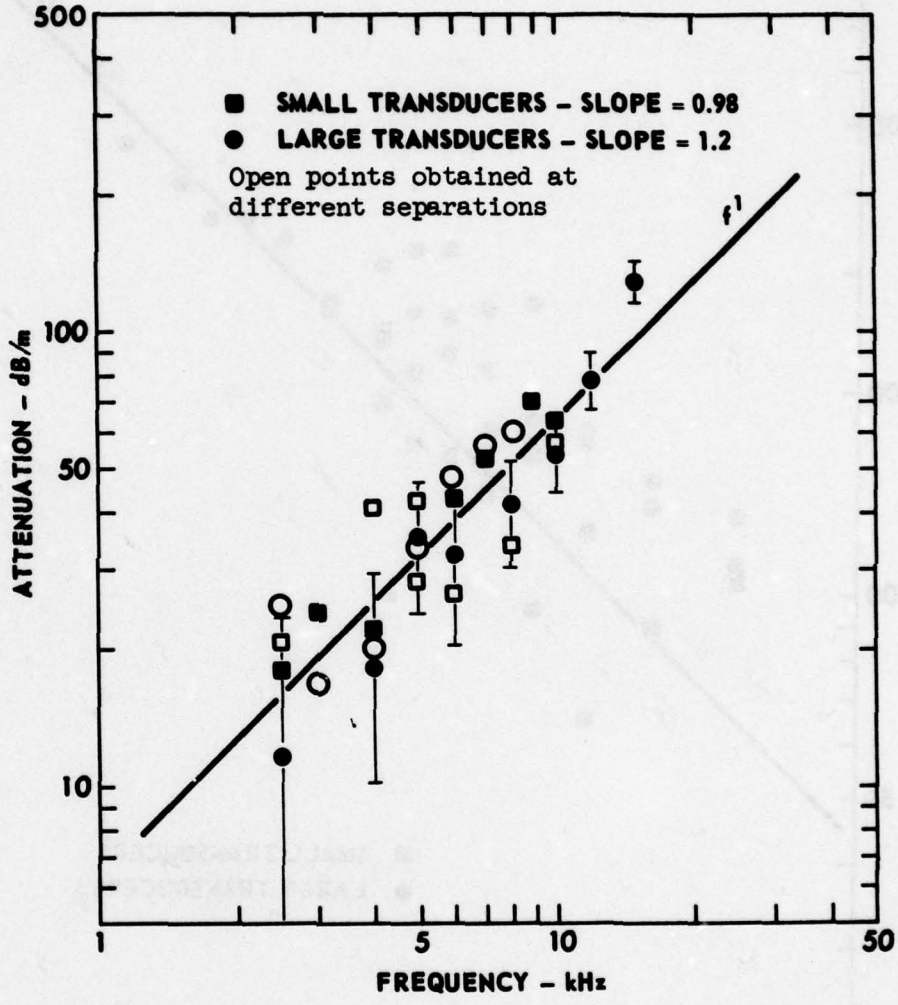

FIGURE VII-6
SHEAR WAVE ATTENUATION versus FREQUENCY
DRY PC SAND

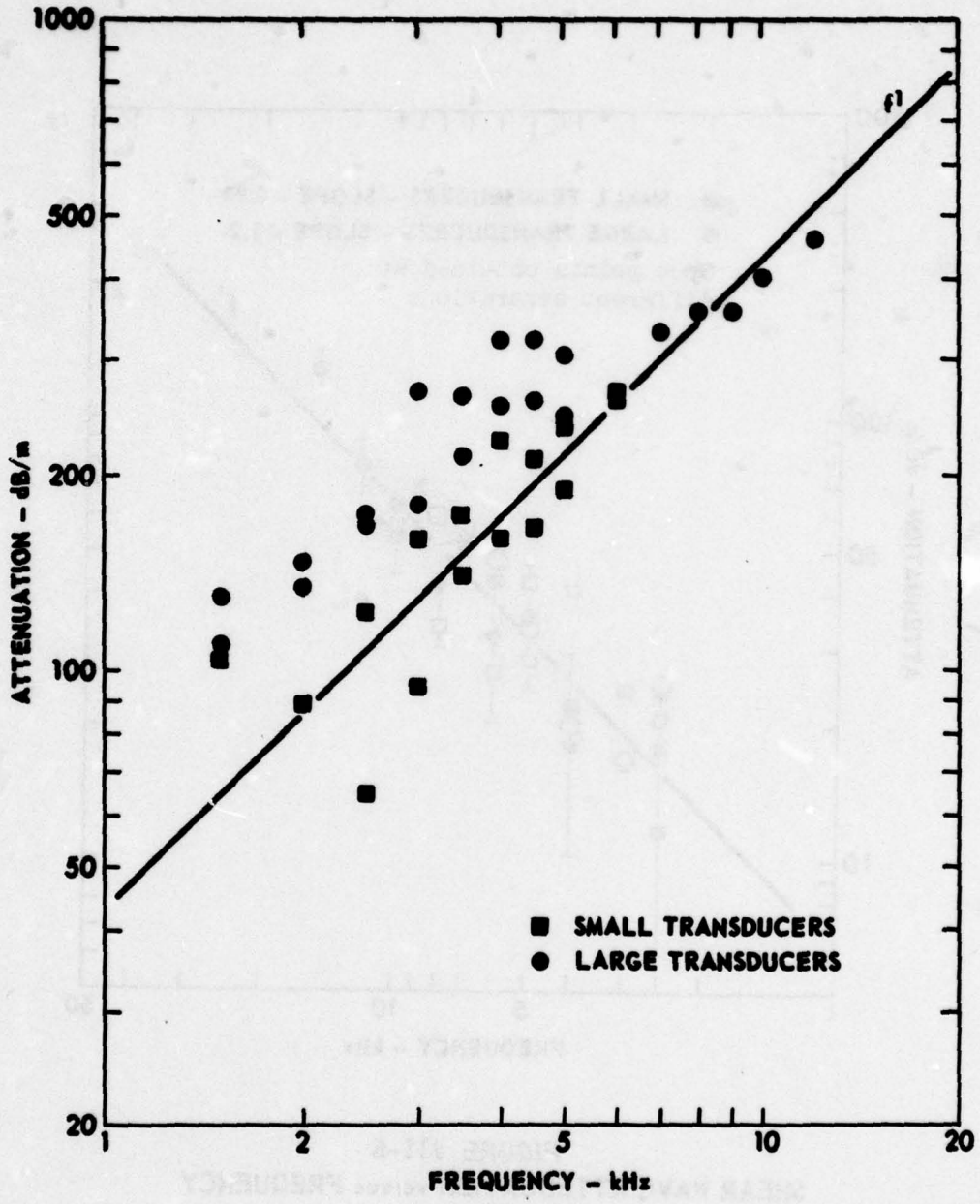

FIGURE VII-7
SHEAR WAVE ATTENUATION versus FREQUENCY
SATURATED PC SAND

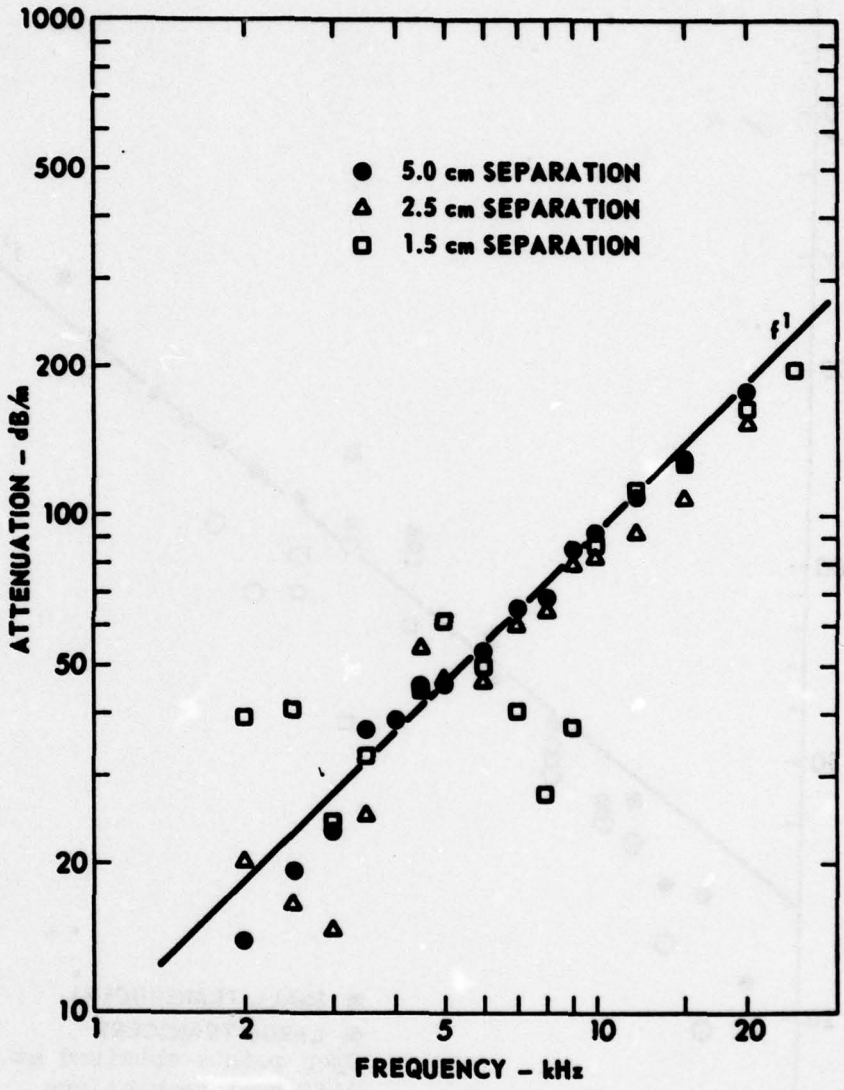

FIGURE VII-8
SHEAR WAVE ATTENUATION versus FREQUENCY
DRY MH BEADS

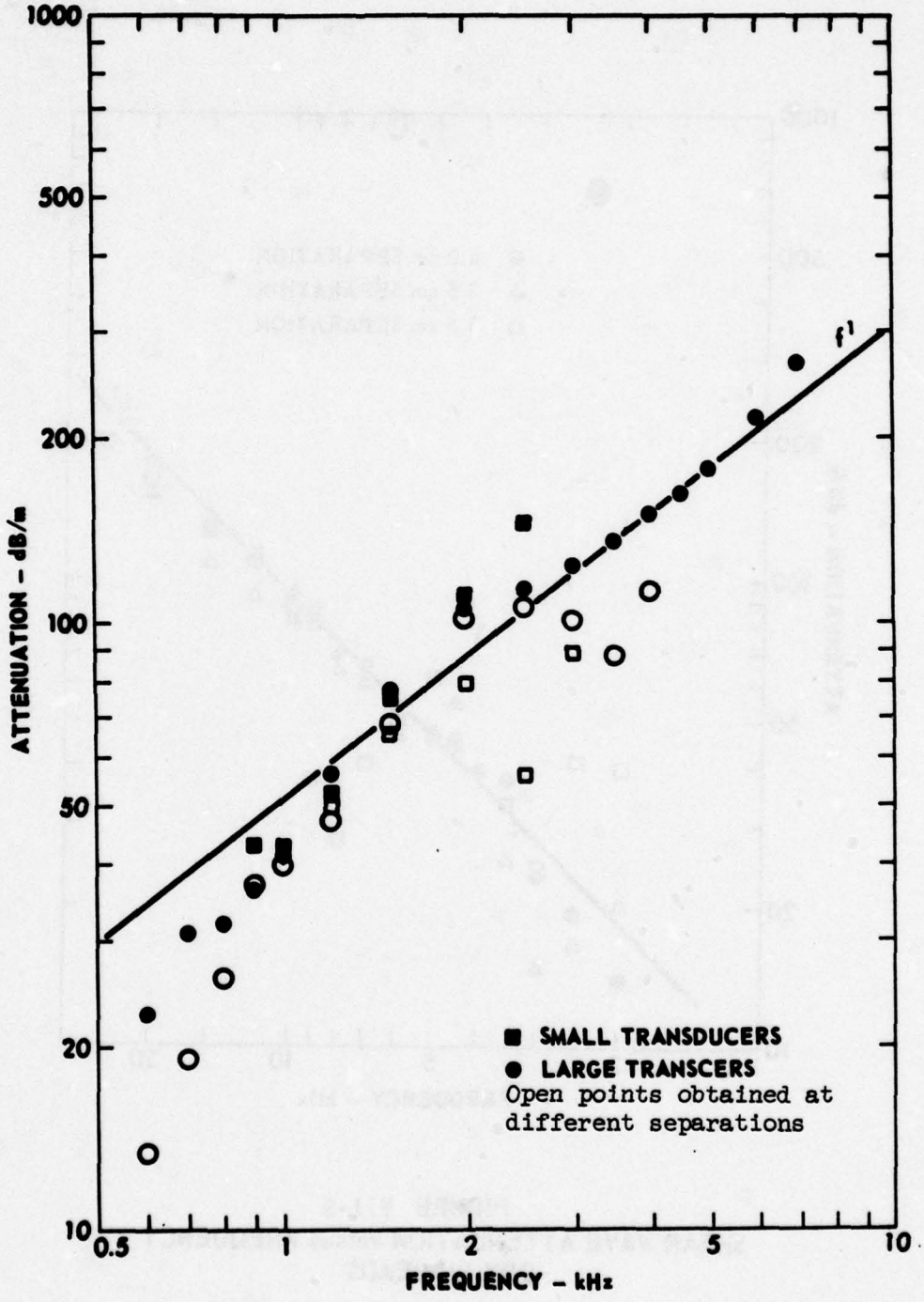

FIGURE VII-9
SHEAR WAVE ATTENUATION versus FREQUENCY
SATURATED MH BEADS

absolute values. However, the results were repeatable for both sizes of transducer elements and should therefore represent a fair picture of the true variation of attenuation with frequency. The lines with unity slope depict a linear dependence of attenuation on frequency. They are included as a reference and do not necessarily represent the best possible fit to the data.

A summary of the acoustic properties of the sediments as determined in the present report are presented in Table II.

TABLE II

SEDIMENT ACOUSTIC PROPERTIES

Small Tank Results								
Sediment	Saturated				Dry			
Beads	V_p	δ_p	V_s	δ_s	V_p	δ_p	V_s	δ_s
L	1850	.096	63	.87	98	.34	95	2.0
MH	1810	.054	65	.37	95	1.2	84	1.1
XHX	1830	.040	82	.32	110	1.4	122	2.8
XPX	1820	.035	53	.31	--	--	76	1.3
Sands								
Red	1710	.045	55	1.2	--	--	73	.59
PC	1740	.015	105	.34	220	.58	220	.4
OTT	1800	.055	47	2.0	--	--	66	1.2
Large Tank Results								
MH	1850	.079	100	.48	--	--	124	.14
PC	--	--	145	.72	--	--	185	.14

V_p = Compressional Wave Speed (m/sec)

V_s = Shear Wave Speed (m/sec)

$\delta = \alpha V / 8.686\ f$

C H A P T E R V I I I

DISCUSSION OF RESULTS

The compressional wave speeds and attenuations presented in Table II for the saturated sediments are in accord with the findings of other investigators. The speed is essentially independent of grain size for the graded glass beads. Part of the variation that does exist can be attributed to changes in temperature for which no correction has been applied. The average value agrees with a speed of 1,850 m/sec reported by Wylie et al. (1956) for seven sizes of glass beads. Speeds observed in the natural sands are slightly lower than those in the beads. This is expected since glass has a higher bulk modulus than quartz. The damping shows a smooth decrease with increasing grain size as expected for sand size particles (Hamilton, 1972). The damping is smaller in the angular PC sand than in the other samples.

The three values of compressional wave speed obtained in the dry glass beads are also independent of grain size. The values agree with longitudinal speeds of

98 to 113 m/sec found in beads by Schmidt (1954). Wylie et al. (1956) estimated a speed of 400 m/sec in dry beads but disclaim reliance on this figure due to poor arrivals and scatter in repeated measurements. Such a speed corresponds to values found in the present investigation when very slight frame pressures were applied.

Little confidence should be placed in the quoted values of compressional wave damping in the dry materials due to the difficulties with transducer coupling and the resulting poor signal quality. The values do agree reasonably well with decrements obtained by Nyborg et al. (1950) of roughly 1.2 to 1.6 and by Koltonski and Malecki (1958) of .23 to .42 for dry sands using pulse transmission techniques. Recall that the attenuations observed by these investigators did not vary linearly with frequency. Longitudinal decrements obtained in dry materials at small confining pressures are considerably lower. For example, Pilbeam and Vaisnys (1973) quote a Q value that corresponds to a decrement of .07 for longitudinal vibrations in a sample of MH beads at .095 MPa with a speed of 380 m/sec. This value did not vary with frequency.

The shear wave speeds in Table II show a greater percentage variation with grain size than do the

compressional wave results. However, the variation follows no discernable trend with either the grain size or the porosity. The dry sediment speeds follow the same pattern but at higher values.

The shear wave decrements for the saturated beads decrease slightly with increasing grain size. Of the nine shear wave decrements given in Table II for the saturated samples, four fall within the range of .3 ± .15 suggested by Hamilton (1976b) as typical for surficial sands. The others are higher.

A decrease in shear wave speed with saturation was anticipated from the theoretical considerations outlined in Chapter III and from the experimental results for rocks and pressurized sands reviewed in Chapter II. All of the samples studied in the present report exhibit this behavior. An increase in shear wave attenuation with saturation was also expected. This was observed in all of the natural sands and in the MH beads in the large tank.[1]

---

[1]The log decrement of the dry PC sand in the small tank is slightly higher than that in the saturated sample. However, the attenuation, that is, the loss in amplitude with distance rather than wavelength, is less. Also, difficulties with the pulse shape were encountered in the small tank at high velocities.

On the other hand, the glass beads all display larger attenuations when dry than when saturated. This difference is apparently due to the instability of the dry glass beads in the small tank.

The extreme sensitivity in the small tank of the dry glass bead measurements to very minor physical disturbances makes it unlikely that the measured values should be taken as the frame parameters when the same beads are saturated. That is, the contact stresses between the dry beads in the wooden box probably differ substantially from those in the saturated beads in the small aluminum tank even though the sediment was at the same depth in each case. Presumably, the increase in overburden pressure in the large tank imparts enough rigidity to the bead packing that the frame parameters in that instance change only slightly with saturation. The angular sand grains are less subject to changes in particle arrangement due to minor vibrations and are also less susceptible to static electric charges. The sand frame parameters should therefore be less influenced by saturation.

While the exact influence on the frame of grain angularity and overburden pressure cannot be determined from the few measurements shown in Table II, important

effects can be attributed to both. The angular PC sand has higher shear wave speeds and lower attenuations when dry and when saturated than the other samples at the same depth. The Red sand, which is a mixture of angular and smooth grains, has the next lowest shear wave attenuation in the unsaturated state. However, there is not enough information available to assess the influences of poor sorting in this sediment. The effect of overburden pressure is also pronounced. Both the saturated MH beads and the PC sand show approximately a 50 percent increase in shear wave speed with an increase in depth from 9 to 20 cm. The attenuations of the saturated samples change only slightly, but those of the dry samples decrease dramatically with minor increases in depth.

There have been theoretical efforts to relate ratios of compressional and shear wave speeds to ratios of the corresponding decrements. The resulting equations are of the form (Hamilton, 1976)

$$\delta_s/\delta_p = kV_p^2/V_s^2 \quad ,$$

with predicted values of k cited as .75 or .50. Hamilton notes that available data indicate values of k in the range of .02 to .2 for natural sediments. The data in

Table II yield k = .012 ± .005 for the beads and k = .05 ± .03 for the sands. On this basis, the above equation is not a particularly accurate means of estimating shear wave attenuation.

A linear increase in attenuation with freqeuncy has been found in the large tank for both the dry MH beads and the dry PC sand over approximately a decade of frequency (Figure VII-6 and Figure VII-8). A linear increase with frequency is also compatible with the results obtained in the saturated sediments, although the scatter in the measurements allows other interpretations. In particular, it is of interest to compare the results with the predictions of the viscous loss model outlined in Chapter III. At first glance, the observed behavior satisfies the major theoretical predictions. That is, the shear wave speeds decrease and the attenuations increase with water saturation. Also, the attenuation of the frame can be characterized by a constant log decrement.

Figures VIII-1 and VIII-2 compare the attenuations predicted by Eq. III-19 with the experimental data shown in earlier figures. The frame parameters, μ and μ', were taken from the dry sediment measurements. The pore size parameter necessary for the determination of the

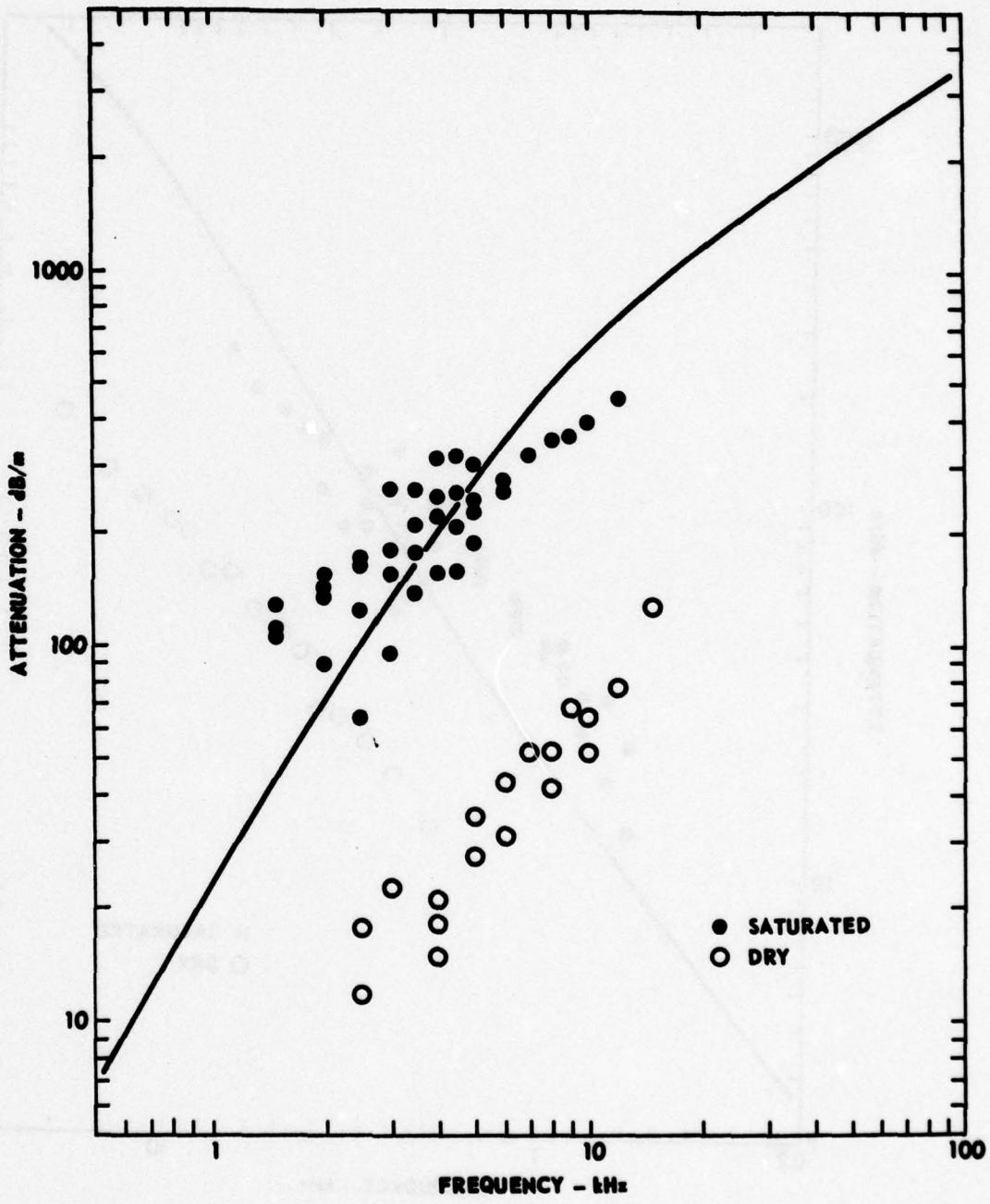

FIGURE VIII-1
SHEAR WAVE ATTENUATION COMPARED WITH
PREDICTED VISCOUS LOSS - PC SAND

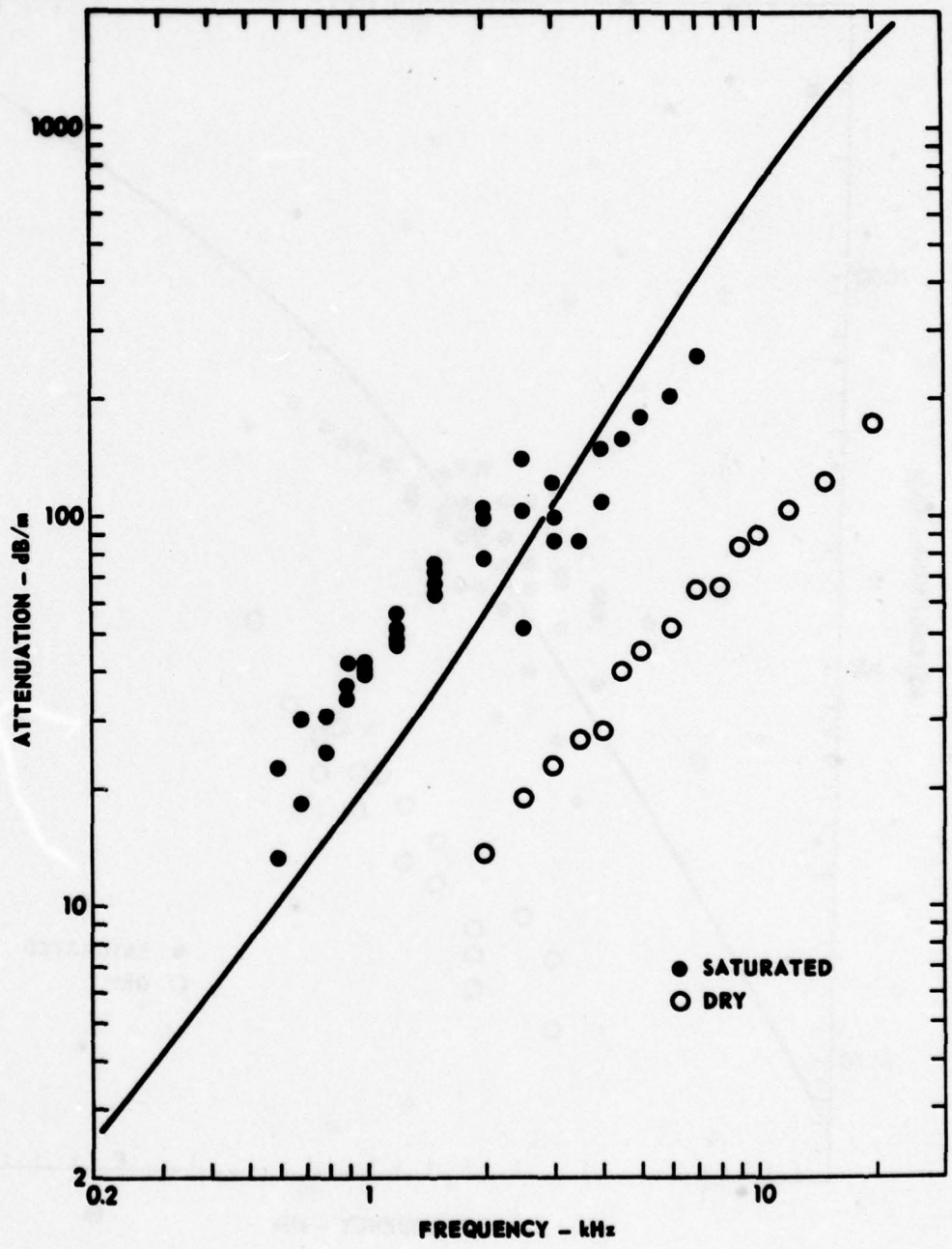

FIGURE VIII-2
SHEAR WAVE ATTENUATION COMPARED WITH
PREDICTED VISCOUS LOSS - MH BEADS

effective density was obtained from Eq. IV-4 and the data in Table I. The predicted increase in attenuation due to viscous loss is in general agreement with the data for both the MH beads and the PC sand. The predicted dispersion in each case is less than the scatter in the velocity measurements. However, the predicted speeds are slightly higher than those actually measured. Minor adjustments in the frame parameters can result in better agreement.

The general agreement of the measured attenuations with those predicted by the theoretical model implies that relative movement between the frame and pore fluid occurs during an acoustic disturbance. This in turn suggests that theories which assume perfect coupling between the frame and the fluid, such as that of Gassman (1951), may be inadequate for a complete description of sediment acoustic properties. This contention is supported by the shear wave velocity measurements of Hardin and Richart (1963) and Domenico (1977) who found that the saturated speeds in sands were greater than those predicted by the addition of the total mass of the water.

If the viscous loss is indeed an important mechanism, then shear wave decrements measured at a single frequency cannot be confidently extrapolated to frequencies

decades removed on the basis of a simple linear dependence of attenuation on frequency. Furthermore, this statement should apply equally to compressional wave measurements. This in turn may explain the variation in the frequency dependence of compressional wave attenuation reported in the literature for sands.

The relative importance of the viscous loss term depends on the magnitude of the frame loss and the ease with which the fluid moves with respect to the frame. The highly permeable sediments studied in the present report were specially chosen so that the expected viscous loss would be comparable to dissipation in the frame. This may seldom be the case in natural marine sediments. The frame loss is expected to dominate in low permeability sediments such as silts and clays. Also, increased rigidity due to overburden pressure will cause both the frame and the viscous losses to decrease, although not necessarily in proportion. At higher pressures, the relative displacement of the fluid and the frame may be negligible even in sands. A definite statement on the practical importance of viscous loss awaits extended measurements, preferably in situ.

C H A P T E R I X

CONCLUSIONS

The data contained in the present report apparently represent one of the first major attempts to measure the viscoelastic shear wave properties of saturated, unconsolidated media without application of external confining pressure. Relevant conclusions can therefore be drawn not only from the measurements themselves but also from the measurement techniques. These include the following.

1. High quality shear wave signals can be generated and detected by bender elements in low rigidity unconsolidated sediments. The broadband characteristics of these transducers allow speeds and attenuations to be measured over more than a decade of frequency with the same device. However, further development can lead to additional refinement. In particular, a better understanding is needed of the transducer response to a change in sediment load and of the coupling of energy into the sediment.

2. Control of minor stresses that influence the rigidity of the sediment is necessary for a successful laboratory program of shear wave measurement. Both the finite

size of the test chamber and the method of compaction can influence the packing of sand sized particles. Techniques which exert a controlled external frame pressure can avoid some of the problems associated with minor disturbances of the sediment. However, the resulting measurements should not be considered as appropriate to surficial sediments without additional confirmation.

The 150 liter sediment tank used in the present study represents a convenient size for laboratory measurements in sand. There is sufficient sediment mass to reduce the influence of minor vibrations on the packing, and yet the mass is not too large to vibrate at amplitudes necessary to reach minimum porosity. The tank is also small enough to allow deaeration of the entire sediment at once.

3. An irregular porous foam liner has been found to be an efficient absorber of shear wave energy. This allows interference from reflections to be minimized.

4. Minor changes in the physical properties of a sediment exert a larger influence on shear wave propagation than on compressional wave parameters. Shear waves therefore offer a greater potential for acoustic characterization of sediments.

5. Increases in grain angularity and overburden pressure both cause significant increases in sediment rigidity and decreases in shear wave damping.

6. Shear wave dispersion, if present, is small.

7. Shear wave attenuation over a limited frequency range is adequately described by a linear variation with frequency. There is evidence, however, that viscous interaction can be a significant loss mechanism in highly permeable sediments. Theoretical models based on viscous interaction predict a change in log decrement with frequency.

B I B L I O G R A P H Y

B I B L I O G R A P H Y

Akal, T.
1972 The relationship between the physical properties of underwater sediments that affect bottom reflection, Marine Geology 13:251-266.

Ament, W. S.
1953 Sound propagation in gross mixtures, J. Acoust. Soc. Am. 25(4) p. 638.

American Society for Testing and Materials, Permeability of granular soils (constant head), ASTM D 2434-68 (reapproved 1974).

Anderson, A. L.
1974 Acoustics of gas bearing sediments, ARL-TR-74-19 Applied Research Lab., Univ. of Texas at Austin.

Attwell, P. B., and Y. V. Ramana
1966 Wave attenuation and internal friction as functions of frequency in rocks, Geophysics 31:1049-1056.

Barkan, D. D.
1962 Dynamics of Bases and Foundations, McGraw-Hill.

Bennett, L. C., Jr.
1967 In situ measurements of acoustic absorption in unconsolidated sediments (abstract), Trans. Am. Geophys. Union 48:144.

Biot, M. A.
1956a Theory of propagation of elastic waves in fluid-saturated porous solid I. Low frequency range, J. Acoust. Soc. Am. 28(2) p. 168.

Biot, M. A.
1956b II. Higher frequency range, J. Acoust. Soc. Am. 28(2) p. 179.

Biot, M. A.
1962 Mechanics of deformation and acoustic propagation in porous media, J. Appl. Phys. 33(4) p. 1482.

Birch, F., and D. Bancroft
1938 The effect of pressure on the rigidity of rocks, J. Geol. 46:59-83;113-141.

Bland, D. R.
1960 The Theory of Linear Viscoelasticity, Pergamon Press.

Born, W. T.
1941 The attenuation constant of earth materials, Geophysics 6:132-148.

Brandt, H.
1960 Factors affecting compressional wave velocity in unconsolidated marine sand sediments, J. Acoust. Soc. Am. 32(2) p. 171-179.

Brown, R.J.S., and J. Korringa
1975 On the dependence of the elastic properties of a porous rock on the compressibility of the pore fluid, Geophysics 40(4) p. 608-616.

Brutsaert, W.
1964 The propagation of elastic waves in unconsolidated unsaturated granular mediums, J. Geophys. Res. 69 (2) p. 243-257.

Busby, J., and E. G. Richardson
1957 The absorption of sound in sediments, Geophysics 22(4) p. 821-828.

Chae, Y. S.
1968 Viscoelastic properties of snow and sand, J. Engn. Mech. Div. ASCE 94:1379-1394.

Chase, D. M.
1979 Wave propagation in liquid saturated open cell foam, J. Acoust. Soc. Am. 65(1) p. 1-8.

Carman, P. C.
1956 Flow of Gases through Porous Media, Academic Press, N.Y.

Cherry, J. T., and K. H. Waters
1968 Shear wave recording using continuous signal methods I. Early development, Geophysics 33:229-239.

Cole, B. F.
1965 Marine sediment attenuation and ocean bottom reflected sound, J. Acoust. Soc. Am. 38 p. 291-297.

Collins, F., and C. C. Lee
1956 Seismic wave attenuation characteristics from pulse experiments, Geophysics 21:16-39.

CRC
1963 Handbook of Physics and Chemistry, 44th ed., C. Hodgman, ed., Chemical Rubber Publishing Co., Cleveland Ohio.

Cunny, R. W., and Z. B. Fry
1973 Vibratory in situ and laboratory soil moduli compared, J. Soil Mech. Found. Div. ASCE 99 SM12 p. 1055-1076.

Davies, D.
1965 Dispersed Stoneley waves on the ocean bottom, Bull. SSA 55:903-918.

Deresiewicz, H., and J. T. Rice
1962 The effect of boundaries on wave propagation in a liquid filled porous solid: IV Reflection of plane waves at a free boundary, Bull. SSA 52:595-625.

Deresiewicz, H., and J. T. Rice
1964 V. Transmission across a plane interface, Bull. SSA 54:595-625.

Dobrin, M. B.
1976 Introduction to Geophysical Prospecting, 3 ed. McGraw-Hill.

Domenico, S. N.
1977 Elastic properties of unconsolidated porous sand reservoirs, Geophysics 42(7) p. 1339-1368. (Discusion, Geophysics 44(4) p. 830 1979)

Elliott, S. E., and B. F. Wiley
1975 Compressional velocities of partially saturated, unconsolidated sands, Geophysics 40(6) p. 949-954.

Faust, L. Y.
1951 Seismic velocity as a function of depth and geologic time, Geophysics 16 p. 192

Ferrero, M. A., and G. G. Sacerdote
1951 Parameters of sound propagation in granular absorbent materials, Acustica 1 p. 137.

Fry, J. C., and R. W. Raitt
1961 Sound velocities at the surface of deep sea sediments, J. Geophys. Res. 66(2) p. 589-597.

Gardner, G., M. Wyllie, and D. Droschak
1964 Effects of pressure and fluid saturation on the attenuation of elastic waves in sands, J. Petroleum Tech. AIME 16 p. 189-198.

Gassmann, F.
1951 Elastic waves through a packing of spheres, Geophysics 16(4) p. 673, errata Geophysics 18(1) p. 269, 1953.

Geertsma, J., and D. C. Smit
1961 Some aspects of elastic wave propagation in fluid saturated porous solids, Geophysics 26(2) p. 169-181.

Geyer, R. L., and S. T. Martner
1969 SH waves from explosive sources near horizontal discontinuities, Geophysics 15 p. 673-685.

Gliko, A. O.
1976 Effective elastic moduli and structure of two phase media, Izv. Earth Physics 5 p. 32-45.

Grant, F. S., and G. F. West
1965 Interpretation Theory in Applied Geophysics, McGraw-Hill.

Gregory, A. R.
1975 Some aspects of rock physics from laboratory and log data that are important to seismic interpretation, preprint, Bureau of Economic Geology, Univ. of Texas at Austin.

Gregory, A. R.
1976 Fluid saturation effects on the dynamic elastic properties of sedimentary rocks, Geophysics 41(5) p. 895-921.

Gregory, A. R., and A. L. Podio
1970 Dual mode ultrasonic apparatus for measuring compressional and shear wave velocities of rock samples, IEEE Trans. Sonics Ultrasonics SU 17(2) p. 77-85.

Hall, J. R., and F. E. Richard, Jr.
1963 Dissipation of elastic wave energy in granular soils, J. Soil Mech. Found. Div. ASCE 89 SM6 p. 27-56.

Hamilton, E. L.
1972 Compressional wave attenuation in marine sediments, Geophysics 37(4) p. 620-646.

Hamilton, E. L.
1976a Sound attenuation as a function of depth in the sea floor, J. Acoust. Soc. Am. 59(3) p. 528-535.

Hamilton, E. L.
1976b Attenuation of shear waves in marine sediments, J. Acoust. Soc. Am. 60(2) p. 334.

Hamilton, E. L.
1976c Shear wave velocity vs. depth in marine sediments--a review, Geophysics 41(5) p. 985-996.

Hamilton, E. L.
1978 Sound velocity-density relations in sea floor sediments and rocks, J. Acoust. Soc. Am. 63(2) p. 336-377.

Hamilton, E. L., R. T. Bachman, T. R. Curry, and D. G. Moore
1977 Sediment velocities from sonobuoys: Bengal Fan, Sunda Trench, Adaman Basin and Nicobar Fan, J. Geophys. Res. 82(20) p. 303-3012.

Hamilton, E. L., H. P. Bucker, D. L. Keir, and J. A. Whitney
1970 Velocity of compressional and shear waves in marine sediments determined from a research submersible, J. Geophys. Res. 75 p. 4039-4049.

Hamilton, E. L., G. Shumway, H. W. Menard, and C. J. Shipek
1956 Acoustic and other physical properties of shallow water sediments off San Diego, J. Acoust. Soc. Am. 28 p. 1-15.

Hampton, L. D.
1967 Acoustic properties of sediments, J. Acoust. Soc. Am. 42(4) p. 882-890.

Hanna, A. S.
1973 Short range transmission loss and evidence for bottom refracted energy, J. Acoust. Soc. Am. 53(6) p. 1686-1690.

Hardin, B. O., and V. P. Drnevich
1972 Shear modulus and damping in soils: measurement and parameter effects, J. Soil Mech. Found. Div. ASCE SM6 p. 603-625.

Hardin, B. O., and F. Richart
1963 Elastic wave velocities in granular soils, J. Soil Mech. Found. Div. ASCE SM 1 p. 33.

Helmberger, D. V., and G. B. Morris
1970 Transformed shear waves, Bull. SSA 60(2) p. 593-600.

Hill, M. N., ed.
1963 The Sea, Vol. 3, Interscience, John Wiley and Sons, N.Y.

Horton, C. W.
1959 A loss mechanism for the Pierre shale, Geophysics 24 p. 667-680.

Horton, C. W.
1978 The reflection of a plane acoustic wave at the interface between water and water filled sediment when allowance is made for the second wave of Biot, preprint, Applied Research Lab., Univ. of Texas at Austin.

Houtz, R. E.
1978 Preliminary sonobouy study of rapidly accumulating shelf sediments, J. Geophys. Res. 83(B11) p. 5397-5404.

Houtz, R. E., and J. I. Ewing
1963 Detailed sediment velocity from seismic refraction profiles in the western north Atlantic, J. Geophys. Res. 68(18) p. 5233-5258.

Hovem, J. M., and G. D. Ingram
1979 Viscous attenuation of sound in saturated sand, preprint, Applied Research Lab., Univ. of Texas at Austin.

Hunter, A., R. Legge, and E. Matsukawa
1961 Measurements of acoustic attenuation and velocity in sand, Acustica 11 p. 26.

Hurlbut, C. S.
1971 Dana's Manual of Mineralogy, 18th ed., John Wiley and Sons.

Johnston, D. H., and M. N. Toksoz
1978 Ultrasonic P and S wave attenuation in dry and saturated rocks under pressure, preprint submitted for publication.

Johnston, D. H., M. N. Toksoz, and A. Timur
1978 Attenuation of seismic waves in dry and saturated rocks II. mechanisms, preprint, submitted for publication. Geophysics 44(4) p. 691, 1979.

Jolly, R. N.
1956 Investigation of shear waves, Geophysics 21 p. 905-938.

Kennett, B.L.N.
1976 A comparison of travel time inversions, Geophy. J. R. Astr. Soc. 44 p. 517-536.

Kennett, B.L.N., and J. A. Orcutt
1976 A comparison of travel time inversions for marine refraction profiles, J. Geophys. Res. 81(23) p. 4061-4070.

King, M. S.
1966 Wave velocities in rocks as a function of changes in overburden pressure and pore fluid saturants, Geophysics 31(1) p. 50-73.

Knopoff, I., and G.J.F. MacDonald
1958 Attenuation of small amplitude stress waves in solids, Rev. Mod. Phy. 30:1178-1192.

Koltonski, W., and I. Malecki
1958 Ultrasonic methods for the exploration of the properties and structure of mineral layers, Acustica 8:307.

Kudo, K., and E. Shima
1970 Attenuation of shear waves in soil, Bull. Earthquake Res. Inst., Univ. Tokyo 48:145-158.

Kuster, G. T., and M. N. Toksoz
1974 Velocity and attenuation of seismic waves in two phase media, parts 1 and 2, Geophysics 39(5) p. 507-606; 233-260.

Laughton, A. S
1957 Sound propagation in compacted ocean sediments, Geophysics 22(2) p. 233-260.

McCann, C., and D. M. McCann
1969 The attenuation of compressional waves in marine sediments, Geophysics 34(6) p. 882-892.

McDonal, F. J., F. A. Angona, R. L. Mills, R. L. Sengbush, R. G. Van Nostrand, and J. E. White
1958 Attenuation of shear and compressional waves in Pierre shale, Geophysics 23:421-439.

McLeroy, E. G., and A. DeLoach
1968 Sound speed and attenuation from 15 to 1,500 kHz, measured in natural sea floor sediments, J. Acoust. Soc. Am. 44(4) p. 1148-1150.

Mengi, Y., and H. D. McNiven
1977 Response of fluid-filled porous media to a transient input, J. Acoust. Soc. Am. 61(1) p. 84-94.

Mengi, Y.
1978 Propagation and decay of waves in porous media, J. Acoust. Soc. Am, 64(4) p. 1125-1131.

Morse, R. W.
1952 Acoustic propagation in granular media, J. Acoust. Soc. Am. 24(6) p. 696.

Nafe, J. E., and C. L. Drake
1957 Variation with depth in shallow and deep water marine sediments of porosity, density and the velocities of compressional and shear waves, Geophysics 22:523-552.

Nolle, A. W., W. A. Hoyer, J. F. Mifsud, W. R. Runyan, and M. A. Ward
1963 Acoustical properties of water filled sands, J. Acoust. Soc. Am. 35(9) p. 1394-1408.

Nur, A.
1972 Dilantancy, pore fluids and permonitory variations of t_s/t_p travel times, Bull. SSA 62(5) p. 1217-1222.

Nur. A., and G. Simmons
1969 The effect of saturation on velocity in low porosity rocks, Earth Planet Sci. Lett. 7:183-193.

Nyborg, W. L., I. Rudnick, and H. K. Schilling
1950 Experiments on acoustic absorption in sand and soil, J. Acoust. Soc. Am. 22(4) p. 422-425.

Otha, Y., and E. Shima
1967 Experimental study on generation and propagation of S waves, II. Preliminary experiments on generation of SV waves, Bull. Earthquake Res. Inst., Univ. Tokyo 45(1) p. 32-42.

Peselnick, L., and W. F. Outerbridge
1961 Internal friction in shear and shear modulus of Solenhofen limestone over a frequency range of 10^7 cycles per second, J. Geophys. Res. 66:581-588.

Peselnick, L., and I. Zietz
1959 Internal friction of fine grained limestones at ultrasonic frequencies, Geophysics 24:285-296.

Pilbeam, C. C., and J. R. Vaisnys
1973 Acoustic velocities and energy losses in granular aggregates, J. Geophys. Res. 78(5) p. 810-824.

Le Pichon, X., J. Ewing, and R. E. Houtz.
1968 Deep sea sediment velocity determinations made while reflection profiling, J. Geophys. Res. 73 (8) p. 2597-2614.

Plona, T. J., and L. Tsang
1979 Characterization of the average microscopic dimension in granular media using ultrasonic pulses: Theory and experiments (abstract) Geophysics 44(3) p. 344-355.

Ricker, N., and R. P. Lynn
1950 Composite reflections (Shear waves), Geophysics 15(1) p. 30-49.

Robin, P-Y.F.
1973 Note on effective pressure, J. Geophys. Res. 78(4) p. 434-2441.

Rogers, J.J.W., and W. B. Head
1961 Relationships between porosity, median size, and sorting coefficients of synthetic sands, J. Sed. Petrology 31(3) p. 467-470.

Rutherford, S. R.
1976 Analytical techniques for determining subbottom velocity profiles in unconsolidated sediments, ARL-TR-76-58, Applied Research Lab., Univ. of Texas at Austin.

Schmidt, H.
1954 Die schallausbreitung in körnigen substanzen (in German, English summary), Acustica 4:639-652.

Shima, E., and Y. Ohta
1967 Experimental study on generation and propagation of S waves I. Designing of SH wave generator and its field tests, Bull. Earthquake Res. Inst., Univ. of Tokyo 45(1) p. 19-32.

Shirley, D. J.
1977 Laboratory and in situ sediment acoustics, ARL-TR-77-46, Applied Research Lab., Univ. of Texas at Austin.

Shirley, D. J.
1978 An improved shear wave transducer, J. Acoust. Soc. Am. 63(5) p. 1643-1645.

Shirley, D. J., and A. L. Anderson
1975a Studies of sediment shear waves, acoustical impedence and engineering properties, ARL-TR-75-23, Applied Research Lab., Univ. of Texas at Austin.

Shirley, D. J., and A. L. Anderson
1975b Acoustical and engineering properties of sediments, ARL-TR-75-58, Applied Research Lab., Univ. of Texas at Austin.

Shirley, D. J., and A. L. Anderson
1975c In situ measurement of marine sediment acoustical properties during coring in deep water, IEEE Trans. Geosci. Electronics GE 13(4).

Shirley, D. J., and D. W. Bell
1978 Acoustics of in situ and laboratory sediments, ART-TR-78-36, Applied Research Lab., Univ. of Texas at Austin.

Shirley, D. J., and L. D. Hampton
1978 Shear wave measurements in laboratory sediments, J. Acoust. Soc. Am. 63 p. 607.

Shumway, G.
1958 Sound velocity vs. temperature in water saturated sediments, Geophysics 23:494-505.

Shumway, G.
1960 Sound speed and absorption studies of marine sediments by a resonance method, parts 1 and 2, Geophysics 25:451-467;659-682.

Simmons, G.
1964 Velocity of shear waves in rocks to 10 kilobars, I, J. Geophys. Res. 69(6) p. 1123-1130.

Smith, P., and R. Greenkorn
1972 Theory of acoustical wave propagation in porous media, J. Acoust. Soc. Am. 52 p. 247-253.

Smith, P., R. Greenkorn, and R. Barile
1974 Infrasonic response characteristics of gas and liquid filled porous media, J. Acoust. Soc. Am. 56(3) p. 781.

Stokoe, K. H., II and, R. D. Woods
1972 In situ shear wave velocity by cross hold method, J. Soil Mech. Found. Div. ASCE 98 SM5 p. 443-460.

Stoll, R. D.
1974 Acoustic waves in saturated sediments, in Physics of Sound in Marine Sediments, L. Hampton, ed., Plenum Press, N.Y.

Stoll, R. D.,
1977 Acoustic waves in ocean sediments, Geophysics 42(4) 715-725.

Stoll, R. D., and G. M. Bryan
1970 Wave attenuation in saturated sediments, J. Acoust. Soc. Am. 47 p. 1440-1447.

Sutton, G. H., H. Berchemer, and J. E. Nafe
1957 Physical analysis of deep sea sediments, Geophysics 22(4) p. 779-812.

Taner, M. T., and F. Koehler
1969 Velocity spectra-Digital computer derivation and applications of velocity functions, Geophysics 34(6)p. 859-881.

Tathan, R. H., and R. L. Stoffa
1976 V_p/V_s--A potential hydrocarbon indicator, Geophys., 41(5) p. 837-849.

Timur, A.
1977 Temperature dependence of compressional and shear wave velocities in rocks, Geophysics 42(5) p. 950-956.

Toksoz, M. N., D. H. Johnston, A. Timur
1978 Attenuation of seismic waves in dry and saturated rocks: I. Laboratory measurements, preprint-submitted for publication. Geophysics 44(4) 681, 1979.

Tyce, R. C.
1976 Near bottom observations of 4 kHz acoustic reflectivity and attenuation, Geophysics 41(4) p. 673-699.

Urick, R. J.
1948 The absorption of sound in a suspension of irregular particles, J. Acoust. Soc. Am. 20 p. 283-289.

Urick, R. J.
1975 Principles of Underwater Sound, 2nd ed. McGraw-Hill.

Walsh, J. B.
1966 Seismic wave attenuation in rock due to friction, J. Geophys. Res. 71 p. 2591-2599.

Walsh, J. B.
1968 Attenuation in partially melted material, J. Geophys. Res. 73(6).

Walton, K.
1975 Effective elastic moduli of model sediments, Geophys. J. R. Astr. Soc. 43 p. 293-306.

Walton, K.
1977 Theoretical wave propagation in model sediments, Proc. Inst. Acoustics p. 7-10-1, 7-10-4.

Warrick, R. E.
1974 Seismic investigation of a San Francisco Bay Mud Site: Bull. SSA 64 375-385.

White, J. E.
1965 Seismic Waves: Radiation, Transmission and Attenuation, McGraw-Hill.

White, J. E., and R. L. Sengburh
1953 Velocity measurements in near surface formations, Geophysics 18(1) p. 54-69.

Wood, A. B.
1930 A Textbook of Sound, 3rd ed., 1955, McGraw-Hill.

Wood, A. B., and D. E. Weston
1964 The propagation of sound in mud, Acustica 14 p. 156-162.

Wood, R. A.
1978 Converted wave reflections in exploration seismic records, MA thesis, Univ. of Texas at Austin.

Wu, T. H.
1971 Soil Dynamics, Allyn and Bacon, Boston.

Wyllie, M.R.J., A. R. Gregory, and L. W. Gardner
1956 Elastic wave velocities in heterogenous and porous media, Geophysics 21(1) p. 41-70.

Wyllie, M.J.R., G.H.F. Gardner, and A. R. Gregory
1962 Studies of elastic wave attenuation in porous media, Geophysics 27(5) p. 569-589.

Yew, C. H., and P. N. Jogi
1976 Study of wave motions in fluid-saturated porous rocks, J. Acoust. Soc. Am. 60(1) p. 2.

Zwikker, C., and C. W. Kosten
1949 Sound Absorbing Materials, Elsevier Publishing Co., N.Y.

14 May 1979

DISTRIBUTION LIST FOR
ARL-TR-79-31
UNDER CONTRACT N00014-76-C-0117
UNCLASSIFIED

Copy No.

Commanding Officer
Naval Ocean Research and Development Activity
NSTL Station, MS 39529
1 Attn: R. R. Goodman (Code 110)
2 R. D. Gaul (Code 600)
3 A. L. Anderson (Code 320)
4 S. Marshall (Code 340)
5 J. Paquin (Code 500)
6 J. Matthews (Code 362)

Commanding Officer
Office of Naval Research
Arlington, VA 22217
7 Attn: J. B. Hersey (Code 102-OS)
8 A. Sykes
9 T. Pyle (Code 48B)
10 H. Bezdek (Code 460)
11 M. Odegard (Code 48D)

Commanding Officer
Naval Electronic Systems Command
Department of the Navy
Washington, DC 20360
12 Attn: J. Sinsky (Code 320)
13 J. Reeves (Code PME 124-34)

Commander
Naval Sea Systems Command
Department of the Navy
Washington, DC 20362
14 Attn: A. P. Franceschetti

Chief of Naval Material
Department of the Navy
Washington, DC 20360
15 Attn: CDR E. Young (Code 08724)

Commanding Officer
Naval Oceanographic Office
NSTL Station, MS 39529
16 Attn: W. Geddes

Distribution List for ARL-TR-79-31 under Contract N00014-76-C-0117

Copy No.

Commander
Naval Ocean Systems Center
Department of the Navy
San Diego, CA 92132
17 Attn: M. A. Pedersen (Code 307)
18 R. R. Gardner (Code 40)
19 E. L. Hamilton
20 H. P. Bucker (Code 409)

Director
Naval Research Laboratory
Department of the Navy
Washington, DC 20375
21 Attn: Code 2627
22 O. Diachok

Chief of Naval Operations
Department of the Navy
Washington, DC 20350
23 Attn: R. S. Winokur CNO (OP-95E1)

Commander
Naval Air Development Center
Department of the Navy
Warminster, PA 18974
24 Attn: C. L. Bartberger

Commander
New London Laboratory
Naval Underwater Systems Center
Department of the Navy
New London, CT 06320
25 Attn: P. Herstein

Commanding Officer
Naval Coastal Systems Laboratory
Panama City, FL 32401
26 Attn: E. G. McLeroy, Jr.
27 B. Tolbert

Superintendent
Naval Postgraduate School
Monterey, CA 93940
28 Attn: H. Medwin
29 Library

Woods Hole Oceanographic Institution
Woods Hole, MA 02543
30 Attn: C. Hollister

Distribution List for ARL-TR-79-31 under Contract N00014-76-C-0117

Copy No.

Hawaii Institute of Geophysics
The University of Hawaii
2525 Correa Road
Honolulu, HI 96822
31 Attn: Dr. G. Sutton

The Scripps Institution of Oceanography
The University of California/San Diego
San Diego, CA 92152
32 Attn: P. Lonsdale

Department of Geological Oceanography
Texas A&M University
College Station, TX 77840
33 Attn: Dr. W. R. Bryant

Underwater Systems, Inc.
3121 Georgia Avenue
Silver Spring, MD 20910
34 Attn: M. S. Weinstein

Geophysics Laboratory
Marine Science Institute
The University of Texas
700 The Strand
Galveston, TX 77550
35 Attn: J. Worzel
36 E. W. Beherns

Tracor, Inc.
1601 Research Boulevard
Rockville, MD 20850
37 Attn: R. J. Urick

The Catholic University of America
6220 Michigan Avenue, NE
Washington, DC 20017
38 Attn: H. M. Uberall

Lamont-Doherty Geological Observatory
Palisades, NY 10964
39 Attn: G. Bryan
40 W. J. Ludwig
41 B. Tucholke
42 R. D. Stoll

Department of Civil and Ocean Engineering
The University of Rhode Island
Kingston, RI 02881
43 Attn: Dr. A. J. Silva

Distribution List for ARL-TR-79-31 under Contract N00014-76-C-0117

Copy No.

University College of North Wales
Marine Science Laboratories
Menai Bridge
Anglesey, NORTH WALES
44 Attn: D. Taylor Smith
45 P. Schultheiss

Director
SACLANT ASW Research Centre
La Spezia, ITALY
46 Attn: T. Akal

The University of Auckland
Auckland, NEW ZEALAND
47 Attn: A. Kibblewhite, Physics Department

48 Defence Research Establishment Pacific
CF Dockyard
Victoria, B. C., CANADA

49 Defence Research Establishment Atlantic
Grove Street
Dartmouth, N. S., CANADA

Department of Civil Engineering
The University of Texas at Austin
Austin, TX 78712
50 Attn: K. Stokoe

51 - 60 Commanding Officer and Director
Defense Documentation Center
Defense Services Administration
Cameron Station, Building 5
5010 Duke Street
Alexandria, VA 22314

61 Office of Naval Research
Resident Representative
Room 582, Federal Building
Austin, TX 78701

62 Environmental Sciences Division, ARL:UT

63 David T. Blackstock, ARL:UT

64 Harlan G. Frey, ARL:UT

Distribution List for ARL-TR-79-31 under Contract N00014-76-C-0117

Copy No.	
65	Loyd D. Hampton, ARL:UT
66	Kenneth E. Hawker, ARL:UT
67	Thomas G. Muir, ARL:UT
68	Donald J. Shirley, ARL:UT
69	Reuben H. Wallace, ARL:UT
70	Library, ARL:UT
71 - 80	Reserve, ARL:UT